CELLULAR INTERACTIONS OF THE CYTOLETHAL DISTENDING TOXINS

BY

AMANDEEP GARGI

DISSERTATION

Submitted in partial fulfillment of the requirements
for the degree of Doctor of Philosophy in Microbiology
in the Graduate College of the
University of Illinois at Urbana-Champaign, 2015

Urbana, Illinois

Doctoral Committee:

Professor Steven Blanke, Chair
Professor Brenda Wilson
Professor Gary Olsen
Professor Richard Tapping

ABSTRACT

Over the course of evolution, pathogens have adapted and co-evolved with their respective hosts, with infectious diseases being one of the leading health concerns. Pathogens have developed several strategies to colonize the host, of which only a few have been characterized in molecular details. Utilizing host uptake and trafficking system, pathogenic effector proteins, called toxins, have exploited existing pathways as a mean to access intracellular targets and modulate host cellular functions. Among known targets in the human host, nucleus has been an infrequent, covert, and a coveted target, and very few external factors have been known to reach nucleus. Cytolethal Distending Toxin (CDT), the first known bacterial toxin to reach the mammalian-cell nucleus, presents an excellent model to study the retrograde trafficking of cargo to the nucleus. CDTs comprise a family of intracellular acting bacterial toxins whose actions upon eukaryotic cells cause DNA-damage, resulting in the induction of DNA-damage repair response, thus leading to the modulation of host cell functions. Most CDTs are hetero-tripartite assemblies of CdtA, CdtB, and CdtC, with CdtB required for CDT-mediated cell cycle arrest, and CdtA and CdtC required to deliver the catalytically active moiety inside the cell. Although all CDTs are generally considered to function as genotoxins, the extent of similarity and differences within the members of the CDT-family in their cellular intoxication properties, and the molecular components of host cellular machinery that plays a role in CDT-mediated intoxication, are poorly understood.

In this dissertation I have identified the host factors that play an important role in the trafficking of CDTs to the nucleus. I have also characterized the similarities and divergence in the retrograde trafficking pathway utilized by different members of the CDT family, including the CDT produced by *Aggregatibacter actinomycetemcomitans, Campylobacter jejuni Escherichia coli,* and *Haemophilus ducreyi*. I have addressed the events spanning from cell-surface binding, to the trafficking of CDT through the subcellular compartments of the host cell, as a prerequisite for toxin to reach nucleus to exert its cytotoxic effects.

My findings have enhanced the understanding of CDT intoxication mechanism and its potential role in the virulence properties of CDT-producing pathogens. Moreover, my studies will also aid in the design of novel tools to target specific subcellular compartments and host cell functions. For future studies, it will be interesting to test the premise that the functional differences between CDTs reflect the diversity of host cells, and tissues, that comprise the infection microenvironments targeted by CDT-producing pathogenic bacteria.

ACKNOWLEDGEMENTS

I wish to acknowledge the contribution and support of certain people, without whom my doctoral work would not have been possible.

First and foremost, I want to thank to my mentor, Steve Blanke, with whom I have my longest and most fruitful professional association. Apart from what is expected of a mentor, to help one learn how to conduct scientific research, he also taught me the critical, yet underappreciated aspects enveloping bench-work research – how to plan research, impacting my critical thinking; and how to communicate scientific findings – in journals and scientific meetings, impacting my professional development and contribution to science. Further, I am appreciative of Steve's efforts to help develop my skills by encouraging and enthusiastically supporting me to attend professional meetings and training programs. Finally, I am thankful to Steve for the financial support he provided through research grants, allowing me to finish my work.

I want to thank my research committee members, Brenda Wilson, Richard Tapping, and Gary Olsen, for their guidance and scientific insights through the course of my doctoral program. My special thanks are due to Ken Bradley and his research group at the University of California, Los Angeles, for their scientific collaboration and constructive criticism on my research. I also want to thank John Cronan, Head of Department of Microbiology, for making our program a proud unit to be part of. Thanks to the University of Illinois' School of Molecular Cell Biology for the teaching fellowship, James Beck, and Francis & Harlie Clark for

research fellowships, and National Institute of Health for research grants, providing me with the financial means to complete this project. Thanks to Elizabeth Good and Shawna Naidu for their supervision during my teaching responsibilities.

I am grateful to my colleagues Tamilselvam Batcha, Aria Eshraghi, Bomy Kim, Brandon Banks, Michael Prouty, Ana Medrano, Tommie Lincecum, Eugene Gillespie, Sophia Son, Brendan Powers, Christian McNeely, and Quynh Vu, who have directly impacted, or contributed to my work. I also want to thank my past and current lab-mates: Robin Holland, Michael Reno, D'feau Jia Lieu, Henry Chen, Hyungjung Kim, Ik Jung Kim, Seung Oh, Prashant Jain, Reshma Kulkarni, Vijay Gupta, Carlos Nossa, Hetal Patel, Pia Muyot, and Theresa Cay, for their immense support, and creating a collaborative and fun work-culture.

I am also thankful for the strong administrative support I enjoyed during my program, which allowed me to focus on my scientific quest. I am thankful to Deb Lebaugh, Diane Tsevelekos, and Shawna Smith, administrative staff of the Department of Microbiology, for their friendly yet constant support throughout my graduate program. I thank Gail Scott and Kelly Clem from the Life Sciences Storeroom, Scott Baker from the Machine Shop, Bill Flesher from the Electronics Shop, Dick Overturf from the Grants and Accounts Administration, Dan Ozier and Don Gerard from the Office of Facilities and Operations, Sara Bingaman from the Procurement Department, Barbara Pilas and Ben Montez from the Flow cytometry facility, and Jeff Haas, Karl Schlipf, and Bemi Ekwejunor from the

Office of Information Technology, for seamless provision of infrastructure and facilities enabling me to execute my project.

DEDICATION

This dissertation is dedicated to my family who has always encouraged me to work to the best of my abilities, and make a difference. To my wife Supreet Gargi, for her patience, adjusting with and supporting me through the difficult times, and constantly motivating me to learn, grow, and outperform myself – sometimes being a companion, and sometimes being an example. To my mother and father, Uma and Goralal Gargi, for instilling strong work ethics, and countless sacrifices they made to help me reach where I am today. To my brother, sister-in-law, and nephew - Manjish, Manisha, and Aditya Gargi, for being the source of inspiration and joy in my life. To my father- and mother-in-law, Surinderpal and Amarjit Kahlon, for their immense support, understanding, and encouragement throughout my graduate school. And to all friends and relatives who have motivated, impacted, and inspired me.

TABLE OF CONTENTS

CHAPTER 1: INTRODUCTION

1.1. Host-Pathogen Interactions

Be it quorum sensing, symbioses, or pathogenesis, interactions between biological systems involves interplay of genetic and environmental factors, leading to outcomes that decide the fate of their relationship (Casadevall & Pirofski, 2000). Pathogens adapt their behavior and genetic expression depending on surrounding environment, and express factors that allow their optimal survival (Young, Hussell, & Dougan, 2002). Once inside the hostile environment of a host, pathogens deploy strategies not only to evade host-defense barriers, but also to survive, and modulate host cell functions to establish a successful infection (Lara-Tejero & Galan, 2002; Oswald, Nougayrede, Taieb, & Sugai, 2005). A common way utilized by pathogens for the host cell modulation, is through the expression of virulence factors, called toxins, which may act in the vicinity where they are released to modulate the site where they are present, or diffuse away to find distant targets for a more generalized effect on the host. Virulence factors ultimately create conditions favorable for pathogen survival, and or colonizing of the host. Understanding interactions of virulence factors with host cells not only address the host-pathogen relationship, but it also sheds light on the physiology of the host cell, sometimes learning about the role of biomolecules with previously unknown function (Sandvig et al., 1992; Sandvig & van Deurs, 2005). For instance, our understanding of cell biology, in recent past, has been significantly aided by studying host-pathogen

interactions as tools to identify new host factors, or discover new functions (Johannes & Popoff, 2008). These discoveries have a potential impact on several fields, including but not restricted to, understanding basic cell biology, molecular pathogenesis, developing therapies, and designing novel bioengineering tools (Baillie, 2009; Chaddock, 2013).

1.2. Cytolethal Distending Toxin (CDT)

Pathogenic bacteria have acquired attributes that promote adaptation to the specific and often diverse environments encountered within the host. Successful pathogens often actively alter, or remodel, host cells and tissues in order to create a more suitable niche for colonization, often through the direct action of bacterial protein toxins and effectors (Blanke, 2006). A novel class of bacterial toxins that interfere with the eukaryotic cell cycle, are called cyclomodulins, which includes virulence factors that either stimulate, or inhibit the cell cycle, creating conditions favorable for pathogen survival, and colonization of the host (Nougayrede, Taieb, De Rycke, & Oswald, 2005). The first bacterial toxins known to act in the nucleus of the target cell are Cytolethal Distending Toxins (CDTs), which block the host cell cycle at the transition between the G_2 and M phases by producing direct DNA lesions (Lara-Tejero & Galan, 2000; Whitehouse et al., 1998), acting as inhibitory cyclomodulins. DNA damage produced by CDTs is enough to activate cell cycle checkpoints, triggering cell cycle arrest, and activation of pathways associated with DNA-damage, which potentially allow CDT producing pathogens to modulate the host cell environment

for successful colonization (Comayras et al., 1997; Cortes-Bratti, Karlsson, Lagergard, Thelestam, & Frisan, 2001; Escalas et al., 2000; Sert et al., 1999).

CDTs were discovered approximately 25 years ago as heat labile factors within culture filtrates of enterotoxigenic *Escherichia coli* (Johnson & Lior, 1988b) and *Campylobacter spp*. (Johnson & Lior, 1988a) that induced remarkable distention of mammalian cells. Since their initial discovery, CDTs have been associated with over two dozen Gram-negative pathogenic bacteria (Figure 1.1), which occupy a diverse array of host niches, including the urogenital tract, gastrointestinal tract, and the oral cavity (Guerra, Cortes-Bratti, Guidi, & Frisan, 2011) mostly from the gamma- and epsilon-proteobacter families (Gargi, Reno, & Blanke, 2012) (Figure 1.2). Important Gram-negative pathogens that produce CDT include *Aggregatobacter actinomycetemcomitans* (Aa-CDT), *Campylobacter jejuni* (Cj-CDT), *Escherichia coli* (Ec-CDT), *Haemophilus ducreyi* (Hd-CDT), *Helicobacter hepaticus* (Hh-CDT), and *Shigella dysenteria* (Sd-CDT) (Gargi et al., 2012) (Figure 1.2).

1.2.1. CDT in bacterial pathogenesis

The importance of CDT in the pathogenicity of the Gram-negative pathogen comes from several clinical and human epidemiological studies, where the presence of genes for CDT have been linked with aggressive infections (Guerra, Guidi, & Frisan, 2011; Wising et al., 2005). While CDT from *A. actinomycetemcomitans* is associated with aggressive periodontitis (Tan, Song, & Ong, 2002), the toxin is thought to confer cytotoxicity to chancroid-causing *H.*

ducreyi isolates (Cope et al., 1997). Hd-CDT induced neutralizing antibodies when injected in rabbits, and caused dose-dependent pathologic skin reactions in both naive and immune rabbits, characterized by increased inflammatory responsiveness after each immunization (Wising et al., 2002). The presence of CDT genes was also found to be significantly associated with *E. coli* induced hemolytic uremic syndrome, characterized by haemolysis and renal failure (Bielaszewska et al., 2004). Furthermore, most *C. jejuni* isolates from Danish broiler chickens had CDT activity on Vero cells (Bang et al., 2001). Furthermore, CDTs have been demonstrated to possess immunomodulatory properties, as it is involved not only in the inhibition of mitogen-induced proliferation of T-cells and B-cells (Svensson, Tarkowski, Thelestam, & Lagergard, 2001), but also in the apoptosis of B- and T-cells (J. L. Smith & Bayles, 2006). These findings strongly suggest that CDT is an important virulence factor that contributes towards the pathogenesis of the source bacteria.

1.2.2. CDT expression and secretion

The *cdt* genes are expressed from a polycistronic operon and are well conserved among the toxin producing species (Akifusa, Poole, Lewthwaite, Henderson, & Nair, 2001; Mao & DiRienzo, 2002; Saiki, Konishi, Gomi, Nishihara, & Yoshikawa, 2001). In nearly all CDT-producing bacteria, CdtA, CdtB and CdtC subunits are encoded by slightly overlapping *cdtA, cdtB* and *cdtC* genes which together form a constitutively expressed operon on the chromosome (Figure 1.1). Amongst CDT producing bacteria, *E. coli* is unique as

this single species has at least five divergent variants of CdtB, which are also differentially segregated per *E. coli* pathotypes (Janka et al., 2003). Information concerning the molecular mechanism of bacterial synthesis and secretion of CDT is limited (Deng, Latimer, Lewis, & Hansen, 2001; Ueno et al., 2006), but it's thought that processed toxin subunits assemble in the periplasm of the bacterium. Valuable insights into the mechanism by which CDT holotoxin might be synthesized and assembled in the bacterium came from a study by Ueno and co-workers (Ueno et al., 2006). Each of the three subunits were translated with an N-terminal leader sequence that allows the proteins to cross the cytoplasmic membrane of the bacterium. Ueno hypothesized that CdtB and CdtC precursors are transported across the membrane via a sec-dependent pathway coordinated with cleavage of the leader sequences by signal peptidase I. This results in accumulation of the mature proteins in the periplasmic space. Precursor CdtA protein is processed by signal peptidase II and modified with a glycerolipid. The modified hydrophobic CdtA is inserted into the periplasmic space side of the outer membrane, via a lipid-binding consensus sequence (lipobox), where it forms a complex with the mature forms of CdtB and CdtC. The precursor holotoxin is further processed by an unidentified protease, that removes the N-terminus along with the glycerolipid. This cleavage step allows the now hydrophilic holotoxin to exit the bacterium. The cleavage of CdtA is supported by another study conducted on *H. ducreyi*, in which both 23- and 17-kDa CdtA peptides were found in *H. ducreyi* extracts. Similar results were reported for the Aa-Cdt (Frisk et al., 2001; Shenker et al., 2004).

1.2.3. Structure and activity of CDT holotoxin and subunits

CDT holotoxin is a heterotrimeric complex comprised of three proteins: CdtA, CdtB and CdtC, with corresponding molecular masses ranging between 23–30, 28–29 and 19–21 kDa, respectively, depending on the bacterial host species (Haghjoo & Galan, 2004; Hu, Nesic, & Stebbins, 2006) (Figure 1.4). The crystal structure of CDT from *H. ducreyi* (Hd-CDT) and *A. actinomycetemcomitans* (Aa-CDT) revealed that three subunits interact extensively with each other to make a stable tripartite complex (Nesic, Hsu, & Stebbins, 2004; Yamada, Komoto, Saiki, Konishi, & Takusagawa, 2006), and all three subunits are required to confer full activity to the holotoxin (Cao, Volgina, Huang, Korostoff, & DiRienzo, 2005; Lara-Tejero & Galan, 2001; Nesic et al., 2004; Nesic & Stebbins, 2005; Saiki, Gomi, & Konishi, 2004; Saiki et al., 2001; Shenker et al., 2004; Wising et al., 2002).

Similar to several other intracellular acting bacterial protein toxins, CDT is believed to possess a two-component A-B toxin's functional architecture. While B-component facilitates toxin binding and uptake into sensitive host cells, A-component, carrying the catalytic activity of the toxin, acts upon specific intracellular targets in a manner that will alter normal cellular function. Sharing structural homology with the B-chain repeats of the plant toxin ricin, CdtA and CdtC together are believed to comprise the B-component of CDT (Hu & Stebbins, 2006; Lara-Tejero & Galan, 2001; Nesic & Stebbins, 2005). Both these subunits present non-globular amino acid extensions at the amino- and carboxyl-termini, which interact with each other and with the CdtB subunit.

An interesting exception to the CdtA/CdtB/CdtC tripartite structure characteristic of the CDT superfamily was discovered within *S. enterica*, serovar Typhi CDT (St-CDT) (Haghjoo & Galan, 2004), for which the gene encoding CdtB is not associated with genes resembling cdtA or cdtC. Instead, the cellular modulatory activity of St-CDT is dependent upon expression of two genes, *pltB* (pertussis-like toxin B) and *pltA* (pertussis-like toxin A) (Figure 1.1), which encode proteins resembling the B components of pertussis toxin, an unrelated AB5-intracellular acting toxin. The reconstituted CdtB/PltA/PltB tripartite complex was demonstrated to induce DNA damage within intoxicated eukaryotic cells (Spano, Ugalde, & Galan, 2008). Infection studies revealed that bacterial uptake into host cells triggers expression of cdtB/pltA/pltB, and that the PltB and PltA subunits are required for transport of intracellular St-CDT to the extracellular medium, where St-CDT then acts upon uninfected host cells in a paracrine manner (Spano et al., 2008). Such a mechanism has not been previously described for any AB-toxin, and suggests an expanded role beyond the canonical functions normally associated with the B components of intracellular-acting toxins.

The CdtB subunit is the most conserved component of the holotoxin amongst all the CDT-producing bacteria (Hu et al., 2006). Adopting the canonical four-layered fold of the DNase I family, CdtB comprises the catalytically active A-component of the holotoxin (Nesic et al., 2004). CDT was first demonstrated as a genotoxin when homology between the CdtB subunit from Ec-CDT, and Cj-CDT, was identified with the mammalian DNase I (Elwell & Dreyfus, 2000; Lara-Tejero

& Galan, 2000) (Figure 1.5). The crystal structure confirms previous data, demonstrating that CdtB shares five conserved residues with the active site of the mammalian DNase I, and possesses DNase-I like activity *in vitro* or when introduced in the mammalian cells by microinjection, or ectopic expression (McSweeney & Dreyfus, 2004). CdtB was shown to completely degrade an *in vitro* DNA plasmid substrate, and ectopic expression of CdtB was shown to induce nuclear fragmentation and a marked chromatin disruption in HeLa cells . Mutations of the conserved residues required for catalysis or for Mg^{2+} binding abolished the ability of CdtB to cleave DNA *in vitro* or to induce DNA damage responses *in vivo* (Elwell & Dreyfus, 2000; Guerra et al., 2005; Lara-Tejero & Galan, 2000).

1.2.4. Cell surface binding

While the cell surface binding of CDTs is still not fully characterized, several groups have made attempts at mapping the residues on CDTs important for host cell binding, and also studying the chemical nature of CDT-receptor. So far, conflicting views have emerged on the chemical nature of putative CDT-receptor, which might be dependent on the cell line and species-specific CDT used in the study. In one study, Cao and co-workers used a modified enzyme-linked immunosorbent assay (ELISA), with thyroglobulin-coated plastic plates to study the binding kinetics of wild-type and mutated Aa-CdtA and Aa-CdtC subunits (Cao et al., 2005). In this study, Aa-CdtA alone was able to bind specifically to thyroglobulin with saturation kinetics. In contrast, Aa-CdtC

demonstrated much lower ligand to receptor binding ratio. However, a study by our collaborators was not able to confirm role of N-linked glycans and glycolipids in the toxin binding (Eshraghi et al., 2010). Another study reported that binding of Ec-CdtA and CdtC to HeLa cells was blocked with N-linked fucose-containing glycoproteins, suggesting fucose might be an important part of receptor at least for Ec-CDT (McSweeney & Dreyfus, 2005). Recent reports have suggested the biochemical nature of the putative CDT receptor, with plasma membrane cholesterol, cell surface glycoproteins, and glycosphingolipids playing a major role in aiding cell surface binding of different CDTs (Eshraghi et al., 2010; Lin et al., 2011). While testing the ability of cholesterol supplementation to increase host cell sensitivity, it was found that increasing plasma cholesterol resulted in increased sensitivity to some CDTs, but not to Cj-CDT (Eshraghi et al., 2010), which suggested that cholesterol might be an important component for binding of most CDTs, but Cj-CDT. Contrarily, another group later showed that cholesterol depletion results in resistance to Cj-CDT (Lin et al., 2011). These results, and further studies that identified a cholesterol recognition amino acid consensus (CRAC) sequence in Aa-CdtC and a non-traditional CRAC sequence in CdtC from *Haemophilus parasuis* suggests that cholesterol may play a role in the binding of most, if not all, CDTs to the host cell surface (Boesze-Battaglia et al., 2009; Zhou, Zhang, Zhao, & Jin, 2012). A genetic screen revealed a putative G protein–coupled receptor, TMEM181, contributes to cellular binding and sensitivity to Ec-CDT (Carette et al., 2009), thus proposing TMEM181 as the potential CDT-receptor. Later studies questioned the presence of TMEM181 on

the cell surface, refuting its claim as a toxin-receptor. Further studies will be required to fully characterize the CDT-receptor, but so far we do know that the receptor is rich in cholesterol and might involve the lipid rafts.

In contrast to the studies involving CDT-receptor, studies that have characterized the importance of molecular determinants on CDTs, are much less conflicting. So far there is a general consensus that CdtA plays a major role as the B-moiety of the holotoxin, while CdtC playing a relatively minor or supportive role (Cao et al., 2005; Gargi et al., 2012). A large aromatic cluster of eight bulky side-chains in CdtA is conserved throughout CDT family, and is believed to be important for the toxin engagement with the host cell surface (Cao, Bandelac, Volgina, Korostoff, & DiRienzo, 2008; Nesic et al., 2004; Yamada et al., 2006). Mutations of the aromatic patch of Hd-CdtA do not change the stability of the ternary complex, but completely abolished the ability of the toxin to cause cell cycle arrest in HeLa cells, suggesting that it plays an indispensible role in toxin binding to its receptor (Nesic et al., 2004). Binding studies employing the thyroglobulin assay to examine the effect of single amino acid substitutions in CdtA supported the idea that surface-exposed heterocyclic amino acids in the aromatic patch region of CdtA might be essential for holotoxin binding to the cell surface (Cao et al., 2008). Another study later identified a tryptophan residue (W115) outside of the aromatic patch that is required for receptor binding, suggesting the binding domain on CdtA may not be restricted to just one aromatic patch (Li et al., 2013). Other aromatic and heterocyclic residues present on the surface of CDT are yet to be mapped and defined.

Another peculiar topological feature of CDT is a deep groove formed by the juxtaposition of CdtA and CdtC subunits, which is also thought to be required for binding to host cell receptor (Hu & Stebbins, 2006; Nesic et al., 2004). CDT contains putative cholesterol recognition/interaction amino acid consensus (CRAC) domain, which aids in the binding of CdtA/CdtC to cholesterol, a major component in lipid rafts, on mammalian cells (Boesze-Battaglia et al., 2009; Lai et al., 2013; Zhou et al., 2012) (Figure 1.3). Mutation in CRAC domain of CdtC resulted in decreased cell binding (Boesze-Battaglia et al., 2009; Lai et al., 2013), leading to reduced capacity for intracellular transfer of the active toxin subunit, CdtB (Boesze-Battaglia et al., 2009), and decreased cell toxicity (Boesze-Battaglia et al., 2009; Zhou et al., 2012).

1.2.5. CDT and cell cycle arrest

The CDT-induced cell cycle arrest resembles the checkpoint response to ionizing radiation (IR), characterized by activation of the ATM kinase and ATM-dependent induction of the tumor suppressor p53 and its transcriptional target, the cyclin-dependent kinase inhibitor p21, phosphorylation of histone H2AX, and re-localization of the DNA repair proteins, such as MRE11 and RAD50, to the sites of DNA double-strand breaks (Hassane, Lee, & Pickett, 2003; Sato et al., 2002; Yamamoto et al., 2004). Direct demonstration of CDT-induced DNA fragmentation was shown using pulsed field gel electrophoresis (PFGE) analysis both in mammalian cells intoxicated with Hd-CDT, and in budding yeast carrying a conditional Cj-CdtB expressing plasmid (Frisan, Cortes-Bratti, Chaves-Olarte,

Stenerlow, & Thelestam, 2003; Hassane, Lee, Mendenhall, & Pickett, 2001). Prolonged exposure to DNA damage chronically activates the DNA damage response machinery, including the ATM-Chk2-p53 axis, resulting in either cell death or a long-term cell cycle arrest state known as cellular senescence (J. Smith, Tho, Xu, & Gillespie, 2010), potentially giving an advantage to pathogens to establish successful infection, especially in the conditions where the fast turnover rate of cells might present a barrier for pathogens (Abuoun et al., 2005; Biswas et al., 2006).

Cell cycle arrest induced by CDTs leads to downstream events like apoptosis, or if the exposure is sub-lethal and prolonged, to genomic destabilization of the affected host cells (Bezine, Vignard, & Mirey, 2014; Gargi et al., 2012; Guerra, Guidi, et al., 2011). Because the DNA content of a cell is easy to quantify, cell cycle arrest has been widely used as a standard measure of the toxin activity. In this study, we have extensively used the quantification of cellular DNA to evaluate the sensitivity of mammalian cells against CDTs, and also to compare the biological activity of CDTs produced by different Gram-negative pathogens, or the point mutations to study the structural and functional implications on the toxin activity (Gargi et al., 2013; Lara-Tejero & Galan, 2001; Nesic et al., 2004; Peres et al., 1997; Whitehouse et al., 1998). To measure the cell cycle progression in intoxicated cells, we determined $CCAD_{50}$ (i.e. cell cycle arrest $dose_{50}$) values, which we defined as the toxin concentrations required to induce G_2/M arrest in 50% of the cell population not already in G_2/M (Gargi et al., 2013).

1.2.6. CDT as a phosphatase

There is not universal agreement that the cellular effects associated with CDT intoxication are due to the DNA degrading activity of the CdtB subunit. Indeed, sequence homology of CdtBs with members of a broad metalloenzyme superfamily led to the proposal that CdtB induces cell cycle arrest as a phosphatase rather than a DNase (Dlakic, 2001). Support for this hypothesis emerged from studies reporting that *in vitro*, Aa-CdtB demonstrates phosphatidylinositol-3,4,5-triphosphate (PIP3) phosphatase activity (Shenker et al., 2007). Mutant proteins with altered residues known to be important for phosphatase activity ablated the *in vitro* activity of Aa-CdtB, as well as the capacity of Aa-CDT to induce G_2/M arrest in human lymphocytes. The fact that CdtB is a member of the large metalloenzyme superfamily led to the proposal that the toxin acted upon susceptible cells or cell lines by dephosphorylation of the Wee1 kinase or Cdc25 phosphatase (Dlakic, 2001). These two enzymes are important for regulating the phosphorylation of tyrosine residues in Cdc2 kinase. An increase in Cdc2 phosphorylation leads to cell cycle arrest. This rationale led to the hypothesis that the primary mode of action of CdtB might be that of a phosphatase, rather than a nuclease. Additional support for the phosphatase mode of action came from studies showing that Aa-CdtB behaved as a Phosphatase and tensin homolog (PTEN) in lymphoid cell lines, which is a hydrolase that removes a phosphate group from PIP3 found in the plasma membrane of cells (Shenker et al., 2007). PIP3 activates downstream signaling components such as the protein kinase Akt, an activator of anabolic signaling

pathways necessary for cell growth. It was proposed that the action of the Cdt in lymphocytes causes a depletion of PIP3, which in turn inactivates the Akt pathway leading to cell cycle arrest and apoptosis. Examination of the PTEN activity of Aa-CDT was further extended to include human macrophages (Shenker, Walker, Zekavat, Dlakic, & Boesze-Battaglia, 2014). Unlike lymphocytes, macrophages did not undergo CDT-mediated apoptosis.

To date, phosphatase activity has not been reported for any CDT other than Aa-CDT. Several studies have reported data suggesting that at least some of the cellular consequences of Aa-CDT cellular intoxication are not likely due to phosphatase activity of Aa-CdtB. Ectopic expression of Aa-CdtB in *Saccharomyces cerevisiae* induced DNA damage and S/G_2 cell cycle arrest, although yeast does not possess the substrate for the reported Aa-CdtB phosphatidylinositol-3,4,5-triphosphate phosphatase activity (Matangkasombut et al., 2010). Moreover, Aa-CDT mediated apoptosis in proliferating U937 monocytes was demonstrated to depend solely on the DNase activity of the Aa-CdtB subunit (Rabin, Flitton, & Demuth, 2009). The phosphatidylinositol-3,4,5-triphosphate phosphatase activity is not likely to be idiosyncratic for Aa-CdtB, as this subunit shares a nearly identical sequence to that of the CdtB subunit from *H. ducreyi* (Hd-CdtB), but further studies will be required to establish the ubiquity of phosphatase activity across all members of CDT family, and its importance in the virulence properties of the toxin.

1.2.7. CDT and apoptosis

Depending on the cell type, eukaryotic cells exposed to CDTs have been shown to arrest in the G_1 and/or G_2 phases of the cell cycle, or undergo apoptosis (Comayras et al., 1997; Cortes-Bratti et al., 2001; Sert et al., 1999; Shenker et al., 1999). In general, CDT intoxication of cells of non-haematopoietic origin results in cell cycle arrest preceding apoptosis (Jinadasa, Bloom, Weiss, & Duhamel, 2011). In contrast, CDT intoxication of haematopoietic cells results in rapid apoptosis, indicating differential cellular responses to the action of CDTs (Ohara, Oswald, & Sugai, 2004; Shenker, Demuth, & Zekavat, 2006; Shenker et al., 2001). While CDT-intoxicated cells have been demonstrated to undergo apoptosis, there are reports that in some cases, CDTs also trigger cell survival pathways (Frisan et al., 2003). The survival of CDT intoxicated cells is dependent on the activation of the small GTPase RhoA (Frisan et al., 2003), which induces actin stress fiber formation, and prevents cell death via activation of the mitogen-activated protein kinase p38 and its downstream target mitogen-activated protein kinase-activated protein kinase 2 (Guerra et al., 2008). The activation of RhoA is dependent on the dephosphorylation of the RhoA-specific guanine nucleotide exchange factor Net1, and it appears to be part of the DNA damage repair responses because it requires a functional ATM (Guerra et al., 2008). CDT intoxicated Jurkat T cells displayed increased caspase-2 and -7 activity and increased cell surface presentation of phosphatidylserine (Ohara et al., 2004). Shenker and group suggested that DNA fragmentation occurred via the apoptotic cascade and not directly due to DNA damage induced by CDT (Shenker et al.,

2006). This report hypothesized that the CdtB phosphatase activity leads to induction of apoptosis and subsequent activation of endogenous nucleases, which result in DNA fragmentation. In this study, two inhibitors of apoptosis, overexpression of Bcl-2 and the caspase-3 inhibitor zvad, blocked apoptosis, DNA fragmentation as judged by the TUNEL assay and histone H2AX phosphorylation, but had no effect on G_2 arrest (Shenker et al., 2006). Taken together, these data suggest that CDT may cause apoptosis in monocytes and T cells to limit the host immune response to the CDT-producing bacteria.

1.2.8. CDT and carcinogenesis

Several studies have begun to address whether infection with CDT-producing pathogenic bacteria may induce changes in the host associated with an early neoplastic process. Using NF-κB-deficient mice to study persistent *C. jejuni* infection, one study indicated a proinflammatory role for Cj-CDT *in vivo*, as toxin producing strains were associated with significantly enhanced severity of gastritis and significantly higher occurrence of gastric hyperplasia and dysplasia, which are markers of an early neoplastic process (Fox et al., 2004). For *Helicobacter hepaticus*, which causes chronic hepatitis and typhlocolitis in some mice, CDT was demonstrated to be critical for persistent infection of Swiss Webster mice, which is characterized with severe inflammation (Ge et al., 2005). In another study, *H. hepaticus* infection of A/JCr mice demonstrated a significantly higher inflammatory response in strains producing Hh-CDT than isogenic mutant strains (Ge et al., 2007). The presence of CDT was associated

with a progression of inflammation to dysplasia. CDT activation of survival responses in cells harboring DNA damage could contribute to the accumulation of genetic instability within the developing inflammatory microenvironment, which may constitute the conditions for promoting the transformation of pre-neoplastic cells to malignant cells in the host.

1.3. Retrograde Trafficking and Molecular Pathogenesis

Following receptor engagement on the plasma membrane, endocytosis and endosomal protein sorting are critical events for diverse cellular functions such as signaling, nutrient uptake, and development. Of these processes, the mechanisms underlying clathrin-dependent and -independent internalization (Conner & Schmid, 2003; Kirkham & Parton, 2005; Mayor & Pagano, 2007), receptor recycling to the plasma membrane (Maxfield & McGraw, 2004), and membrane trafficking to compartments of the late endocytic pathway (Gruenberg & Stenmark, 2004) have been studied in some detail. In contrast, much less is known about endosomal trafficking to the biosynthetic/secretory compartments, which is known as retrograde transport. Exit from endosomal compartments is termed retrograde sorting and occurs in different parts of the endocytic pathway. Retrograde sorting acts on cargo molecules targeted to endosomes from the Golgi apparatus or the plasma membrane. These cargo proteins or lipids are then transported to the trans-Golgi network (TGN), Golgi membranes, or, in some cases, the endoplasmic reticulum (ER) via the retrograde route (Bonifacino & Rojas, 2006; Sandvig & van Deurs, 2005). Virulence factors also rely on these

transport routes to enter host cell and access its intracellular target. Thus, structural and mechanistic studies on pathogen products and cellular factors have led to the first molecular models for trafficking between endosomes and the TGN. Distinct features of trafficking by the retrograde route have expanded our understanding of cell biology, and provided new therapeutic strategies in immunotherapy and drug delivery.

1.3.1. Receptor engagement and endocytosis

The presence or absence of receptors on the plasma membrane surface often dictates the sensitivity or resistance, respectively, of host cells to specific intracellular-acting bacterial toxins (Blanke, 2006). Using ligand blotting assays, very early studies reported the binding of partially purified Cj-CDT to two peptides with approximate molecular masses of 45 and 59 kDa from HeLa cell membrane preparations and 59 kDa from CHO cell membrane preparations (Bag, Ramamurthy, & Nair, 1993), suggesting the presence of molecular components on the surface of host cells that might function as CDT receptors.

To date, bonafide CDT receptors have not yet been identified. One study implicated fucose as an important determinant for Ec-CDT, as lectins targeting fucose moieties inhibited toxin interactions with cells to a greater extent than lectins targeting alternative glycans (McSweeney & Dreyfus, 2005). Another study indicated that the Aa-CDT holotoxin binds to surface glycosphingolipids, and that inhibitors of glycosphingolipid synthesis can prevent intoxication of the human monocytic U937 cell line (Mise et al., 2005). Mutagenesis of a human cell

line haploid for most chromosomes identified cell lines deficient in the membrane-expressed protein TMEM181 that were resistant to Ec-CDT, although it is not yet clear that TMEM181 functions as a cell surface receptor for this toxin (Carette et al., 2009).

A recent study in which Aa-CDT, Cj-CDT, Ec-CDT, and Hd-CDT were compared in a head to head fashion revealed considerable differences in the potencies of these toxins, as well as the target cell requirements important for intoxication (Eshraghi et al., 2010). For example, cholesterol was found to be important for the cellular activities of Aa-CDT, Cj-CDT, and Hd-CDT, but not for those of Cj-CDT. Using mutant CHO cell lines lacking N-linked complex- or hybrid-carbohydrates, glycosphingolipids, or fucose, the study also reported the unexpected finding that N- and O-glycan, or fucosylated structures are in fact not required for mediating toxin binding (Eshraghi et al., 2010). The diversity of cell surface determinants important for CDT interactions identified in these early studies suggest that individual CDTs may each bind to a different receptor. It is attractive to speculate that CDT receptor diversity reflects the tissue tropism of individual CDT-producing pathogens. Following engagement with the host cell surface, CDTs are taken up in the endolysosomal compartments before being targeted retrogradely towards the nucleus. Information on the cellular uptake is limited, but the experiments studying Hd-CDT suggest that the toxin enters cells by a dynamin-dependent endocytosis that may be clathrin-dependent or independent (Cortes-Bratti, Chaves-Olarte, Lagergard, & Thelestam, 2000).

1.3.2. Retrograde trafficking of CDT

In order to reach the nucleus, CDT exploits the retrograde trafficking pathway of the host cell (Figure 1.3). As an intracellular-acting genotoxins, CDT has several fundamental problems to solve in order to exert their modulatory activities, with the most glaring being how to transport soluble CdtB moieties from the cell surface to the nucleus. There are some recent indications that host cell requirements for the genotoxic activity of CDTs from different species may be divergent, raising the possibility that not all CdtB moieties travel from the cell surface to the nucleus along a single transport pathway (Gargi et al., 2013). Biochemical and fluorescence imaging studies suggest that CDTs are transported in a retrograde manner from the endolysosomal system to the ER via the Golgi complex (Guerra et al., 2005). Analogous to several other toxins, including Cholera- and Shiga-toxins, the catalytically active subunit (CdtB) is believed to escape degradation within the endocytic trafficking pathway, and later, translocated from the ER to the cytosol by exploiting the ER degradation pathway, which normally translocates misfolded proteins to the cytosol via protein translocons within the ER membrane (Blanke, 2006; Eshraghi et al., 2014). One study reported that Hd-CdtB was not detected within the cytosol of intoxicated cells (Guerra et al., 2009). In fact, to date, there is no experimental evidence that any CDT subunit is translocated from the ER to the cytosol of intoxicated cells, leading to the suggestion that the CdtB subunits may be translocated directly from the ER to the nucleus (Guerra et al., 2009). On the contrary, given the possibility of potentially transient nature of CdtB in the cytosol,

detection parameters used, studies supporting the importance of ERAD pathway for translocation of CdtB from ER lumen to the cytosol (Eshraghi et al., 2014), and idea that CdtB proteins carry a nuclear localization signal, hint that CdtB might transition through the cytosol before reaching the nucleus (McSweeney & Dreyfus, 2004; Nishikubo et al., 2003). More studies are required to address this query.

1.4. Gaps in Knowledge

CDT is the only known bacterial toxin that reaches the nucleus of the host cell to cause DNA damage. Although the role of toxin in producing DNA damage and triggering downstream pathways is well known, mechanistic details of how the toxin is transported to its target are still poorly understood. Limited studies have tried to address the cell surface engagement (Bag et al., 1993; Boesze-Battaglia et al., 2006; Cao et al., 2008; Eshraghi et al., 2010; Mise et al., 2005), followed by uptake of toxin into the cell (Cortes-Bratti et al., 2000; Guerra et al., 2005), and involvement of specific organelles (Eshraghi et al., 2014; Guerra et al., 2005) in the trafficking of the toxin, but the details of the subcellular compartments and the host factors essential for CDT trafficking within the mammalian cells are largely unknown. Clearly, a major gap in the mechanism underlying CDT-mediated cellular intoxication is how CdtB reaches its site of action. The putative nuclear localization signals identified for two members of the CDT family, Aa-CDT and Ec-CDT, are highly divergent, suggesting that the mechanisms by which these two toxins are transported to the nucleus may not

be identical (McSweeney & Dreyfus, 2004; Nishikubo et al., 2003). Moreover, findings from our research group also indicate that CDTs from different pathogens might follow different paths to reach nucleus (Eshraghi et al., 2010; Gargi et al., 2013).

1.5. Significance of This Study

The objective of this study is to address the mechanistic details of intoxication process of CDTs in general, and identifying the similarities and differences between holotoxins that are similar or distant in their sequence and structural homology. Another major objective of this work is to identify the host cell factors that are involved in the transportation process of CDTs, as an important step for the toxin to reach its target and elaborate its biological activity.

In this study, we directly compared the cellular intoxication mechanisms employed by CDTs produced by *C. jejuni*, *E. coli*, and *H. ducreyi*, three pathogens that colonize similar, or highly divergent host niches (i.e. the intestinal and urogenital tracts, respectively). Amongst CDT family, holotoxin from these three pathogens share relatively low sequence identity in their CdtA and CdtC subunits, suggesting the possibility that these toxins might interact with host cells in fundamentally different ways. Our studies revealed differences in the cellular requirements for toxin intracellular trafficking. Overall, these studies suggest that CDTs from different pathogens are transported within cells by distinct pathways, potentially relevant to their colonization niche within the host.

Our study also addresses the host factors that facilitate CDT transportation to its target. We demonstrate the importance of an intact and functional Golgi apparatus for CDT activity, and localization of active subunit of Cj-CDT to the nucleus. We demonstrate the time dependent and transient localization of Cj-CdtB with the Golgi apparatus, and evidence supporting that Cj-CdtB utilizes the cellular machinery from the late-endosomal compartments to the Golgi apparatus. We show that Cj-CDT trafficking and intoxication properties are independent of early endosome to the Golgi apparatus transition, but are sensitive to the endosomal maturation, and the toxin is predominantly trafficked out of vesicles marked by STX10, and rab9, both indicators of transition through the late endosomal compartments, before reaching the Golgi apparatus. Blocking the Golgi apparatus sorting function by small molecule inhibitors abrogated downstream trafficking and activity of the toxin. Moreover, when the Golgi apparatus block was removed, the toxin already present in the cell proceeded to the nucleus, and caused cell cycle arrest, suggesting that Golgi apparatus is a bottleneck in the CDT intoxication of host cells. We also addressed the importance of Golgi-membrane resident protein, COG complex, in the trafficking and activity of CDTs. Barring limited work done on SubAB and Shiga toxin, role of COG complex on the trafficking of proteins remained largely underexplored (R. D. Smith et al., 2009; Willett et al., 2013). In this study we applied novel strategies to identify components of molecular machinery involved in the transition of CDTs from the endolysosomal system to the Golgi apparatus.

Together, our findings suggest an important role of the Golgi apparatus in both function and trafficking of Cj-CdtB to the ER, and ultimately to the nucleus, and identifies specific host cell determinants required for the intracellular transportation, and biological activity of CDTs.

1.6. Figures

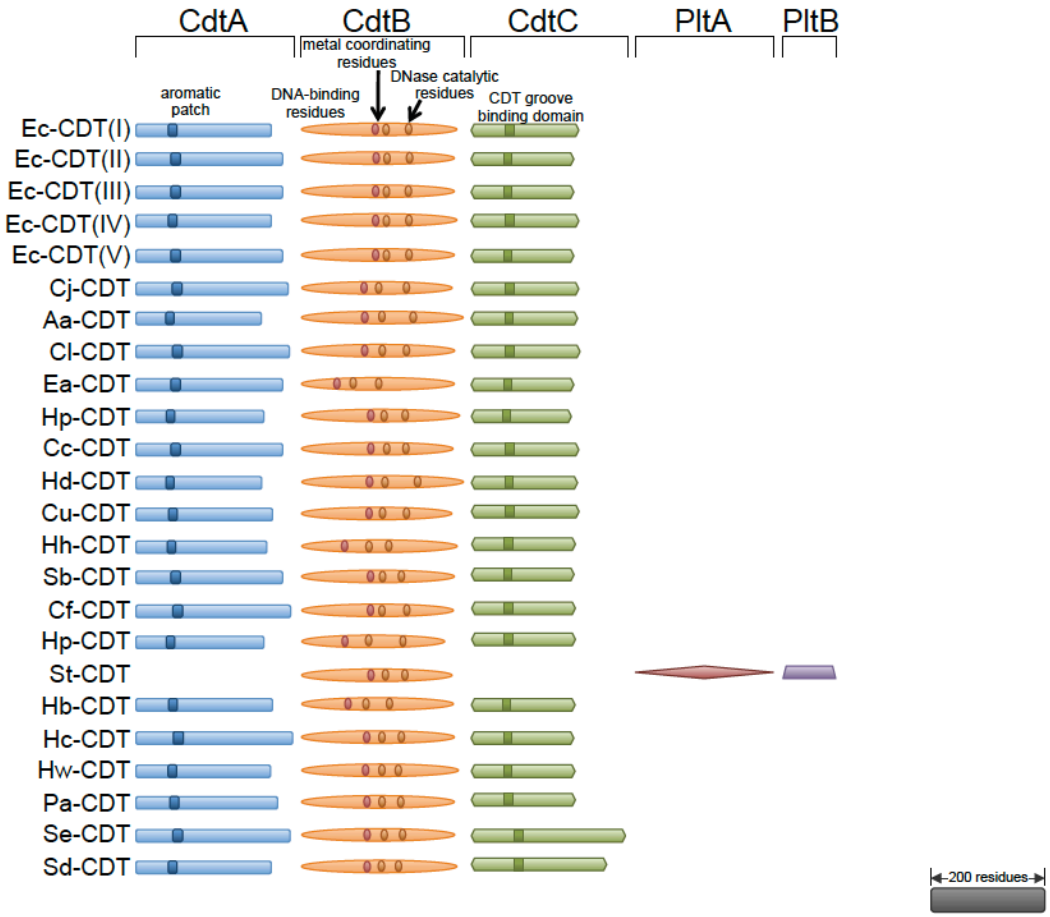

Figure 1.1. Three independent proteins are required to make CDT holotoxin. Most of the known CDTs are composed of CdtA, CdtB, and CdtC, with some exceptions like *S. typhi* where PltA and PltB make holotoxin with CdtB. All CdtAs contain an aromatic patch, demonstrated to be important in binding to the surface of mammalian cells. CdtBs are most conserved amongst three proteins, and are the catalytic subunit of the toxin carrying conserved metal coordinating residues, DNase catalytic residues, and residues homologous to DNA contacting residues of DNase I. CdtCs contain conserved residues believed to be important in formation of a cell-surface binding groove. The scale bar represents primary sequence length equivalent to 200 residues. CDT, Cytolethal Distending Toxin; Plt, Pertussis like toxin. Individual genuses and species are abbreviated as follows: *Escherichia coli* (Ec), *Campylobacter jejuni* (Cj), *Aggregatobacter actinomycetemcomitans* (Aa), *Campylobacter lari* (Cl), *Escherichia albertii* (Ea), *Haemophilus parasuis* (Hp), *Campylobacter coli* (Cc), *Haemophilus ducreyi* (Hd), *Campylobacter upsaliensis* (Cu), *Helicobacter hepaticus* (Hh), *Shigella boydii* (Sb), *Campylobacter fetus* (Cf), *Helicobacter pullorum* (Hp), *Salmonella typhi* (St), *Helicobacter bilis* (Hb), *Helicobacter cinaedi* (Hc), *Helicobacter winghamensis* (Hw), *Providencia alcalifaciens* (Pa), *Salmonella enterica* (Se), *Shigella dysenteriae* (Sd).

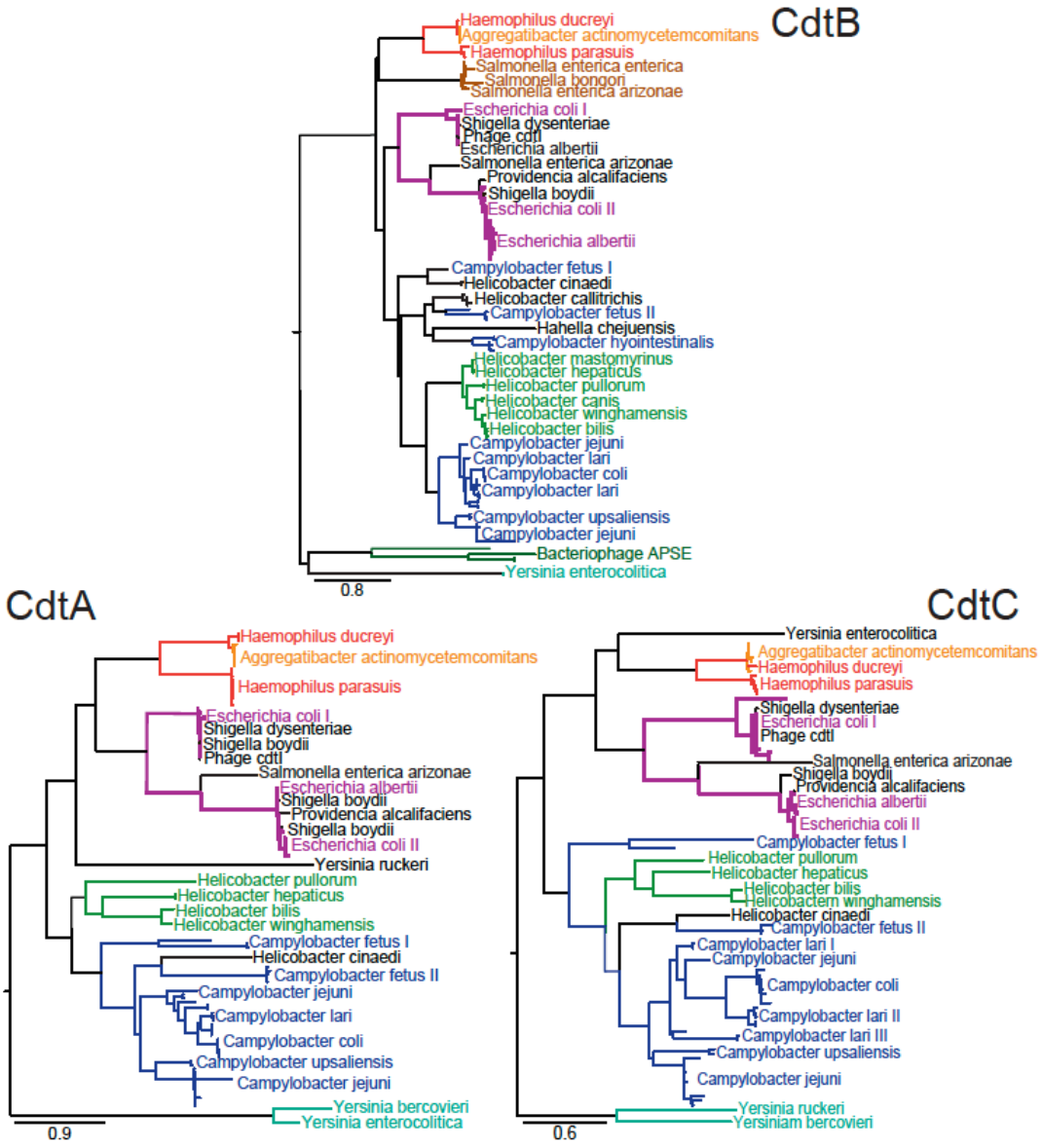

Figure 1.2. Amino acid maximum likelihood phylogenies of the three subunits of CDT. Sequences were extracted from the NCBI non-redundant protein database using BLAST with the criteria that sequences have at least 30% identity and 50% coverage against a known set of CDT subunit sequences from *H. ducreyi, A. actinomycetemcomitans, E. coli, E. albertii, S. dysenteriae, S. enterica, C. jejuni, and H. bilus*. Sequences below these threshold cut-offs were too divergent to be reliably aligned for phylogenetic analyses. Multiple identical sequences from the same species were reduced to unique representatives. The sequences were aligned using a combination of MAFFT and MUSCLE. Phylogenies were inferred using PhyML according to the LG substitution matrix. Clades are colored according to the dominant genus with likely horizontal gene transfer candidates in black. Clades dominated by sequences from a single species are labeled once and distinct clades of sequences from the same species are numbered.

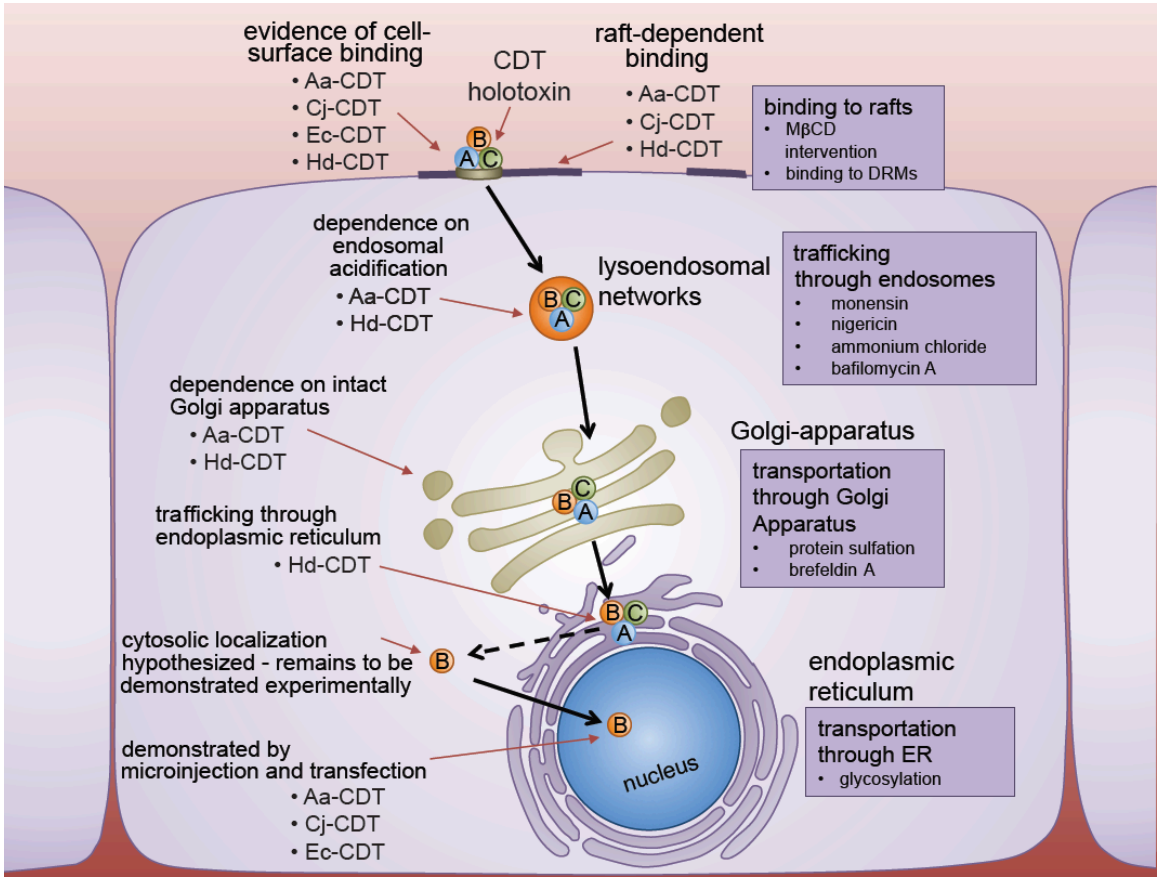

Figure 1.3. Host cell-surface binding and internalization of CDT. CDT binds to a cell surface determinant, and in some cases, is affected by perturbations in lipid rafts. Following internalization by clathrin-coated pits to the endosomes, CDT is trafficked in a retrograde fashion to the Golgi-apparatus, and the endoplasmic reticulum (ER). From the ER, CdtB localizes to the nucleus by a yet unconfirmed route directly, or through the cytoplasm. Experimental techniques used to identify the pathway employed by CDT to trafficking inside the cell, are represented next to the organelles involved.

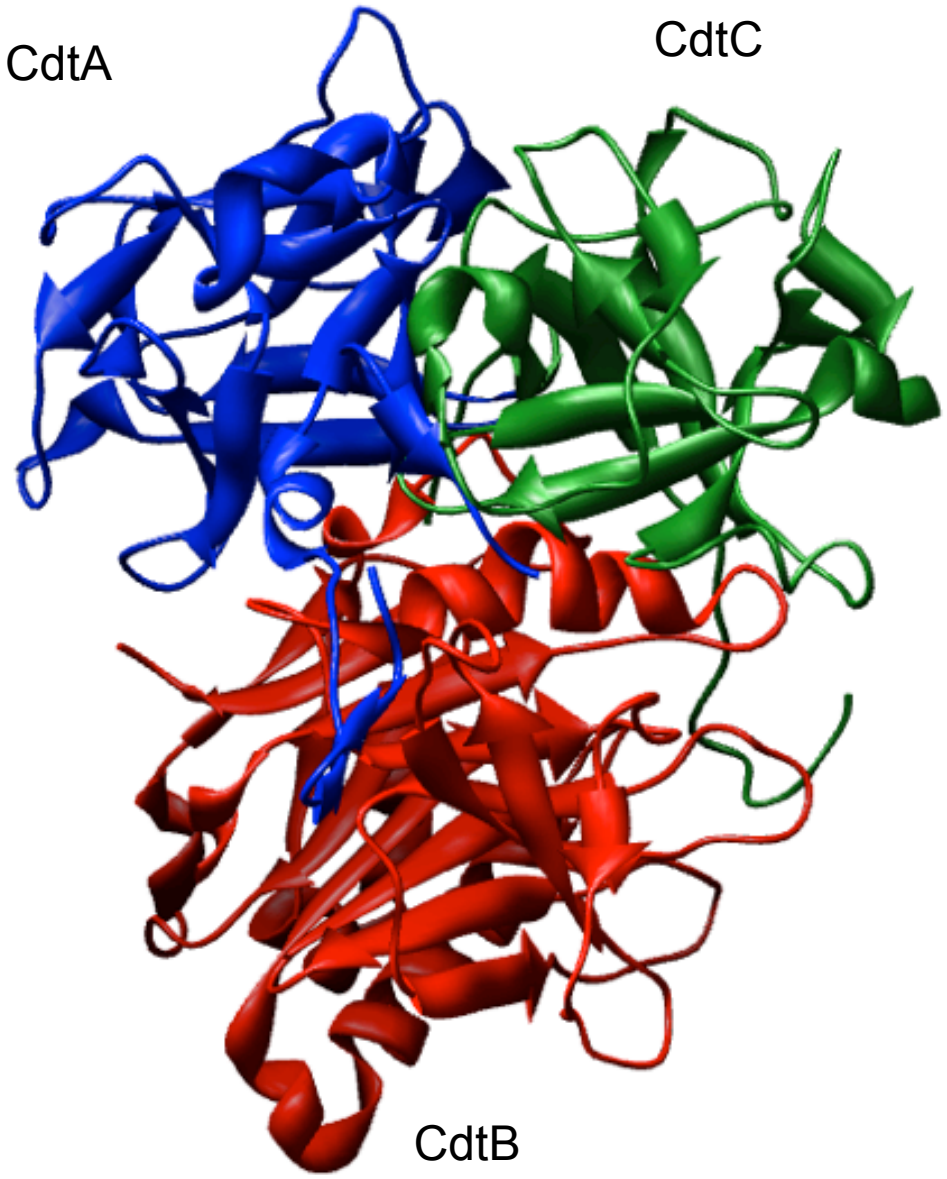

Figure 1.4. Crystal structure of Hd-CDT. CDT is a ternary complex comprised of three proteins: CdtA (modeled in blue), CdtB (red), and CdtC (green). CdtA and CdtC possess amino and carboxy termini that project as non-globular polypeptides and interact extensively with each other and with CdtB. Ribbon cartoon of Hd-CDT was constructed using Chimera (Pettersen et al., 2004), fetching PDB model 1SR4 for Hd-CDT (Nesic et al., 2004).

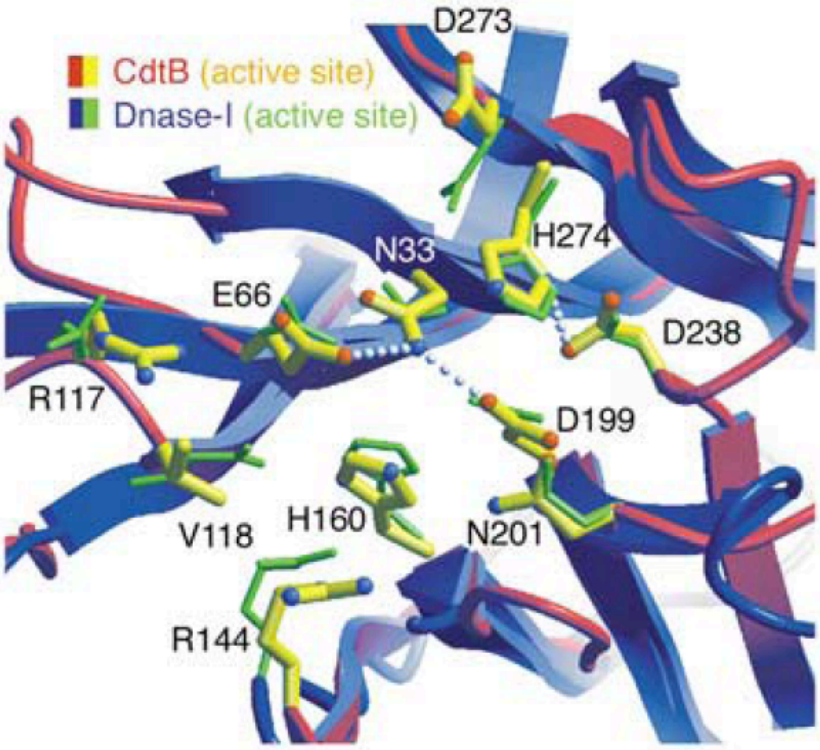

Figure 1.5. Structural homology between CdtB and DNase I enzymes. Catalytically active subunit of CDT has conserved residues homologous to DNase I enzymes. Main-chain/side-chain atoms of CdtB and DNase-I are shown in red/yellow and blue/green, respectively. Mutation in the highlighted conserved residues lead to loss in the DNA-digestion properties of the protein. Model adapted from Nesic et al., 2004 (Nesic et al., 2004).

1.7. References

1. Abuoun, M., Manning, G., Cawthraw, S. A., Ridley, A., Ahmed, I. H., Wassenaar, T. M., & Newell, D. G. (2005). Cytolethal distending toxin (CDT)-negative *Campylobacter jejuni* strains and anti-CDT neutralizing antibodies are induced during human infection but not during colonization in chickens. *Infect Immun, 73*(5), 3053-3062.

2. Akifusa, S., Poole, S., Lewthwaite, J., Henderson, B., & Nair, S. P. (2001). Recombinant *Actinobacillus actinomycetemcomitans* cytolethal distending toxin proteins are required to interact to inhibit human cell cycle progression and to stimulate human leukocyte cytokine synthesis. *Infect Immun, 69*(9), 5925-5930.

3. Bag, P. K., Ramamurthy, T., & Nair, U. B. (1993). Evidence for the presence of a receptor for the cytolethal distending toxin (CLDT) of *Campylobacter jejuni* on CHO and HeLa cell membranes and development of a receptor-based enzyme-linked immunosorbent assay for detection of CLDT. *FEMS Microbiol Lett, 114*(3), 285-291.

4. Baillie, L. W. (2009). Is new always better than old?: The development of human vaccines for anthrax. *Hum Vaccin, 5*(12), 806-816.

5. Bang, D. D., Scheutz, F., Ahrens, P., Pedersen, K., Blom, J., & Madsen, M. (2001). Prevalence of cytolethal distending toxin (cdt) genes and CDT production in *Campylobacter spp.* isolated from Danish broilers. *J Med Microbiol, 50*(12), 1087-1094.

6. Bezine, E., Vignard, J., & Mirey, G. (2014). The cytolethal distending toxin effects on Mammalian cells: a DNA damage perspective. *Cells, 3*(2), 592-615.

7. Bielaszewska, M., Fell, M., Greune, L., Prager, R., Fruth, A., Tschape, H., Karch, H. (2004). Characterization of cytolethal distending toxin genes and expression in shiga toxin-producing *Escherichia coli* strains of non-O157 serogroups. *Infect Immun, 72*(3), 1812-1816.

8. Biswas, D., Fernando, U., Reiman, C., Willson, P., Potter, A., & Allan, B. (2006). Effect of cytolethal distending toxin of *Campylobacter jejuni* on adhesion and internalization in cultured cells and in colonization of the chicken gut. *Avian Dis, 50*(4), 586-593.

9. Blanke, S. R. (2006). Portals and Pathways: Principles of Bacterial Toxin Entry into Host Cells. *Microbe, 1*, 26 - 32.

10. Boesze-Battaglia, K., Besack, D., McKay, T., Zekavat, A., Otis, L., Jordan-Sciutto, K., & Shenker, B. J. (2006). Cholesterol-rich membrane microdomains mediate cell cycle arrest induced by *Actinobacillus actinomycetemcomitans* cytolethal-distending toxin. *Cellular Microbiology, 8*(5), 823-836.

11. Boesze-Battaglia, K., Brown, A., Walker, L., Besack, D., Zekavat, A., Wrenn, S., Shenker, B. J. (2009). Cytolethal distending toxin-induced cell cycle arrest of lymphocytes is dependent upon recognition and binding to cholesterol. *Journal of Biological Chemistry, 284*(16), 10650-10658.

12. Bonifacino, J. S., & Rojas, R. (2006). Retrograde transport from endosomes to the trans-Golgi network. *Nat Rev Mol Cell Biol, 7*(8), 568-579.

13. Cao, L., Bandelac, G., Volgina, A., Korostoff, J., & DiRienzo, J. M. (2008). Role of aromatic amino acids in receptor binding activity and subunit assembly of the cytolethal distending toxin of *Aggregatibacter actinomycetemcomitans. Infect Immun, 76*(7), 2812-2821.

14. Cao, L., Volgina, A., Huang, C. M., Korostoff, J., & DiRienzo, J. M. (2005). Characterization of point mutations in the cdtA gene of the cytolethal distending toxin of *Actinobacillus actinomycetemcomitans*. *Mol Microbiol, 58*(5), 1303-1321.

15. Carette, J. E., Guimaraes, C. P., Varadarajan, M., Park, A. S., Wuethrich, I., Godarova, A., Brummelkamp, T. R. (2009). Haploid genetic screens in human cells identify host factors used by pathogens. *Science, 326*(5957), 1231-1235.

16. Casadevall, A., & Pirofski, L. A. (2000). Host-pathogen interactions: basic concepts of microbial commensalism, colonization, infection, and disease. *Infect Immun, 68*(12), 6511-6518.

17. Chaddock, J. (2013). Transforming the domain structure of botulinum neurotoxins into novel therapeutics. *Curr Top Microbiol Immunol, 364*, 287-306.

18. Comayras, C., Tasca, C., Peres, S. Y., Ducommun, B., Oswald, E., & De Rycke, J. (1997). *Escherichia coli* cytolethal distending toxin blocks the HeLa cell cycle at the G_2/M transition by preventing cdc2 protein kinase dephosphorylation and activation. *Infect Immun, 65*(12), 5088-5095.

19. Conner, S. D., & Schmid, S. L. (2003). Regulated portals of entry into the cell. *Nature, 422*(6927), 37-44.

20. Cope, L. D., Lumbley, S., Latimer, J. L., Klesney-Tait, J., Stevens, M. K., Johnson, L. S., Hansen, E. J. (1997). A diffusible cytotoxin of *Haemophilus ducreyi*. *Proceedings of the National Academy of Sciences of the United States of America, 94*(8), 4056-4061.

21. Cortes-Bratti, X., Chaves-Olarte, E., Lagergard, T., & Thelestam, M. (2000). Cellular internalization of cytolethal distending toxin from *Haemophilus ducreyi*. *Infect Immun, 68*(12), 6903-6911.

22. Cortes-Bratti, X., Karlsson, C., Lagergard, T., Thelestam, M., & Frisan, T. (2001). The *Haemophilus ducreyi* cytolethal distending toxin induces cell cycle arrest and apoptosis via the DNA damage checkpoint pathways. *Journal of Biological Chemistry, 276*(7), 5296-5302.

23. Deng, K., Latimer, J. L., Lewis, D. A., & Hansen, E. J. (2001). Investigation of the interaction among the components of the cytolethal distending toxin of *Haemophilus ducreyi*. *Biochemical & Biophysical Research Communications, 285*(3), 609-615.

24. Dlakic, M. (2001). Is CdtB a nuclease or a phosphatase? *Science, 291*(5504), 547.

25. Elwell, C. A., & Dreyfus, L. A. (2000). DNase I homologous residues in CdtB are critical for cytolethal distending toxin-mediated cell cycle arrest. *Mol Microbiol, 37*(4), 952-963.

26. Escalas, N., Davezac, N., De Rycke, J., Baldin, V., Mazars, R., & Ducommun, B. (2000). Study of the cytolethal distending toxin-induced cell cycle arrest in HeLa cells: involvement of the CDC25 phosphatase. *Experimental Cell Research, 257*(1), 206-212.

27. Eshraghi, A., Dixon, S. D., Tamilselvam, B., Kim, E. J., Gargi, A., Kulik, J. C., Damoiseaux, R., Blanke, S.R., & Bradley, K. A. (2014). Cytolethal distending toxins require components of the ER-associated degradation pathway for host cell entry. *PLoS Pathog, 10*(7), e1004295.

28. Eshraghi, A., Maldonado-Arocho, F. J., Gargi, A., Cardwell, M. M., Prouty, M. G., Blanke, S. R., & Bradley, K. A. (2010). Cytolethal distending toxin family members are differentially affected by alterations in host glycans and membrane cholesterol. *Journal of Biological Chemistry, 285*(24), 18199-18207.

29. Fox, J. G., Rogers, A. B., Whary, M. T., Ge, Z., Taylor, N. S., Xu, S., Horwitz, B.H., & Erdman, S. E. (2004). Gastroenteritis in NF-kappaB-deficient mice is produced with wild-type *Camplyobacter jejuni* but not with *C. jejuni* lacking cytolethal distending toxin despite persistent colonization with both strains. *Infect Immun, 72*(2), 1116-1125.

30. Frisan, T., Cortes-Bratti, X., Chaves-Olarte, E., Stenerlow, B., & Thelestam, M. (2003). The *Haemophilus ducreyi* cytolethal distending toxin induces DNA double-strand breaks and promotes ATM-dependent activation of RhoA. *Cellular Microbiology, 5*(10), 695-707.

31. Frisk, A., Lebens, M., Johansson, C., Ahmed, H., Svensson, L., Ahlman, K., & Lagergard, T. (2001). The role of different protein components from the *Haemophilus ducreyi* cytolethal distending toxin in the generation of cell toxicity. *Microbial Pathogenesis, 30*(6), 313-324.

32. Gargi, A., Reno, M., & Blanke, S. R. (2012). Bacterial toxin modulation of the eukaryotic cell cycle: are all cytolethal distending toxins created equally? *Front Cell Infect Microbiol, 2*, 124.

33. Gargi, A., Tamilselvam, B., Powers, B., Prouty, M. G., Lincecum, T., Eshraghi, A., Maldonado-Arocho, F.J., Wilson, B.A., Bradley, K.A., & Blanke, S. R. (2013). Cellular interactions of the cytolethal distending toxins from *Escherichia coli* and *Haemophilus ducreyi*. *Journal of Biological Chemistry, 288*(11), 7492-7505.

34. Ge, Z., Feng, Y., Whary, M. T., Nambiar, P. R., Xu, S., Ng, V., Fox, J. G. (2005). Cytolethal distending toxin is essential for *Helicobacter hepaticus* colonization in outbred Swiss Webster mice. *Infect Immun, 73*(6), 3559-3567.

35. Ge, Z., Rogers, A. B., Feng, Y., Lee, A., Xu, S., Taylor, N. S., & Fox, J. G. (2007). Bacterial cytolethal distending toxin promotes the development of dysplasia in a model of microbially induced hepatocarcinogenesis. *Cellular Microbiology, 9*(8), 2070-2080.

36. Gruenberg, J., & Stenmark, H. (2004). The biogenesis of multivesicular endosomes. *Nat Rev Mol Cell Biol, 5*(4), 317-323.

37. Guerra, L., Carr, H. S., Richter-Dahlfors, A., Masucci, M. G., Thelestam, M., Frost, J. A., & Frisan, T. (2008). A bacterial cytotoxin identifies the RhoA exchange factor Net1 as a key effector in the response to DNA damage. *PLoS ONE [Electronic Resource], 3*(5), e2254.

38. Guerra, L., Cortes-Bratti, X., Guidi, R., & Frisan, T. (2011). The biology of the cytolethal distending toxins. *Toxins, 3*(3), 172-190.

39. Guerra, L., Guidi, R., & Frisan, T. (2011). Do bacterial genotoxins contribute to chronic inflammation, genomic instability and tumor progression? *FEBS J, 278*(23), 4577-4588.

40. Guerra, L., Nemec, K. N., Massey, S., Tatulian, S. A., Thelestam, M., Frisan, T., & Teter, K. (2009). A novel mode of translocation for cytolethal distending toxin. *Biochim Biophys Acta, 1793*(3), 489-495.

41. Guerra, L., Teter, K., Lilley, B. N., Stenerlow, B., Holmes, R. K., Ploegh, H. L., Sandvig, K., Thelestam, M., Frisan, T. (2005). Cellular internalization of cytolethal distending toxin: a new end to a known pathway. *Cellular Microbiology, 7*(7), 921-934.

42. Haghjoo, E., & Galan, J. E. (2004). *Salmonella typhi* encodes a functional cytolethal distending toxin that is delivered into host cells by a bacterial-internalization pathway. *Proceedings of the National Academy of Sciences of the United States of America, 101*(13), 4614-4619.

43. Hassane, D. C., Lee, R. B., Mendenhall, M. D., & Pickett, C. L. (2001). Cytolethal distending toxin demonstrates genotoxic activity in a yeast model. *Infect Immun, 69*(9), 5752-5759.

44. Hassane, D. C., Lee, R. B., & Pickett, C. L. (2003). *Campylobacter jejuni* cytolethal distending toxin promotes DNA repair responses in normal human cells. *Infect Immun, 71*(1), 541-545.

45. Hu, X., Nesic, D., & Stebbins, C. E. (2006). Comparative structure-function analysis of cytolethal distending toxins. *Proteins, 62*(2), 421-434.

46. Hu, X., & Stebbins, C. E. (2006). Dynamics and assembly of the cytolethal distending toxin. *Proteins, 65*(4), 843-855.

47. Janka, A., Bielaszewska, M., Dobrindt, U., Greune, L., Schmidt, M. A., & Karch, H. (2003). Cytolethal distending toxin gene cluster in enterohemorrhagic *Escherichia coli* O157:H- and O157:H7: characterization and evolutionary considerations. *Infect Immun, 71*(6), 3634-3638.

48. Jinadasa, R. N., Bloom, S. E., Weiss, R. S., & Duhamel, G. E. (2011). Cytolethal distending toxin: a conserved bacterial genotoxin that blocks cell cycle progression, leading to apoptosis of a broad range of mammalian cell lineages. *Microbiology, 157*(Pt 7), 1851-1875.

49. Johannes, L., & Popoff, V. (2008). Tracing the retrograde route in protein trafficking. *Cell, 135*(7), 1175-1187.

50. Johnson, W. M., & Lior, H. (1988a). A new heat-labile cytolethal distending toxin (CLDT) produced by *Campylobacter spp*. *Microbial Pathogenesis, 4*(2), 115-126.

51. Johnson, W. M., & Lior, H. (1988b). A new heat-labile cytolethal distending toxin (CLDT) produced by *Escherichia coli* isolates from clinical material. *Microbial Pathogenesis, 4*(2), 103-113.

52. Kirkham, M., & Parton, R. G. (2005). Clathrin-independent endocytosis: new insights into caveolae and non-caveolar lipid raft carriers. *Biochim Biophys Acta, 1746*(3), 349-363.

53. Lai, C. H., Lai, C. K., Lin, Y. J., Hung, C. L., Chu, C. H., Feng, C. L., Chang, C.S., & Su, H. L. (2013). Characterization of putative cholesterol recognition/interaction amino acid consensus-like motif of *Campylobacter jejuni* cytolethal distending toxin C. *PLoS ONE [Electronic Resource], 8*(6), e66202.

54. Lara-Tejero, M., & Galan, J. E. (2000). A bacterial toxin that controls cell cycle progression as a deoxyribonuclease I-like protein. *Science, 290*(5490), 354-357.

55. Lara-Tejero, M., & Galan, J. E. (2001). CdtA, CdtB, and CdtC form a tripartite complex that is required for cytolethal distending toxin activity. *Infect Immun, 69*(7), 4358-4365.

56. Lara-Tejero, M., & Galan, J. E. (2002). Cytolethal distending toxin: limited damage as a strategy to modulate cellular functions. *Trends Microbiol, 10*(3), 147-152.

57. Li, L., Ding, C., Duan, J. L., Yang, M. F., Sun, Y., Wang, X. Q., & Xu, Y. (2013). A new functional site W115 in CdtA is critical for *Aggregatibacter actinomycetemcomitans* cytolethal distending toxin. *PLoS ONE [Electronic Resource], 8*(6), e65729.

58. Lin, C. D., Lai, C. K., Lin, Y. H., Hsieh, J. T., Sing, Y. T., Chang, Y. C., Chen, K., Wang, W., Su, H., & Lai, C. H. (2011). Cholesterol depletion reduces entry of *Campylobacter jejuni* cytolethal distending toxin and attenuates intoxication of host cells. *Infect Immun, 79*(9), 3563-3575.

59. Mao, X., & DiRienzo, J. M. (2002). Functional studies of the recombinant subunits of a cytolethal distending holotoxin. *Cellular Microbiology, 4*(4), 245-255.

60. Matangkasombut, O., Wattanawaraporn, R., Tsuruda, K., Ohara, M., Sugai, M., & Mongkolsuk, S. (2010). Cytolethal distending toxin from *Aggregatibacter actinomycetemcomitans* induces DNA damage, S/G_2 cell cycle arrest, and caspase- independent death in a *Saccharomyces cerevisiae* model. *Infect Immun, 78*(2), 783-792.

61. Maxfield, F. R., & McGraw, T. E. (2004). Endocytic recycling. *Nat Rev Mol Cell Biol, 5*(2), 121-132.

62. Mayor, S., & Pagano, R. E. (2007). Pathways of clathrin-independent endocytosis. *Nat Rev Mol Cell Biol, 8*(8), 603-612.

63. McSweeney, L. A., & Dreyfus, L. A. (2004). Nuclear localization of the Escherichia coli cytolethal distending toxin CdtB subunit. *Cellular Microbiology, 6*(5), 447-458.

64. McSweeney, L. A., & Dreyfus, L. A. (2005). Carbohydrate-binding specificity of the Escherichia coli cytolethal distending toxin CdtA-II and CdtC-II subunits. *Infect Immun, 73*(4), 2051-2060.

65. Mise, K., Akifusa, S., Watarai, S., Ansai, T., Nishihara, T., & Takehara, T. (2005). Involvement of ganglioside GM3 in G_2/M cell cycle arrest of human monocytic cells induced by *Actinobacillus actinomycetemcomitans* cytolethal distending toxin. *Infect Immun, 73*(8), 4846-4852.

66. Nesic, D., Hsu, Y., & Stebbins, C. E. (2004). Assembly and function of a bacterial genotoxin. *Nature, 429*(6990), 429-433.

67. Nesic, D., & Stebbins, C. E. (2005). Mechanisms of assembly and cellular interactions for the bacterial genotoxin CDT. *PLoS Pathog, 1*(3), e28.

68. Nishikubo, S., Ohara, M., Ueno, Y., Ikura, M., Kurihara, H., Komatsuzawa, H., Oswald, E., & Sugai, M. (2003). An N-terminal segment of the active component of the bacterial genotoxin cytolethal distending toxin B (CDTB) directs CDTB into the nucleus. *Journal of Biological Chemistry, 278*(50), 50671-50681.

69. Nougayrede, J. P., Taieb, F., De Rycke, J., & Oswald, E. (2005). Cyclomodulins: bacterial effectors that modulate the eukaryotic cell cycle. *Trends Microbiol, 13*(3), 103-110.

70. Ohara, M., Oswald, E., & Sugai, M. (2004). Cytolethal distending toxin: a bacterial bullet targeted to nucleus. *J Biochem, 136*(4), 409-413.

71. Oswald, E., Nougayrede, J. P., Taieb, F., & Sugai, M. (2005). Bacterial toxins that modulate host cell-cycle progression. *Curr Opin Microbiol, 8*(1), 83-91.

72. Peres, S. Y., Marches, O., Daigle, F., Nougayrede, J. P., Herault, F., Tasca, C., Oswald, E. (1997). A new cytolethal distending toxin (CDT) from *Escherichia coli* producing CNF2 blocks HeLa cell division in G_2/M phase. *Mol Microbiol, 24*(5), 1095-1107.

73. Pettersen, E. F., Goddard, T. D., Huang, C. C., Couch, G. S., Greenblatt, D. M., Meng, E. C., & Ferrin, T. E. (2004). UCSF Chimera--a visualization system for exploratory research and analysis. *J Comput Chem, 25*(13), 1605-1612.

74. Rabin, S. D., Flitton, J. G., & Demuth, D. R. (2009). *Aggregatibacter actinomycetemcomitans* cytolethal distending toxin induces apoptosis in nonproliferating macrophages by a phosphatase-independent mechanism. *Infect Immun, 77*(8), 3161-3169.

75. Saiki, K., Gomi, T., & Konishi, K. (2004). Deletion and purification studies to elucidate the structure of the *Actinobacillus actinomycetemcomitans* cytolethal distending toxin. *J Biochem, 136*(3), 335-342.

76. Saiki, K., Konishi, K., Gomi, T., Nishihara, T., & Yoshikawa, M. (2001). Reconstitution and purification of cytolethal distending toxin of *Actinobacillus actinomycetemcomitans*. *Microbiol Immunol, 45*(6), 497-506.

77. Sandvig, K., Dubinina, E., Garred, O., Prydz, K., Kozlov, J. V., Hansen, S. H., & van Deurs, B. (1992). Protein toxins: mode of action and cell entry. *Biochemical Society Transactions, 20*(4), 724-727.

78. Sandvig, K., & van Deurs, B. (2005). Delivery into cells: lessons learned from plant and bacterial toxins. *Gene Therapy, 12*(11), 865-872.

79. Sato, T., Koseki, T., Yamato, K., Saiki, K., Konishi, K., Yoshikawa, M., Ishikawa, I., & Nishihara, T. (2002). p53-independent expression of p21(CIP1/WAF1) in plasmacytic cells during G_2 cell cycle arrest induced by *Actinobacillus actinomycetemcomitans* cytolethal distending toxin. *Infect Immun, 70*(2), 528-534.

80. Sert, V., Cans, C., Tasca, C., Bret-Bennis, L., Oswald, E., Ducommun, B., & De Rycke, J. (1999). The bacterial cytolethal distending toxin (CDT) triggers a G_2 cell cycle checkpoint in mammalian cells without preliminary induction of DNA strand breaks. *Oncogene, 18*(46), 6296-6304.

81. Shenker, B. J., Besack, D., McKay, T., Pankoski, L., Zekavat, A., & Demuth, D. R. (2004). *Actinobacillus actinomycetemcomitans* cytolethal distending toxin (Cdt): evidence that the holotoxin is composed of three subunits: CdtA, CdtB, and CdtC. *J Immunol, 172*(1), 410-417.

82. Shenker, B. J., Demuth, D. R., & Zekavat, A. (2006). Exposure of lymphocytes to high doses of *Actinobacillus actinomycetemcomitans* cytolethal distending toxin induces rapid onset of apoptosis-mediated DNA fragmentation. *Infect Immun, 74*(4), 2080-2092.

83. Shenker, B. J., Dlakic, M., Walker, L. P., Besack, D., Jaffe, E., LaBelle, E., & Boesze-Battaglia, K. (2007). A novel mode of action for a microbial-derived immunotoxin: the cytolethal distending toxin subunit B exhibits phosphatidylinositol 3,4,5-triphosphate phosphatase activity. *J Immunol, 178*(8), 5099-5108.

84. Shenker, B. J., Hoffmaster, R. H., Zekavat, A., Yamaguchi, N., Lally, E. T., & Demuth, D. R. (2001). Induction of apoptosis in human T cells by *Actinobacillus actinomycetemcomitans* cytolethal distending toxin is a consequence of G_2 arrest of the cell cycle. *J Immunol, 167*(1), 435-441.

85. Shenker, B. J., McKay, T., Datar, S., Miller, M., Chowhan, R., & Demuth, D. (1999). *Actinobacillus actinomycetemcomitans* immunosuppressive protein is a member of the family of cytolethal distending toxins capable of causing a G_2 arrest in human T cells. *J Immunol, 162*(8), 4773-4780.

86. Shenker, B. J., Walker, L. P., Zekavat, A., Dlakic, M., & Boesze-Battaglia, K. (2014). Blockade of the PI-3K signalling pathway by the *Aggregatibacter actinomycetemcomitans* cytolethal distending toxin induces macrophages to synthesize and secrete pro-inflammatory cytokines. *Cellular Microbiology, 16*(9), 1391-1404.

87. Smith, J., Tho, L. M., Xu, N., & Gillespie, D. A. (2010). The ATM-Chk2 and ATR-Chk1 pathways in DNA damage signaling and cancer. *Adv Cancer Res, 108*, 73-112.

88. Smith, J. L., & Bayles, D. O. (2006). The contribution of cytolethal distending toxin to bacterial pathogenesis. *Crit Rev Microbiol, 32*(4), 227-248.

89. Smith, R. D., Willett, R., Kudlyk, T., Pokrovskaya, I., Paton, A. W., Paton, J. C., & Lupashin, V. V. (2009). The COG complex, Rab6 and COPI define a novel Golgi retrograde trafficking pathway that is exploited by SubAB toxin. *Traffic, 10*(10), 1502-1517.

90. Spano, S., Ugalde, J. E., & Galan, J. E. (2008). Delivery of a *Salmonella typhi* exotoxin from a host intracellular compartment. *Cell Host Microbe, 3*(1), 30-38.

91. Svensson, L. A., Tarkowski, A., Thelestam, M., & Lagergard, T. (2001). The impact of *Haemophilus ducreyi* cytolethal distending toxin on cells involved in immune response. *Microbial Pathogenesis, 30*(3), 157-166.

92. Tan, K. S., Song, K. P., & Ong, G. (2002). Cytolethal distending toxin of *Actinobacillus actinomycetemcomitans*. Occurrence and association with periodontal disease. *J Periodontal Res, 37*(4), 268-272.

93. Ueno, Y., Ohara, M., Kawamoto, T., Fujiwara, T., Komatsuzawa, H., Oswald, E., & Sugai, M. (2006). Biogenesis of the *Actinobacillus actinomycetemcomitans* cytolethal distending toxin holotoxin. *Infect Immun, 74*(6), 3480-3487.

94. Whitehouse, C. A., Balbo, P. B., Pesci, E. C., Cottle, D. L., Mirabito, P. M., & Pickett, C. L. (1998). *Campylobacter jejuni* cytolethal distending toxin causes a G_2-phase cell cycle block. *Infect Immun, 66*(5), 1934-1940.

95. Willett, R., Kudlyk, T., Pokrovskaya, I., Schonherr, R., Ungar, D., Duden, R., & Lupashin, V. (2013). COG complexes form spatial landmarks for distinct SNARE complexes. *Nat Commun, 4*, 1553.

96. Wising, C., Azem, J., Zetterberg, M., Svensson, L. A., Ahlman, K., & Lagergard, T. (2005). Induction of apoptosis/necrosis in various human cell lineages by *Haemophilus ducreyi* cytolethal distending toxin. *Toxicon, 45*(6), 767-776.

97. Wising, C., Svensson, L. A., Ahmed, H. J., Sundaeus, V., Ahlman, K., Jonsson, I. M., Lagergard, T. (2002). Toxicity and immunogenicity of purified *Haemophilus ducreyi* cytolethal distending toxin in a rabbit model. *Microbial Pathogenesis, 33*(2), 49-62.

98. Yamada, T., Komoto, J., Saiki, K., Konishi, K., & Takusagawa, F. (2006). Variation of loop sequence alters stability of cytolethal distending toxin (CDT): crystal structure of CDT from *Actinobacillus actinomycetemcomitans*. *Protein Sci, 15*(2), 362-372.

99. Yamamoto, K., Tominaga, K., Sukedai, M., Okinaga, T., Iwanaga, K., Nishihara, T., & Fukuda, J. (2004). Delivery of cytolethal distending toxin B induces cell cycle arrest and apoptosis in gingival squamous cell carcinoma in vitro. *Eur J Oral Sci, 112*(5), 445-451.

100. Young, D., Hussell, T., & Dougan, G. (2002). Chronic bacterial infections: living with unwanted guests. *Nat Immunol, 3*(11), 1026-1032.

101. Zhou, M., Zhang, Q., Zhao, J., & Jin, M. (2012). Haemophilus parasuis encodes two functional cytolethal distending toxins: CdtC contains an atypical cholesterol recognition/interaction region. *PLoS ONE, 7*(3), e32580.

CHAPTER 2: CELLULAR INTERACTIONS OF THE CDT FROM *E. COLI* AND *H. DUCREYI*

2.1. Introduction

The cytolethal distending toxins (CDTs) comprise a family of multi-subunit bacterial genotoxins that modulate the eukaryotic cell cycle (Ceelen, Decostere, Ducatelle, & Haesebrouck, 2006; Gargi, Reno, & Blanke, 2012; Nougayrede, Taieb, De Rycke, & Oswald, 2005; Ohara, Oswald, & Sugai, 2004; Oswald, Nougayrede, Taieb, & Sugai, 2005). CDT-mediated cell cycle arrest and the disruption of cytokinesis have been proposed to alter the normal barrier and immune functions of both epithelial cells and lymphocytes (Nougayrede et al., 2005). Animal model studies as well as the association of *cdt* gene carriage in disease-causing bacteria from human isolates both support the importance of CDTs for the virulence strategies of specific pathogens (Ge, Schauer, & Fox, 2008; Smith & Bayles, 2006).

Most CDTs function as assembled complexes of three protein subunits, encoded by three contiguous genes (*cdtA*, *cdtB*, *cdtC*) within an operon (Thelestam & Frisan, 2004). Consistent with the canonical AB model of intracellular acting toxins (Blanke, 2006), CdtB appears to function as the enzymatic A-subunit. CdtB has DNase I-like activity (C. A. Elwell & Dreyfus, 2000; Lara-Tejero & Galan, 2000) and localizes to the nucleus when expressed ectopically within the cytosol of mammalian cells (McSweeney & Dreyfus, 2004; Nishikubo et al., 2003; Wising, Magnusson, Ahlman, Lindholm, & Lagergard,

2010), suggesting that this subunit directly causes DNA damage within the nuclei of intoxicated cells. CdtA and CdtC facilitate the delivery of CdtB into cells (Cao, Bandelac, Volgina, Korostoff, & DiRienzo, 2008; Cao, Volgina, Huang, Korostoff, & DiRienzo, 2005; McSweeney & Dreyfus, 2005; Nesic & Stebbins, 2005), although the molecular details of how these subunits facilitate the cell-surface binding, uptake, and intracellular transport of CdtB remain poorly understood.

A diverse group of Gram-negative pathogenic bacteria that colonize distinct niches within the host have been identified to possess *cdt* genes (Pickett & Whitehouse, 1999). The AB_2 toxin architecture as well as a number of other key structural features appear to be generally conserved across the CDT family (Hu, Nesic, & Stebbins, 2006), suggesting that individual toxin members may interact with and intoxicate cells in a similar fashion. However, the cellular intoxication properties of CDTs produced by different pathogenic organisms are poorly understood. Recently, the sensitivity of several cell lines to CDTs from *Aggregatibacter actinomycetemcomitans, Campylobacter jejuni, Escherichia coli*, and *Haemophilus ducreyi* were demonstrated to be differentially affected by alterations in host glycans and membrane cholesterol (Eshraghi et al., 2010), suggesting that host cell requirements for CDT intoxication of mammalian cells may not be universally conserved. However, it remains unclear whether the overall mechanism and molecular basis of toxin binding, uptake, and intracellular transport, are broadly applicable to all members of the CDT family.

The objective of this study was to directly compare the cellular intoxication mechanisms employed by CDTs produced by *E. coli* and *H. ducreyi*, two

pathogens that colonize highly divergent host niches (i.e. the intestinal and urogenital tracts, respectively). Notably, the CDTs from *E. coli* (Ec-CDT) and *H. ducreyi* (Hd-CDT) share only 22% and 19% sequence identity, respectively, in their CdtA and CdtC subunits, suggesting the possibility that these two toxins might interact with host cells in fundamentally different ways. These studies revealed differences in the cellular requirements for toxin intracellular trafficking. Moreover, Ec-CDT and Hd-CDT did not compete with each other for binding to the surface of cells, suggesting that these toxins may target and bind to discrete receptors. Overall, these studies suggest that Ec-CDT and Hd-CDT are transported within cells by distinct pathways, possibly mediated by their interaction with different receptors at the cell surface.

The text of the chapter 2 is similar to the paper published in Journal of Biological Science (Amandeep Gargi, Batcha Tamilselvam, Brendan Powers, Michael G. Prouty, Tommie Lincecum, Aria Eshraghi, Francisco J. Maldonado-Arocho, Brenda A. Wilson, Kenneth A. Bradley and Steven R. Blanke, 2013. Cellular interactions of the cytolethal distending toxins from *Escherichia coli* and *Haemophilus ducreyi*. J. Biol. Chem. 288: 7492-7505.).

2.2. Materials and Methods

Cloning of cdt genes and preparation of expression strains. The cloning of the genes encoding Ec-CDT and Hd-CDT in plasmids for recombinant expression in *E. coli* was previously described (Eshraghi et al., 2010).

Expression and purification of recombinant Ec-CDT and Hd-CDT. Each recombinant protein was expressed and purified as previously described (Eshraghi et al., 2010). Protein concentrations were quantified using the Bradford Protein Assay (Thermo Scientific, Rockford, IL). Recombinant proteins were used only when purified to at least 95% homogeneity, as estimated by resolving the proteins using sodium-dodecyl sulfate (SDS)-polyacrylamide gel electrophoresis (PAGE), and visualizing after staining the gels with Coomassie Brilliant Blue (Bio-Rad, Hercules, CA; data not shown). The purified, denatured subunits were stored at -20 °C in HEPES (20 mM, *N*-[2-Hydroxyethyl] piperazine-*N*-[2-ethanesulphonic acid], Calbiochem, La Jolla, CA), pH 7.5 containing urea (8 M) and NaCl (200 mM).

Ec-CDT and Hd-CDT holotoxins were prepared as previously described (Nesic, Hsu, & Stebbins, 2004). Ec-CDT and Hd-CDT holotoxin integrity was evaluated using the dialysis retention assay, as previously described (Cao et al., 2005). Ec-CDT or Hd-CDT holotoxin (5-20 μM, 1 ml) was dialyzed (100 kDa molecular mass cut-off tubing; Spectrum Laboratories) at 4 °C against four 250 ml volumes of phosphate buffer saline (PBS) pH 7.4 containing 5% glycerol. After 24 h, the dialyzed proteins were evaluated using SDS-PAGE followed by staining with Coomassie Brilliant blue. The gels were scanned with a CanonScan 9950F scanner (Canon, Lake Success, NY) using ArcSoft Photo Studio 5.5 software (ArcSoft, Fremont, CA). The integrity of the holotoxins was quantified by comparing the relative intensities of the bands corresponding to CdtA, CdtB, or CdtC before and after dialysis, as determined by using the UN-SCAN-IT program

(Silk Scientific, Inc., Orem, UT). Individual CDT subunits, each of which has a molecular mass less than 35 kDa, were used as negative controls.

Mammalian cells. All mammalian cell cultures were maintained at 37 °C and under 5% CO_2 within a humidified environment. Human cervical cancer epithelial (HeLa) cells (CCL-2, ATCC) were maintained in Minimal Essential Medium Eagle (MEM, Mediatech, Herndon, VA) with 10% fetal bovine serum (FBS, Mediatech). Chinese hamster ovary (CHO-K1) cells (CCL-61, ATCC) were maintained in Ham's F-12K (Lonza, Walkersville, MD) with 10% FBS. Human epithelial colorectal adenocarcinoma (Caco-2) cells (HTB-37, ATCC) were maintained in MEM (Eagle) with 20% FBS. Human embryonic intestinal (INT-407) cells (CCL-6, ATCC) were maintained in basal medium eagle (Sigma) with 10% FBS. Complete medium was obtained by supplementing each medium described above with L-glutamine (2 mM, Sigma), penicillin (50 IU/ml, Mediatech), and streptomycin (50 μg/ml, Mediatech).

Cell cycle phase determination. The indicated cell lines were seeded (1.5 x 10^5 cells per well) in 6-well plates (Corning Inc., Corning, NY). After 18 h, the cells were further incubated in complete medium with or without Ec-CDT or Hd-CDT at the indicated concentrations, or mock incubated with PBS pH 7.4. After 48 h, the cells were analyzed for arrest at the G_2/M interface, as previously described (Eshraghi et al., 2010). From these data, dose response curves were generated by plotting cells in G_2/M as a function of toxin concentration. From the dose response curves, we determined $CCAD_{50}$ (i.e. cell cycle arrest $dose_{50}$)

values, which we defined as the toxin concentrations required to induce G_2/M arrest in 50% of the cell population not already in G_2/M.

For both Ec-CDT and Hd-CDT, preliminary studies revealed nearly identical dose response curves for G_2/M arrest in the presence or absence of the hexa-histidine tags (Figure 2.1). All subsequent studies were conducted with Ec-CDT or Hd-CDT assembled from subunits that retained their respective hexa-histidine tags.

Some studies were conducted in the presence of the indicated concentrations of brefeldin A (BFA; MP Biomedicals), ammonium chloride (NH_4Cl, Sigma), bafilomycin A1 (LC Laboratories, Woburn, MA), monensin (Sigma), or nigericin (Sigma). These studies were conducted at approximately the $CCAD_{50}$ values determined for Hd-CDT and Ec-CDT in order to best assess whether each pharmacological agent inhibited, potentiated, or had no effect on toxin activity.

Flow cytometry. Analytical flow cytometry-based assays were carried out as previously described (Eshraghi et al., 2010).

DNase assay. The relative *in vitro* DNase activities of either Ec-CdtB or Hd-CdtB were determined as described previously (C. A. Elwell & Dreyfus, 2000), using purified pUC19 as the substrate. Reactions were stopped at 4 h by the addition of EDTA (to a final concentration of 10 mM). DNA gel loading dye (6x; Promega) was added to each sample, and the samples were resolved by employing agarose (0.8%) gel electrophoresis using Tris-acetate-EDTA (TAE, 40

mM Tris base, Fisher Biotech, Fair Lawn, NJ; 20 mM acetic acid, Fisher Scientific; 1 mM EDTA) electrophoresis buffer with constant voltage (100 V). The gels were stained with ethidium bromide (1 μg/ml, Bio-Rad), photographed using a Gel Doc EQ system (Bio-Rad), and the relative pixel densities of stained bands corresponding to supercoiled pUC19 were measured using UN-SCAN-IT. Relative DNase activity was calculated from the pixel densities of ethidium bromide stained bands corresponding to supercoiled pUC19, using the relationship: relative DNase activity = [(super-coiled pUC19 pixels from control reactions lacking Ec-CdtB and Hd-CdtB) – (super-coiled pUC19 pixels from reactions containing Ec-CdtB or Hd-CdtB)] / [super-coiled pUC19 pixels from control reactions lacking Ec-CdtB and Hd-CdtB]. A value of 1.0 corresponds to a complete loss of detectable supercoiled pUC19.

Biotinylation of CDTs. Ec-CDT or Hd-CDT (1 ml at 5-20 μM) in PBS pH 7.4 was incubated overnight at 4 °C with EZ Link Sulfo-NHS-LC-Biotin (10-fold molar excess, Thermo Scientific). The labeling reaction was arrested by the addition of Tris pH 8.0 (to a final concentration of 20 mM). To remove free label, the proteins were dialyzed at 4 °C against four changes of PBS pH 7.4 (250 ml each) containing 5% glycerol. Preliminary studies indicated that biotinylation reactions had no detectable effects on the capacity of either Ec-CDT or Hd-CDT to induce cell cycle arrest in G_2/M.

Internalization assay. Cells were seeded (2×10^4 per well) in 8-well chamber slides (Nunc; Rochester, NY). After 18 h, the slides were incubated on

ice for 30 min. The cells were washed two times with ice-cold PBS pH 7.4, and then further incubated on ice with or without biotinylated Ec-CDT or Hd-CDT (at the indicated concentrations) in PBS pH 7.4 with bovine serum albumin (BSA, 3%, Sigma), or mock incubated in PBS pH 7.4 with BSA (3%). After 30 min of toxin pre-binding on ice, the cells were washed three times with ice-cold PBS pH 7.4.

To monitor CDT binding, the cells were immediately fixed by incubating with ice-cold 2% formaldehyde (Sigma), and then further incubated at room temperature for 30 min. To monitor CDT internalization, after 30 min of toxin pre-binding on ice, the cells were incubated with pre-warmed (37 °C) complete medium. After 10 min, the cells were washed with ice-cold PBS pH 7.4, and fixed with ice-cold 2% formaldehyde. After fixing for 30 min at room temperature, the cells were permeabilized by incubating in PBS 7.4 containing 0.1% Triton X-100 for 15 min, and blocked with 3% BSA for 30 min. To probe for biotinylated Ec-CDT or Hd-CDT, the fixed and permeabilized cells were incubated at room temperature with streptavidin conjugated with Alexa Fluor 488 (1:200 dilution in PBS 7.4; Invitrogen). After 1 h, the cells were washed 3 times with 0.1% Tween-20 (Fisher Scientific) in PBS pH 7.4. The nucleus was stained by incubating with 4',6-diamidino-2-phenylindole (DAPI; 300 nM in PBS pH 7.4, Invitrogen) for 2 min. Slides were washed 3 times with 0.1% Tween-20 in PBS pH 7.4 and air-dried. The slides were mounted with ProLong Gold antifade reagent (Invitrogen) and cured overnight. The cells were then analyzed using DIC/fluorescence microscopy.

DIC/fluorescence microscopy. Chamber slides were analyzed using a DeltaVision RT microscope (Applied Precision; Issaquah, WA), using an Olympus Plan Apo 40x oil objective with NA 1.42 and working distance of 0.17 mm DIC images were collected using a Photometrics CoolSnap HQ camera; (Photometrics, Tucson; AZ). Images were processed using SoftWoRX Explorer Suite (version 3.5.1, Applied Precision Inc). Deconvolution was carried out using SoftWoRX constrained iterative deconvolution tool (ratio mode), and analyzed using Imaris 5.7 (Bitplane AG, Zurich, Switzerland).

CDT localization to the ER. Cells were plated in an 8-well chamber slide to 30-40% confluency. After overnight incubation, cells were washed 2 times with PBS pH 7.4, followed by addition of 100 μl OPTI-MEM (Invitrogen, Grand Island, NY), and further incubated for 2 h before transfection. Approximately 30 min prior to addition to cells, the appropriate dilutions of pDsRed2-ER (0.4 μg/200 μl/well; Clontech, Mountain View, CA), which encodes RFP fused to the ER targeting sequence of calreticulin, and the ER retention sequence, KDEL; and Lipofectamine 2000 reagent (1 μl/200 μl/well; Invitrogen) complex were prepared according to the manufacturers instructions, and allowed to incubate at room temperature. After 30 min, OPTI-MEM was removed, and the plasmid DNA-transfection mixture (100 μl) was added to each well in a drop-wise fashion with gentle agitation, and the cells were immediately incubated at 37 °C and under 5% CO_2. After 4 h, the transfection mixture was removed from the monolayers, and the cells were incubated in complete medium at 37 °C and under 5% CO_2. After overnight incubation, we typically detected 80-90% of the cells within the

monolayer to be transfected based on the percentage of cells with RFP fluorescence, as determined using an Olympus CKX 41 fluorescence microscope (Olympus America Inc., Center Valley, PA).

Cells that had been transfected, as described above, with pDsRed2-ER, were pre-incubated for 30 min in the absence or presence of NH_4Cl (20 mM) at 37 °C and under 5% CO_2. The cells were then further incubated with biotinylated Ec-CDT or Hd-CDT (200 nM), and the cells were stained for each toxin as described above under "*Internalization Assay*". The cells were further stained for actin by incubating with Alexa Fluor 647-labelled phalloidin (1 U/200 μl/well; Invitrogen). Images were collected using DIC/fluorescence microscopy and deconvoluted, as described above. For each cell, images were collected from an average of 30 z-planes, each at a thickness of 0.2 μm. Localization analysis was conducted by using the co-localization module of the DeltaVision SoftWoRx 3.5.1 software suite. Results were expressed as the localization index, which was derived from calculating the Pearson's coefficient of correlation values, which in these studies was a measure of localization of the indicated CDT to the ER in each z plane of the cell. In these studies, a localization index value of 1.0 indicates 100% localization of Ec-CDT or Hd-CDT to the ER, whereas a localization index of 0.0 indicates the absence of Ec-CDT or Hd-CDT localization to the ER. The localization index was calculated from the analysis of a total of 50 images collected over three independent experiments.

Monitoring nuclear localization of Ec-CdtB or Hd-CdtB within the nuclear fraction of CDT-intoxicated cells. Cells were seeded in 100 mm culture dishes (BD Biosciences, Durham, NC). After overnight incubation, the monolayers were treated with bafilomycin A1 (20 nM) for 30 min, and further incubated with Ec-CDT or Hd-CDT (at the indicated concentrations). After 30 min, the cells were further incubated with fresh medium (not containing toxin) for an additional 210 min. After 240 min total internalization of Ec-CDT or Hd-CDT, the cells were harvested by scraping, lysed using hypotonic buffer, and fractionated as per the manufacturer's protocol (Nuclear Extract Kit, Active Motif, Carlsbad, CA). The fractionated samples were evaluated by western blotting, using rabbit polyclonal antibodies against Ec-CdtB (1:20,000 dilution; generated by Thermo Fisher Scientific Inc., Rockford, IL), or rabbit polyclonal antibodies against Hd-CdtB (1:10,000; generated by Immunological Resource Center, University of Illinois, Urbana, IL), cytosolic marker GAPDH (1:200; Abcam, Cambridge, MA), microsomal marker calnexin (1:2,000; Abcam), nuclear marker p84 (1:2,000; Abcam), and cell lysate loading control actin (1:1,000; NeoMarkers, Fremont, CA). Anti-mouse (1:2,000), and anti-rabbit (1:5,000) secondary antibodies were purchased from Pierce Protein Biology Products (Thermo Fisher Scientific Inc.). Relative amounts of CdtB were determined by densitometric analysis of the blot bands using the UN-SCAN-IT program.

H2AX activation assay. Cells were transfected with pDsRed-Rab7 DN (0.4 µg/200 µL/well), using the general transfection procedure as described above under "*CDT localization to the ER."* The transfected monolayers were incubated

at 37°C with Ec-CDT (200 nM) or Hd-CDT (200 nM). After 8 hours, the cells were fixed and permeabilized as described above under "*Internalization Assay*." To monitor activation of H2AX by CDT, samples were stained overnight with a rabbit polyclonal anti-p-H2AX antibody (1:5000 dilution; Invitrogen) at 4 °C, followed by incubation with goat anti-rabbit Alexa Fluor 488 antibody (1:1000 dilution; Invitrogen) at room temperature for 2 h. The cells were further counter stained for actin by incubating with Alexa Fluor 647-labelled phalloidin (1 U/200 μl/well) and for nuclei by incubating with DAPI (1 ng/200 μl, Invitrogen) for 30 min. The slides were mounted with ProLong Gold Antifade Reagent (25 μl/well; Invitrogen). Images were collected using DIC/fluorescence microscopy and deconvoluted, as described above. For each cell, images were collected from an average of 30 z-planes, each at a thickness of 0.2 μm. H2AX activation analysis was conducted by using the DeltaVision SoftWoRx 3.5.1 software suite. Percentage of H2AX activated cells in each group of functional and dysfunctional Rab7 cells were calculated from approximately 50 cells from each group over three independent experiments.

Monitoring nuclear localization of Ec-CdtB or Hd-CdtB using fluorescence microscopy. Cells were transfected with pDsRed-Rab7-DN (0.4 μg/200 μl/well), using the general transfection procedure as described above under "*CDT localization to the ER*" The transfected monolayers were pre-chilled for 30 min on ice and further incubated with Ec-CDT (200 nM) or Hd-CDT (200 nM) on ice for 30 min. After 60 min post internalization, the cells were fixed and permeabilized as described above under "*Internalization Assay*" To monitor Ec-CdtB or Hd-

CdtB localization to the nucleus, cells were incubated with rabbit polyclonal anti-Ec-CdtB or anti-Hd-CdtB antibodies (1:2000 dilution) at 4 °C overnight, followed by incubation with goat anti-rabbit Alexa Fluor 488-labeled antibody (1:1000 dilution; Invitrogen) at room temperature for 2 h. The cells were further counter stained for the nucleus by incubating with DAPI (1 ng/200 µl, Invitrogen) for 30 min at room temperature. The slides were mounted with ProLong Gold Antifade Reagent (25 µl/well; Invitrogen). Images were collected using DIC/fluorescence microscopy and deconvoluted, as described above. For each cell, images were collected from an average of 30 z-planes, each at a thickness of 0.2 µm. Nuclear localization analysis was conducted by using the DeltaVision SoftWoRx 3.5.1 software suite. Percentage of CdtB localization into nucleus in each group of functional and dysfunctional Rab7 cells were calculated from approximately 30 cells from each group over three independent experiments.

CdtB-localization to Rab9-enriched vesicles. Pre-chilled monolayers were incubated with pre-chilled Ec-CDT (200 nM) or Hd-CDT (200 nM) on ice. After internalization, the cells were fixed and permeabilized as described above under "*Internalization Assay*." To probe the localization of CDT in Rab9 enriched vesicles, intoxicated cells were incubated with rabbit polyclonal anti-Ec-CdtB or anti-Hd-CdtB antibodies (1:2000 dilution), along with mouse monoclonal anti-Rab9 antibody (1:50 dilution; Abcam) at 4 °C overnight, followed by incubation with goat anti-rabbit Alexa Fluor 488-labeled antibody (1:1000 dilution; Invitrogen) and donkey anti-mouse Alexa Fluor 568 antibody (1:1000 dilution; Invitrogen) at room temperature for 2 h. The cells were further counter stained for

actin by incubating with Alexa Fluor 647-labeled phalloidin (1 U/200 μl/well; Invitrogen) and for the nucleus by incubating with DAPI (1 ng/200 μl, Invitrogen) for 30 min at room temperature. The slides were mounted with ProLong Gold Antifade Reagent (25 μl/well; Invitrogen).

Images were collected using DIC/fluorescence microscopy and deconvoluted, as described above. For each cell, images were collected from an average of 30 z-planes, each at a thickness of 0.2 μm. Localization analysis was conducted by using the co-localization module of the DeltaVision SoftWoRx 3.5.1 software suite. Results were expressed as the localization index, which was derived from calculating the Pearson's coefficient of correlation values, which in these studies was a measure of localization of the indicated CDT to the Rab9 in each z plane of the cell. In these studies, a localization index value of 1.0 indicates 100% localization of Ec-CdtB or Hd-CdtB to Rab9, whereas a localization index of 0.0 indicates the absence of Ec-CdtB or Hd-CdtB localization to the Rab9. The localization index was calculated from the analysis of a total of 50 images collected over three independent experiments.

Cell binding assays. Mammalian cell binding assays were conducted as previously described (Cao et al., 2005; Lee, Hassane, Cottle, & Pickett, 2003). Cells were seeded (2×10^4/well) in 96-well plates (Fisher). After 18 h, the plates were incubated on ice. After 30 min, the cells were washed two times with ice-cold PBS pH 7.4, and then further incubated on ice with or without biotinylated Ec-CDT or Hd-CDT (at the indicated concentrations) and BSA (3%) in PBS pH

7.4, or mock incubated with BSA (3%) in PBS pH 7.4. After 1 h on ice, the cells were washed three times with ice-cold PBS pH 7.4, and then fixed by adding ice-cold 2% formaldehyde and 0.2% glutaraldehyde, and then further incubated at room temperature. Preliminary studies indicated that maximal binding occurred between 30 and 60 min (not shown). After 15 min, the plate was washed three times with PBS pH 7.4 at room temperature, and then incubated at room temperature with streptavidin-HRP conjugate (1:15,000, GE Healthcare, Little Chalfont, Buckinghamshire, UK) in PBS pH 7.4. After 30 min, the cells were washed five times with PBS pH 7.4, and then incubated at room temperature with TMB Ultra (100 μl, Thermo Scientific). After 30 min, the supernatant from each well was removed and added to an equal volume of sulfuric acid (2 N, Mallinckrodt Baker Inc., Paris, KY) at room temperature. The optical density at 450 nm ($O.D._{450nm}$) was measured using a Biotek Synergy 2 plate reader (Biotek Instruments Inc., Winooski, VT). The $O.D._{450nm}$ measured for supernatants collected from wells containing cells incubated with PBS pH 7.4 alone (background absorbance) was subtracted from the $O.D._{450nm}$ measured for supernatants collected from wells containing cells that had been incubated with Ec-CDT or Hd-CDT. Relative binding was determined by dividing the $O.D._{450nm}$ minus background at each toxin concentration by the $O.D._{450\ nm}$ minus background at the highest concentration of toxin used in these studies (200 nM). The dissociation constants (K_d) were calculated by non-linear regression of the curve generated from plotting relative binding as a function of toxin concentration, using GraphPad Prism (Version 4.03, GraphPad Software, La

Jolla, CA). Competitive binding assays were conducted as described above, except in the absence or presence of 100-fold molar excess of the specified non-biotinylated proteins.

Effects of lectin binding on CDT binding. Cell monolayers were prepared as described above under "*Cell binding assays*." Pre-chilled cells were pre-treated on ice with Euonymus Europaeus Agglutinin lectin (EEA, EY Labs, San Mateo, CA; 40 Mg/ml). After 30 min, the cells were further incubated on ice with or without biotinylated Ec-CDT (100 nM) or Hd-CDT (100 nM) and BSA (3%) in PBS pH 7.4, or mock incubated with BSA (3%) in PBS pH 7.4, in the presence, or absence of 40 Mg/ml EEA. After 30 min on ice, the cells were washed, fixed, and analyzed as described above under "*Cell binding assays*."

Statistics. Unless otherwise indicated, each experiment was performed at least three independent times, each time in triplicate. Statistical analyses were performed using Microsoft Excel (Version 11.0, Microsoft, Redmond, WA) or GraphPad. The *Q*-test was performed to eliminate data that were statistical outliers (Dixon, 1950). Error bars represent standard deviations. All *P* values were calculated with the Student's *t*-test using paired, two-tailed distribution. A *P* value of less than 0.05 indicated that differences in the specified data were considered statistically significant.

2.3. Results

Evaluating the relative sensitivities of mammalian cell lines to Ec-CDT and Hd-CDT. A recent study (Eshraghi et al., 2010) reported that considerably lower concentrations of Hd-CDT than Ec-CDT were required to induce phosphorylation of the histone protein H2AX, a marker of DNA damage, in HeLa, CHO-K1, Balb/3T3, Y-1 cells, OT-1, NIH/3T3, IC-21, and Raw 264.7 cells. To evaluate the relationship between these results and the capacity of Ec-CDT or Hd-CDT to induce G_2/M cell cycle arrest, one of several possible downstream consequences of H2AX activation, we measured cell cycle progression in HeLa and CHO-K1 cells, which have been commonly used as models for studying the function of bacterial toxins, including CDTs (Aragon, Chao, & Dreyfus, 1997; Bag, Ramamurthy, & Nair, 1993; Bouzari & Varghese, 1990; Cope et al., 1997; Cortes-Bratti, Chaves-Olarte, Lagergard, & Thelestam, 1999; Frisan, Cortes-Bratti, Chaves-Olarte, Stenerlow, & Thelestam, 2003; Gelfanova, Hansen, & Spinola, 1999; Johnson & Lior, 1988a, 1988b; Mayer, Bueno, Hansen, & DiRienzo, 1999; Okuda, Kurazono, & Takeda, 1995; Sugai et al., 1998), as a function of Ec-CDT or Hd-CDT concentrations. From the dose response curves, we determined $CCAD_{50}$ (i.e. cell cycle arrest $dose_{50}$) values, which we defined as the toxin concentrations required to induce G_2/M arrest in 50% of the cell population not already in G_2/M. These studies revealed that substantially lower concentrations of Hd-CDT than Ec-CDT were required to induce G_2/M cell cycle arrest in HeLa cells (Figure 2.2). For HeLa cells, $CCAD_{50}$ values of 4 pM and 100 nM were determined for Hd-CDT and Ec-CDT, respectively, indicating that Hd-

CDT is approximately 2.5 x 10^4-fold more potent towards HeLa cells than Ec-CDT (Figure 2.2). In contrast, CHO-K1 cells required only 70-fold higher concentrations of Ec-CDT than Hd-CDT, with $CCAD_{50}$ values of 7 nM and 0.1 nM, respectively (Figure 2.2). These results are consistent with those of the previous study (Eshraghi et al., 2010), which reported that HeLa and CHO-K1 cells required approximately 1.0 x 10^4- and 50-fold higher concentrations, respectively, of Ec-CDT than Hd-CDT to induce H2AX phosphorylation.

We also compared the relative sensitivities towards Hd-CDT and Ec-CDT using two intestinal cell lines (Caco-2, INT-407 cells), which had not been evaluated in the previous study (Eshraghi et al., 2010). These studies revealed that Caco-2 (Figure 2.2) and INT-407 cells (Figure 2.2) were both arrested at the G_2/M interface at considerably lower concentrations of Hd-CDT than Ec-CDT. However, these cell lines again varied in their relative susceptibilities to the two toxins. Caco-2 cells required approximately 3 x 10^2-fold higher concentrations of Ec-CDT ($CCAD_{50}$ = 3 nM) than Hd-CDT ($CCAD_{50}$ = 10 pM), whereas INT-407 cells required approximately 7 x 10^3-fold higher concentrations of Ec-CDT ($CCAD_{50}$ = 40 nM) than Hd-CDT ($CCAD_{50}$ = 6 pM).

To evaluate the possibility that differences in holotoxin stability might underlie the highly divergent cellular potencies of Ec-CDT and Hd-CDT, we investigated the assembly of the heterotrimeric complexes using the dialysis retention assay (Cao et al., 2005; Cao, Volgina, Korostoff, & DiRienzo, 2006). These studies revealed that approximately 60-99% Ec-CDT or Hd-CDT were assembled into holotoxins, as indicated by their retention within dialysis tubing

with a molecular weight cutoff of approximately 100 kDa (Figure 2.3), while CdtC (Figure 2.3) or CdtA or CdtB (data not shown) were not retained. Even in the worst-case scenarios (e.g. 60% holotoxin assembly), the large differences in potencies robustly measured for these two toxins (more than 10^4-fold greater activity for Hd-CDT than Ec-CDT on HeLa cells) cannot readily be attributed to the inability of the holotoxins to assemble.

Relative in vitro DNase activities of Ec-CdtB and Hd-CdtB. CDT-dependent G_2/M arrest of intoxicated cells has been attributed to the activation of cellular DNA repair pathways (Hassane, Lee, & Pickett, 2003; Li et al., 2002) in response to the DNase I-like enzymatic activity associated with the CdtB subunit of several CDTs, including Ec-CDT (C. A. Elwell & Dreyfus, 2000; Lara-Tejero & Galan, 2000) and Hd-CDT (Frisk et al., 2001). To evaluate whether or not differences in the sensitivities of HeLa cells to Ec-CDT and Hd-CDT might be associated with the intrinsic catalytic properties of the CdtB subunits of each toxin, the *in vitro* DNase activities of the purified recombinant Ec-CdtB and Hd-CdtB subunits (in the absence of CdtA and CdtC) were compared. These studies revealed that both Ec-CdtB and Hd-CdtB demonstrated similar DNase activity in a dose-dependent manner (Figure 2.4). Consistent with previous reports (Cao et al., 2005; Frisk et al., 2001; Lara-Tejero & Galan, 2000), Ec-CdtA, Ec-CdtC, Hd-CdtA, or Hd-CdtC did not yield detectable DNase activity (data not shown). These results support the idea that the disparity in cellular potencies of Ec-CDT and Hd-CDT are not likely due to intrinsic divergence in the DNase activities between these toxins' catalytic subunits.

Both Ec-CDT and Hd-CDT are taken up from the plasma membrane into cells within 10 min. Several studies have reported that ectopic expression of CdtB within mammalian cells is sufficient to induce cell cycle arrest in G_2/M, even in the absence of CdtA and CdtC (C. Elwell, Chao, Patel, & Dreyfus, 2001; Lara-Tejero & Galan, 2000; Li et al., 2002; Nishikubo et al., 2003), strongly supporting a model that CdtB acts from an intracellular location. To evaluate the possibility that differences in cell sensitivity to Ec-CDT and Hd-CDT may be due to large disparities between the times required for toxin uptake from the cell surface, we examined the internalization of both toxins into HeLa cells using DIC/fluorescence microscopy. These experiments revealed that under conditions non-permissive for cell entry (4 °C), both Ec-CDT and Hd-CDT were visible at the cell surface (Figure 2.5A, C), indicating that both toxins were bound to the plasma membrane. When the temperature was raised to 37 °C to induce conditions permissive for uptake, both toxins were visible within the cell after just 10 min (Figure 2.5B, D), indicating that Ec-CDT and Hd-CDT were both efficiently internalized from the plasma membrane into cells.

Effect of BFA on toxin-induced G_2/M cell cycle arrest. Hd-CDT mediated cell cycle arrest has been demonstrated to be sensitive to the action of BFA, which disrupts retrograde protein transport from the Golgi complex to the ER (Cortes-Bratti, Chaves-Olarte, Lagergard, & Thelestam, 2000; Guerra et al., 2005), suggesting that this toxin is trafficked by a retrograde mechanism (Blanke, 2006). Because the importance of an intact Golgi complex for intoxication of cells with Ec-CDT had not been previously studied, toxin-mediated cell cycle arrest of

HeLa cells was evaluated in the presence or absence of BFA and at approximately the respective $CCAD_{50}$ values of each toxin (e.g. 5 pM for Hd-CDT, and 100 nM for Ec-CDT). These studies revealed that for Ec-CDT, as well as for Hd-CDT, toxin-mediated G_2/M cell cycle arrest was blocked by BFA (Figure 2.6A, B), which supports a model that both toxins are trafficked to the ER via the Golgi complex.

Effects of endosomal acidification inhibitors on toxin-induced G_2/M cell cycle arrest. The finding that Ec-CDT and Hd-CDT-mediated G_2/M cell cycle is blocked in the presence of BFA prompted us to further evaluate host cell requirements associated with transport from the cell surface to the ER. Transport of a subset of intracellular acting bacterial toxins within the cell requires the lowering of pH within the lumen of endocytic compartments (Blanke, 2006). While an earlier study (Cortes-Bratti et al., 2000) reported that Hd-CDT mediated G_2/M cell cycle arrest in HeLa cells was inhibited by several agents that block endosome acidification, the requirement for endosome acidification associated with Ec-CDT mediated G_2/M cell cycle arrest had not previously been reported. As previously demonstrated (Cortes-Bratti et al., 2000), Hd-CDT mediated G_2/M cell cycle arrest in HeLa cells was inhibited (Figure 2.7A, B) by the lysosomotropic amine, ammonium chloride (Mellman, Fuchs, & Helenius, 1986). In contrast, Ec-CDT mediated cell cycle arrest was not blocked in the presence of NH_4Cl (Figure 2.7A, B). Moreover, bafilomycin A_1, which blocks acidification of intracellular vacuoles by an alternative mechanism, inhibiting the action of vacuolar ATPases (Bowman, Siebers, & Altendorf, 1988), also blocked Hd-CDT-

mediated, but not Ec-CDT-mediated G_2/M cell cycle arrest (Figure 2.7C, D). Finally, the polyether ionophore monensin, which is known to block intracellular protein transport by collapsing proton gradients as a sodium/proton antiporter (Mollenhauer, Morre, & Rowe, 1990), and, the potassium/proton carboxylic ionophore, nigericin (Mellman et al., 1986), both blocked Hd-CDT-mediated, but not Ec-CDT-mediated G_2/M cell cycle arrest (Figure 2.7E). The sensitivity of cells to Ec-CDT was modestly, but reproducibly, elevated in the presence of agents that block acidification of endosomal compartments (Figure 2.7), but we do not currently understand the basis for the slight enhancement in Ec-CDT cellular activity.

Essentially identical results were obtained when using CHO-K1 cells in the presence of NH_4Cl, bafilomycin A1, monensin, or nigericin (data not shown), indicating that the disparate effects of agents that block endosomal acidification on Ec-CDT- or Hd-CDT-mediated cell cycle arrest in G_2/M are not idiosyncratic to HeLa cells. Additional studies confirmed that neither the cellular binding nor the uptake of either Ec-CDT or Hd-CDT into cells from the plasma membrane was affected by NH_4Cl, bafilomycin A1, monensin, or nigericin (data not shown).

To more quantitatively assess whether the presence of the His-tag on the amino-terminus of the recombinant CDT subunits might alter CDT intracellular trafficking, we compared the dose-response curves of the His-tagged and non-His-tagged forms of Ec-CDT and Hd-CDT in the presence or absence of NH_4Cl or bafilomycin A1, both of which inhibited Hd-CDT-mediated G_2/M cell cycle arrest, but not Ec-CDT-mediated G_2/M cell cycle arrest. These studies revealed

that the dose response curves of the His-tagged and non-His-tagged forms of Ec-CDT and Hd-CDT were essentially identical in the presence or absence of NH_4Cl or bafilomycin A1 (Figure 2.1). Taken together, these data indicated that Ec-CDT-mediated G_2/M cell cycle arrest does not require acidification of endosomal compartments, suggesting that Ec-CDT and Hd-CDT are transported from the cell surface to the ER by different pathways.

Effects of inhibiting endosomal acidification on toxin-transport to the ER. While an earlier study indicated that Hd-CDT mediated G_2/M cell cycle arrest in HeLa cells was inhibited by several agents that block endosome acidification (Cortes-Bratti et al., 2000), the importance of endosome acidification for localization of Ec-CDT or Hd-CDT to the ER, the organelle from which CdtB subunits have been proposed to be translocated to the cytosol (Gargi et al., 2012), has not been reported. To evaluate whether acidification of endosomal vesicles is required for intracellular toxin transport to the ER, we used fluorescence microscopy to determine whether Ec-CDT or Hd-CDT localization to the ER is altered in the presence of NH_4Cl. These studies revealed that Ec-CDT localization to the ER is not visibly altered in the presence of NH_4Cl (Figure 2.8A, B, E). In contrast, Hd-CDT localization to the ER was significantly reduced in the presence of NH_4Cl (Figure 2.8C, D, E). Several attempts to evaluate CDT localization specifically to the ER using biochemical fractionation approaches were inconclusive due to the inability to satisfactorily resolve the ER from other membrane-containing fractions, with the exception of the nucleus. These results indicate that transport to the ER of Hd-CDT, but not Ec-CDT, requires

acidification of endosomal vesicles, and moreover, suggests that Ec-CDT and Hd-CDT may be transported to the ER via different trafficking pathways.

Effects of endosomal acidification inhibitors on CdtB localization to the nucleus. Previous reports that CdtB possesses *in vitro* DNase I-like activity (C. A. Elwell & Dreyfus, 2000; Lara-Tejero & Galan, 2000) and localizes to the nucleus when expressed ectopically within the cytosol of mammalian cells (McSweeney & Dreyfus, 2004; Nishikubo et al., 2003; Wising et al., 2010), supports a model that this CDT subunit functions within the nucleus of intoxicated cells. To evaluate whether acidification of endosomal vesicles is required for intracellular toxin transport to the nucleus, we fractionated cells intoxicated for 60 min with Ec-CDT or Hd-CDT in the absence or presence of bafilomycin A1, and used western blotting to determine whether the localization of the CdtB subunit is altered when endosomal acidification was prevented. These studies revealed that most of the internalized Ec-CdtB or Hd-CdtB was associated with the nuclear fraction (Figure 2.9), while neither CdtB subunit was associated with either the cytosolic or microsomal fractions. In contrast to the CdtB subunits, neither the CdtA or CdtC subunits of Ec-CDT or Hd-CDT were detected within the nuclear fractions (data not shown), which is consistent with the model that only the A fragments of retrograde-trafficked bacterial toxins are translocated out of the ER (Blanke, 2006) and more recently, with immunofluorescence studies of the intracellular trafficking of CDT from *Aggregatibacter actinomycetemcomitans* (Damek-Poprawa, Jang, Volgina, Korostoff, & DiRienzo, 2012).

Ec-CdtB was detected within the nuclear fractions prepared from cells that had been incubated with Ec-CDT holotoxin in the presence or absence of bafilomycin A1 (Figure 2.9). In contrast, Hd-CdtB was not detected in either the nuclear fraction or whole cell lysates prepared from cells that had been incubated with Hd-CDT holotoxin in the presence of bafilomycin A1 (Figure 2.9). We speculate that in the presence of bafilomycin A1, Hd-CdtB is either degraded within the endolysosomal system or, alternatively, recycled back to the cell surfaces and released, although we did not investigate either of these possibilities further. These results indicate that the transport of Hd-CdtB, but not Ec-CdtB, to the nucleus requires acidification of endosomal vesicles.

Comparing the importance of late-endosome-targeted carrier vesicle biogenesis for Ec-CDT-and Hd-CDT-mediated H2AX phosphorylation. One of the consequences resulting from inhibition of the V-ATPase-mediated pH drop is inhibition of endosomal carrier vesicle formation, which facilitates transport between endosomal compartments (Hurtado-Lorenzo et al., 2006). To more directly evaluate the importance of late-endosome-targeted carrier vesicle transport for the intracellular activity of Ec-CDT or Hd-CDT, we compared toxin-dependent phosphorylation of H2AX in cells expressing a dominant negative (DN) form of Rab7, a small GTPase required for late-endosome-targeted carrier vesicle biogenesis (Vonderheit & Helenius, 2005). Transiently transfected HeLa cells expressing Rab7 (T22N) fused to DsRed, (DN-DsRed-Rab7 (T22N)), which is defective in nucleotide exchange and has a reduced affinity for GTP (Spinosa et al., 2008) were incubated with either Ec-CDT or Hd-CDT. After 8 h, the

monolayers were examined using fluorescence microscopy to quantify the number of cells with phosphorylated H2AX (p-H2AX). Because approximately 40%-60% of the cells in any well were discovered to be expressing DN-DsRed-Rab7 (T22N), H2AX phosphorylation could be monitored within the same well in both transfected and non-transfected cells. These studies revealed significantly fewer DN-DsRed-Rab7 (T22N) expressing cells with p-H2AX activation than in non-transfected cells (Figure 2.10), supporting the idea that toxin trafficking from early to late endosomal compartments is important for the biological activity of Hd-CDT but not Ec-CDT.

Comparing the importance of late-endosome-targeted carrier vesicle biogenesis for Hd-CdtB trafficking to the nucleus. Because the biological activity of CDTs is generally considered to require their CdtB subunits to function within the nucleus of intoxicated cells (Gargi et al., 2012), we hypothesized that DN-DsRed-Rab7 (T22N) blocked the cellular activity of Hd-CDT by inhibiting the transport of Hd-CdtB to the nucleus. To evaluate this hypothesis, the nuclear localization of Ec-CdtB and Hd-CdtB was compared within transiently transfected HeLa cells expressing DN-DsRed-Rab7 (T22N) to non-transfected HeLa cells. These studies revealed significantly less Hd-CdtB localized to the nucleus of cells expressing DN-DsRed-Rab7 (T22N) than in non-transfected cells (Figure 2.11). In contrast, Ec-CdtB was localized to the nucleus to approximately the same extent in cells expressing or not expressing DN-DsRed-Rab7 (T22N) (Figure 2.11), indicating that late-endosome-targeted carrier vesicle biogenesis is important for intracellular trafficking of Hd-CdtB, but not Ec-CdtB.

Comparing the localization of Ec-CDT-and Hd-CDT to Rab9-enriched vesicles. Because late-endosome-targeted carrier vesicle biogenesis is required to transport cargo from early to late vesicles within the endolysosomal system, we hypothesized that Hd-CdtB, but not Ec-CdtB is transported through late endosomal vesicles. To evaluate this hypothesis, we used fluorescence imaging to investigate the localization of Ec-CdtB and Hd-CdtB to vesicles enriched with the small GTPase Rab9, which contributes to the generation and maintenance of late endocytic compartments (Ganley, Carroll, Bittova, & Pfeffer, 2004). These experiments revealed that after 30 min, visibly more Hd-CdtB co-localized with Rab9-enriched puncta than Ec-CdtB (Figure 2.12), supporting the hypothesis that Hd-CdtB, but not Ec-CdtB, is transported through late endosomal vesicles. Taken together with the data presented above indicating the importance of late-endosome-targeted carrier vesicle biogenesis for Hd-CDT but not Ec-CDT, these results suggest that the catalytic CdtB subunits of these two toxins are trafficked along distinct pathways.

Relative cell binding of Ec-CDT and Hd-CDT. Analogous to all intracellular-acting bacterial exotoxins (Blanke, 2006), CDTs must bind to the surface of target cells prior to internalization (Cao et al., 2008; Mise et al., 2005). Studies to evaluate the binding of Ec-CDT and Hd-CDT to HeLa cells as a function of toxin concentration revealed that both Ec-CDT and Hd-CDT yielded saturable binding curves (Figure 2.13A, B). Moreover, the presence of a 100-fold molar excess of non-biotinylated toxins inhibited the dose-dependent cell association of biotinylated toxins, indicating that the binding of both Ec-CDT and

Hd-CDT was largely specific, with K_d values for specific binding of 172 (±27) nM (Figure 2.13A) and 169 (±35) nM (Figure 2.13B), respectively.

Despite binding to the cell surface with similar properties, it was not clear whether Ec-CDT and Hd-CDT were binding to the same or discrete plasma membrane receptors. To differentiate between these possibilities, we evaluated whether Ec-CDT and Hd-CDT bind competitively to the surface of HeLa cells. These studies revealed that the binding of biotinylated Ec-CDT to the cell surface was inhibited to a greater extent by 100-fold molar excess of unlabeled Ec-CDT than a 100-fold molar excess of unlabeled Hd-CDT (Figure 2.14A). In a similar manner, cell surface binding of biotinylated Hd-CDT was found to be inhibited to a greater extent by 100-fold molar excess of unlabeled Hd-CDT than a 100-fold molar excess of unlabeled Ec-CDT (Figure 2.14B). These data suggest that while the interactions of both Ec-CDT and Hd-CDT with host cells are largely specific, the two toxins may bind to distinct cell surface components. In further support of this idea, the cell surface binding of Ec-CDT, but not Hd-CDT, was partially inhibited in the presence of EEA, a fucose-specific lectin that was previously reported to antagonize Ec-CDT binding to HeLa cells (McSweeney & Dreyfus, 2005) (Figure 2.14C).

2.4. Discussion

The studies presented here revealed differences in the manner in which CDTs from two unrelated pathogenic bacteria intoxicate mammalian cells. Hd-

CDT induces G_2/M cell cycle arrest at substantially lower concentrations than Ec-CDT in all tested cell lines (Figure 2.S1), consistent with a recent report demonstrating that Hd-CDT induces H2AX activation within cells at lower concentrations than Ec-CDT (Eshraghi et al., 2010). The high level of dissimilarity between the protein sequences of the CdtA and CdtC subunits (22% and 19% sequence identity, respectively) does not readily reveal the reasons underlying the divergent potencies of Ec-CDT and Hd-CDT, but is consistent with the idea that these two toxins may interact with and intoxicate cells by disparate mechanisms. Indeed, although both Ec-CDT and Hd-CDT possess similar *in vitro* DNase activities exhibited by their catalytic CdtB subunits (Figure 2.1), are both efficiently taken up by cells (Figure 2.S3), and both require an intact Golgi complex to induce G_2/M cell cycle arrest (Figure 2.2), divergence was discovered in the cellular requirements associated with intracellular toxin transport (Figures 2.3 – 2.8). Hd-CDT-mediated G_2/M arrest and ER localization were inhibited by agents that prevent acidification of endosomal compartments, while Ec-CDT-mediated G_2/M arrest and ER localization were not affected.

How might the requirement for acidification of endosomal compartments relate to the cyclomodulatory activities of Ec-CDT and Hd-CDT? Intoxication of cells by a subset of intracellular-acting bacterial toxins requires a drop of the luminal pH within endosomal compartments (Abrami, Reig, & van der Goot, 2005; Blanke, 2006; Daro, Sheff, Gomez, Kreis, & Mellman, 1997; Sandvig & van Deurs, 2005; Tweten, 2005), which is a normal step in vesicle maturation carried out by the proton-pumping vacuolar ATPase (V-ATPase) (Nishi & Forgac, 2002;

Sun-Wada, Wada, & Futai, 2003, 2004). For diphtheria, anthrax, or botulinum toxins, the pH drop induces conformational changes in the toxin structure required for insertion into the endosomal membrane and translocation of the catalytic fragment into the cytosol (Blanke, 2006; Montecucco, Papini, & Schiavo, 1994). However, preventing acidification of endosomal compartments can also stall the trafficking of proteins along the endosomal pathway, such as the mannose 6-phosphate receptor that is normally transported from late endosomal vesicles to the Golgi complex (Lombardi et al., 1993; Riederer, Soldati, Shapiro, Lin, & Pfeffer, 1994). Inhibition of the V-ATPase-mediated pH drop inhibits trafficking by blocking the formation of endosomal carrier vesicles, which facilitate transport between endosomal compartments (Hurtado-Lorenzo et al., 2006). The finding that the presence of NH_4Cl or bafilomycin A1 significantly inhibited localization of Hd-CDT to the ER (Figure 2.4) or nucleus (Figure 2.5) respectively, suggests that Hd-CDT intoxication requires an intracellular transport pathway involving late endosomal compartments. This idea is further supported by the importance of Rab7, which regulates the biogenesis at early endosomes of transport vesicles targeted for late endosomal compartments (Figures 2.6, 2.7), as well the co-localization of Hd-CdtB with Rab9 (Figure 2.8).

In contrast, our data support a model that Ec-CDT transport to the ER occurs by a mechanism independent of late endosome-mediated trafficking. Notably, several reports have indicated that the retrograde transport mechanisms of other toxins, including Shiga toxin (Mallard et al., 1998), cholera toxin (Lencer et al., 1995; Orlandi, Curran, & Fishman, 1993), or ricin (Simpson, Dascher,

Roberts, Lord, & Balch, 1995), are also insensitive to agents that prevent endosomal acidification, suggesting that these toxins are transported from early endocytic vesicles to the ER through a pathway that bypasses late endosomal compartments. Additional experimental work will be required to more completely define the Ec-CDT and Hd-CDT intracellular trafficking mechanisms, but we speculate that the overall pathway of Ec-CDT transport to the ER may be more similar to that used by Shiga toxin, cholera toxin, or ricin, than the pathway used by Hd-CDT.

The molecular basis underlying the putative targeting of Ec-CDT and Hd-CDT to discrete intracellular trafficking pathways is unclear. However, based on the inability of Ec-CDT or Hd-CDT to competitively bind to the surface of cells (Figure 2.10A, B), we hypothesize that the two toxins utilize distinct cell surface receptors. Inhibition of the cell surface binding of Ec-CDT, but not Hd-CDT, by the fucose-specific lectin EEA (Figure 2.10C) further supports this idea. Receptor recognition and binding is critical for the function of intracellular-acting toxins because the receptor, in part, functions as a molecular “carrier” whose normal uptake and trafficking through the cell directly impacts the final cellular destination of the toxin (Blanke, 2006). A cell surface receptor for Hd-CDT has not yet been identified, but a genetic screen using the KBM7 chronic myeloid leukemia cell line revealed that a putative G protein–coupled receptor, TMEM181, contributes to cellular binding and sensitivity to Ec-CDT (Carette et al., 2009). Our competition studies (Figure 2.10) suggest that Hd-CDT and Ec-CDT do not share the same receptor, but we cannot rule out the possibility of a

role for TMEM181 in conferring cell sensitivity to Hd-CDT. Consistent with the idea that Ec-CDT and Hd-CDT may bind to different receptors on the surface of sensitive cells, a recent study reported that a mutant CHO cell line, characterized by abbreviated glycan sequences on membrane glycoproteins and glycolipids, was hypersensitive to Hd-CDT, but demonstrated the same sensitivity as the parental CHO cells to Ec-CDT (Eshraghi et al., 2010).

Comparing the molecular and structural basis for Ec-CDT and Hd-CDT receptor recognition is currently challenging because, even though the crystal structure has been solved for Hd-CDT (Nesic et al., 2004), high-resolution structural data is not yet available for the Ec-CDT holotoxin. The highly dissimilar protein sequences of the CdtA and CdtC subunits of Ec-CDT and Hd-CDT are consistent with the idea that these two toxins may interact with and intoxicate cells by disparate mechanisms. Additional studies will also be required to determine whether or not differences in intracellular trafficking pathways between Ec-CDT and Hd-CDT directly contribute to the disparity in the potencies exhibited by the two toxins towards sensitive cells. Nonetheless, we speculate that differential cell surface requirements for toxin association is critical for targeting Ec-CDT and Hd-CDT to their respective uptake and intracellular trafficking pathways.

Multiple factors could potentially contribute to the differences in cellular potencies of Ec-CDT and Hd-CDT. For example, discrepancies in the cytosolic localization of the respective CdtB subunits, which is widely thought to precede localization to the nucleus, may contribute to differences in toxin potencies. In

studies to compare the levels of Ec-CdtB and Hd-CdtB within the cytosol of intoxicated cells, we could not detect Ec-CdtB and Hd-CdtB by either fluorescence microscopy or cellular fractionation and western blot analysis (data not shown). We speculate that the levels of Ec-CdtB and Hd-CdtB within the cytosol in these experiments were below our detection limits. A recent study reported the detection of a fluorescent version of CdtB from *A. actinomycetemcomitans* within the cytosol and nucleus (Damek-Poprawa et al., 2012). On the other hand, in another recent study, the authors suggested that Hd-CdtB localization to the nucleus not require that this subunit to be first translocated to the cytosol (Guerra et al., 2009).

In summary, we have identified differences in the intoxication pathways used by CDTs from pathogens that colonize two distinct niches. Because CDTs are generally believed to disrupt the normal functions of epithelial and immune cells comprising the mucosal barrier (Nougayrede et al., 2005; Oswald et al., 2005), we speculate that Ec-CDT and Hd-CDT may have evolved divergently in response to the specific tissue and cell tropisms of the pathogenic microbes that produce these toxins. Finally, these results provide experimental evidence that caution must be applied when extrapolating the properties of individual CDTs to the entire family of these toxins.

2.5. Figures

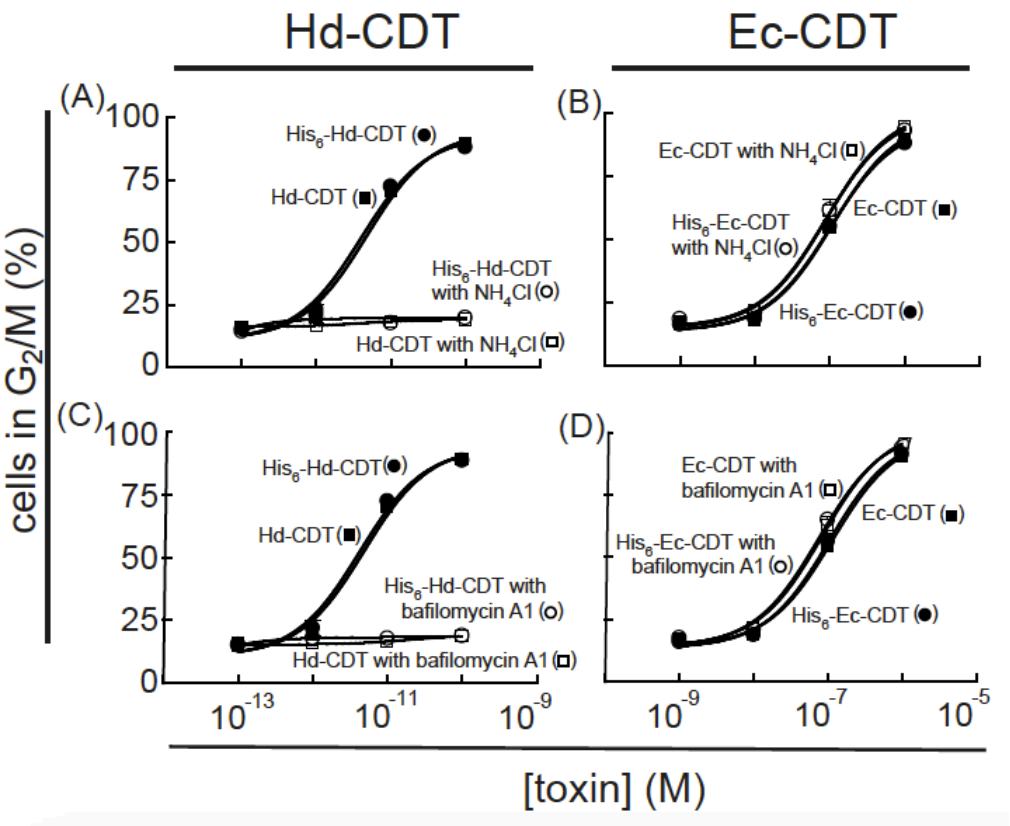

Figure 2.1. Effect of N-terminal His-tag on the activities of Ec-CDT and Hd-CDT. Monolayers of HeLa cells were incubated in presence of the indicated concentrations of Hd-CDT (A, C) or Ec-CDT (B, D), with (circle) or without (square) N-terminal His-tag, in the presence (empty circle or square), or absence (filled circle or square), of NH_4Cl (A, B) or bafilomycin A1 (C, D). After 24 h, the cells were analyzed for arrest in G_2/M using flow cytometry, as described under "Experimental Procedures." The data, which were combined from three independent experiments, were rendered as the percentage of cells in G_2/M as a function of toxin concentration.

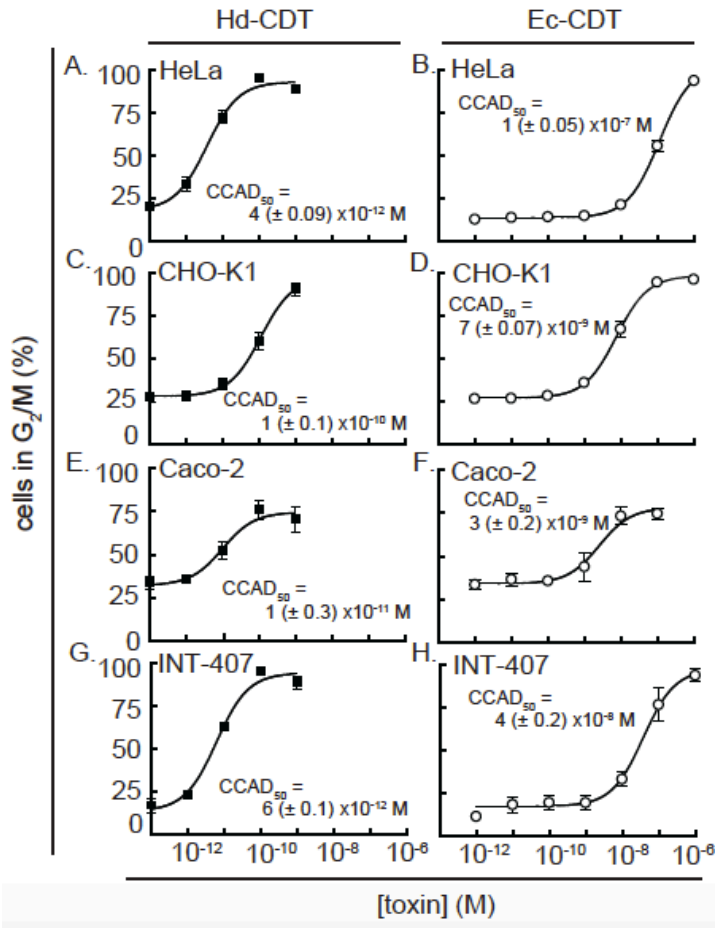

Figure 2.2. Cell line sensitivities to Ec-CDT or Hd-CDT. Monolayers of HeLa (A, B), CHO-K1 (C, D), Caco-2 (E, F), or INT-407 (G, H) cells were incubated in the absence or presence of Hd-CDT (filled squares, 10-13-10-9 M; A, C, E, G) or Ec-CDT (empty circles; 10^{-12}-10^{-6} M; B, D, F, H). After 48 h, the cells were analyzed for arrest in G2/M using flow cytometry, as described under "Experimental Procedures." The data were rendered as the percentage of cells in G_2/M as a function of toxin concentration. For each cell line, there were characteristic differences in the baseline average of untreated cells in G_2/M, as well as the maximum number of toxin-treated cells arrested in G_2/M. The value associated with each dose-response curve is the $CCAD_{50}$ value (+/- standard deviation), which was determined as described under "Experimental Procedures," and derived from data combined from three or more independent experiments.

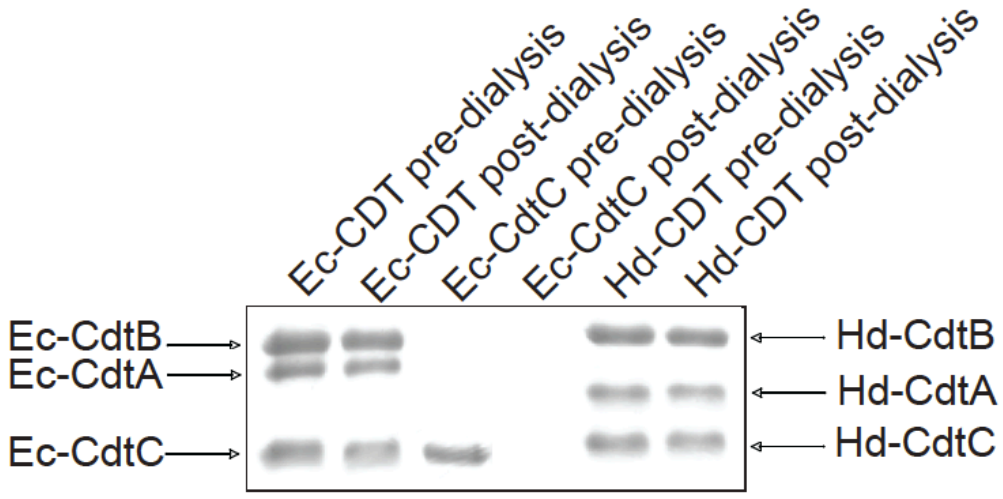

Figure 2.3. Dialysis retention assay of Ec-CDT and Hd-CDT. The assembled Ec-CDT and Hd-CDT holotoxins, as well as the Ec-CdtC subunit alone, were dialyzed in 100 kDa molecular mass cut-off dialysis tubing at 4 °C against four changes of PBS pH 7.4 (total dialysis exchange factor of 1.6 x 10^9) for a total time of 24 h. Identical amounts of dialyzed (labeled as “post-dialysis”) and non-dialyzed (labeled as “pre-dialysis”) samples, were resolved using SDS-PAGE and visualized after staining with Coomassie Brilliant blue and destaining. The data shown are representative of those collected for every preparation of the Ec-CDT or Hd-CDT holotoxins.

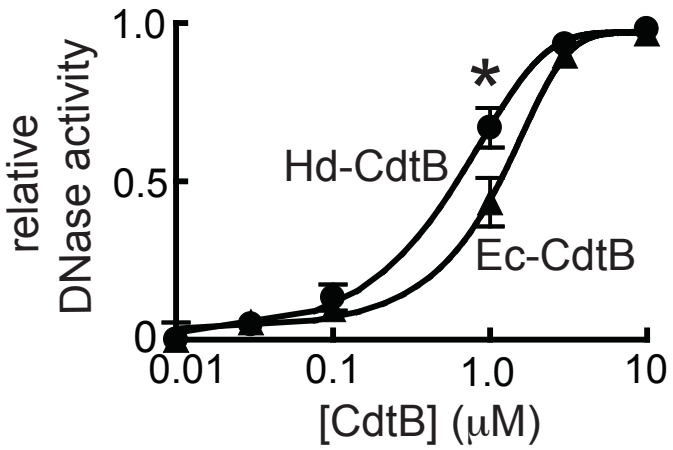

Figure 2.4. *In vitro* DNase activities of Ec-CdtB and Hd-CdtB. The DNase activities of Ec-CdtB (filled triangles) and Hd-CdtB (filled circles) were determined as described under Experimental Procedures, and plotted as a function of toxin concentration. The rendered data were combined from three independent experiments, each conducted in triplicate. Error bars indicate standard deviations. Statistical significance was calculated for the differences in relative DNase activities at the indicated concentrations of Ec-CdtB and Hd-CdtB. * indicates $P < 0.05$.

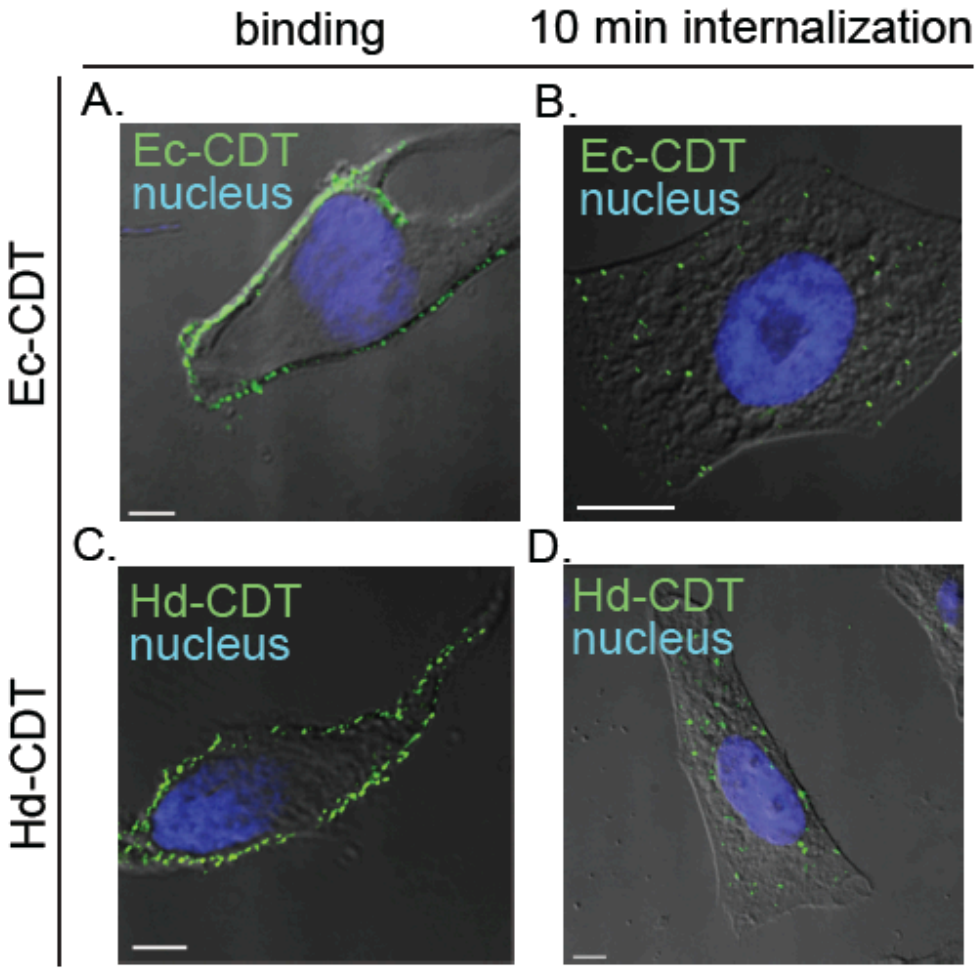

Figure 2.5. Fluorescence microscopy analysis of Ec-CDT and Hd-CDT uptake into cells. Binding (A, C) or internalization (10 min; B, D) of Ec-CDT (A, B) or Hd-CDT (C, D) (both at 100 nM) into HeLa cells was visualized using DIC/fluorescence microscopy, as described under Experimental Procedures. The data were rendered as a single z-plane (5 μm depth within each cell). Green puncta indicate Ec-CDT or Hd-CDT, as indicated, and blue indicates the DAPI-stained nucleus. White bars indicate 10 μm. The data shown are representative of images collected during three independent experiments.

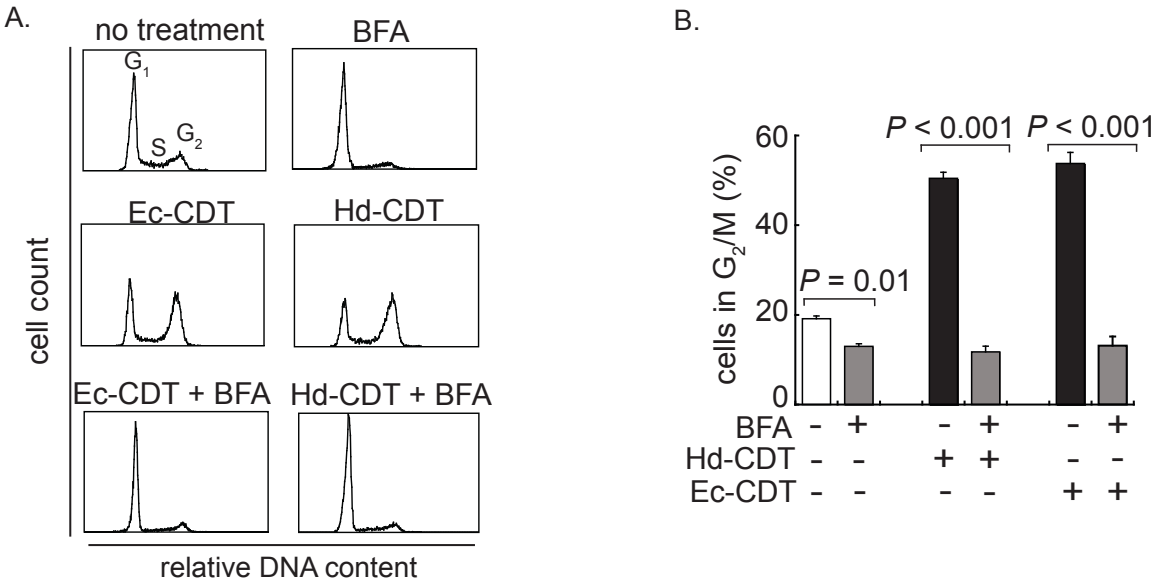

Figure 2.6. Effects of BFA on Ec-CDT- or Hd-CDT-induced cell cycle arrest. Ec-CDT (100 nM)- or Hd-CDT (5 pM)-mediated arrest of HeLa cells in G_2/M was determined in the absence or presence of BFA (0.2 μg/ml). (A) The data are rendered as individual histograms representative of those collected during three independent experiments. Histograms indicate the number of cells (y axis, same scale for each histogram) at a given PI fluorescence intensity (x axis, same scale for each histogram), with, as indicated in the top left histogram, the left peak representing cells in G_0/G_1 phase (designated as G_1) of the cell cycle, the right peak representing cells in G_2/M (designated as G_2), and the area between the peaks representing cells in S phase (designated as S). The results are rendered as bar graphs generated from data combined from three or more independent experiments that compare the percentage of cells arrested in G_2/M in untreated cells (white bar), cells treated with either Ec-CDT or Hd-CDT, as indicated, in the absence of BFA (black bars), or cells treated with BFA in the absence or presence of Ec-CDT or Hd-CDT, as indicated (gray bars). Error bars represent standard deviations. Statistical significance was calculated for the differences between cell populations incubated in the absence or presence of BFA.

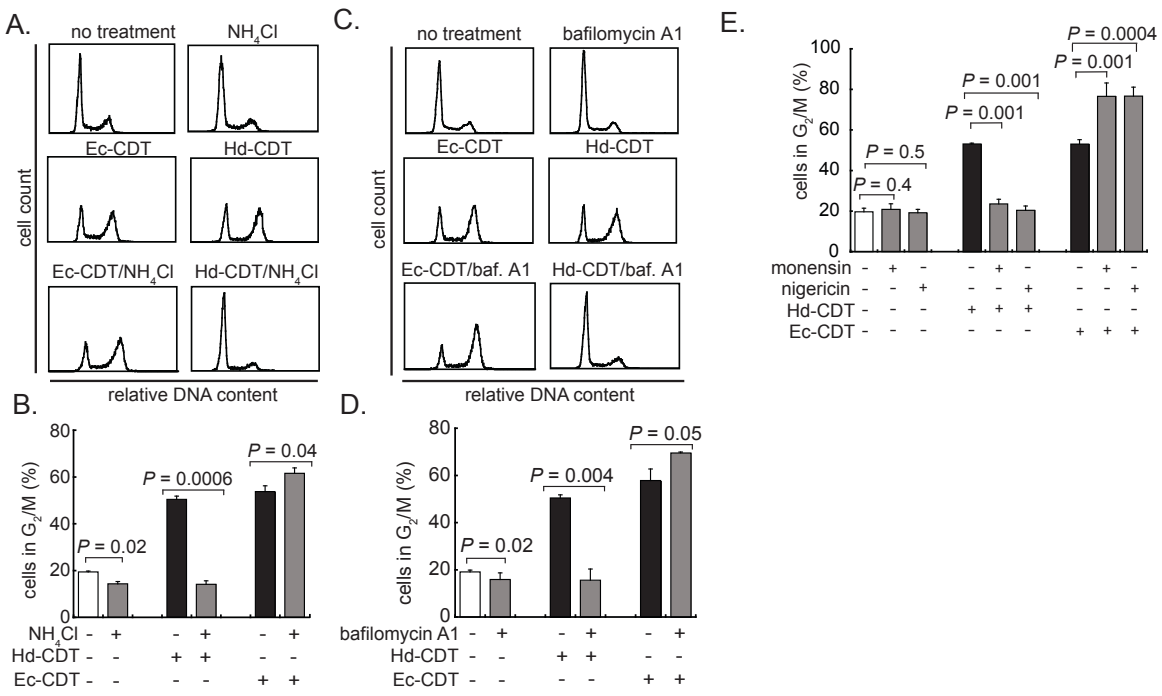

Figure 2.7. Effects of agents that inhibit acidification of endosomal compartments on Ec-CDT- or Hd-CDT-induced cell cycle arrest. Ec-CDT (100 nM)- or Hd-CDT (5 pM)-mediated arrest of HeLa cells in G_2/M was determined, as indicated in the absence or presence of NH_4Cl (20 mM; A, B), bafilomycin A1 (20 nM; C, D), monensin (10 nM; E), or nigericin (100 nM; E). (A, C) The data are rendered as individual histograms representative of those collected during three independent experiments. In (C), bafilomycin A1 is abbreviated as baf. A1 in the 2 lower panels. (B, D, E) The results are rendered as bar graphs generated from data combined from three independent experiments that compare the percentage of cells arrested in G_2/M phase in untreated cells (white bars), cells treated with Ec-CDT or Hd-CDT, as indicated, in the absence of pharmacological agents (black bars), or cells treated with pharmacological agents, as indicated, in the absence or presence of Ec-CDT or Hd-CDT (gray bars). Error bars represent standard deviations. Statistical significance was calculated for the differences between cell populations incubated in the absence or presence of the indicated agent.

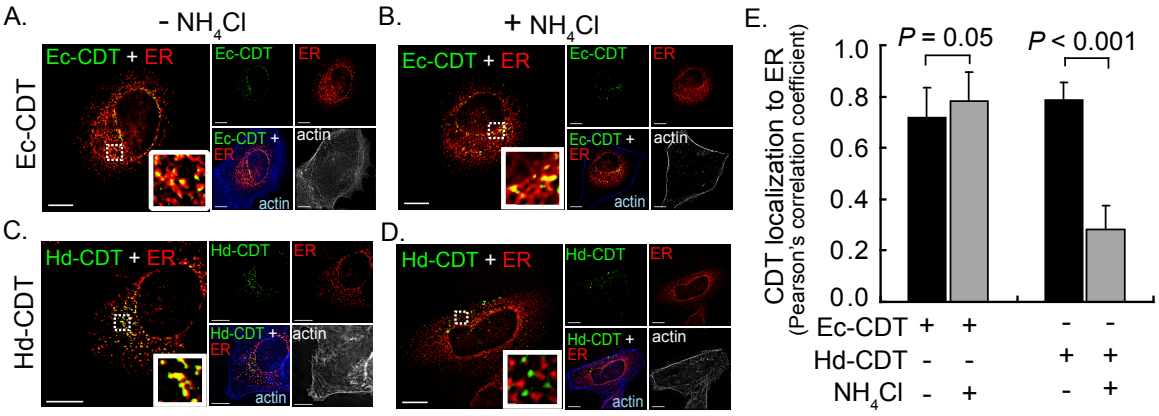

Figure 2.8. Effects of agents that inhibit acidification of endosomal compartments on Ec-CDT or Hd-CDT localization to the ER. HeLa cells that had been transiently transfected with pDsRed2-ER were incubated with Ec-CDT (200 nM; A, B, E) or Hd-CDT (200 nM; C, D, E) at 37 °C for 60 min in the absence (A, C, E) or presence (B, D, E) of NH_4Cl (20 mM), were imaged using fluorescence microscopy. (A-D) Cellular actin was counterstained with phalloidin conjugated with Alexa Fluor 647. Images were representative of those collected from three independent experiments. The data were rendered as a single z-plane (5 μm depth within each cell). As labeled, green puncta indicate either Ec-CDT or Hd-CDT, red puncta indicate ER, white or blue filaments indicate actin, and Ec-CDT or Hd-CDT localized to ER is indicated by yellow puncta. White bars indicate 10 μm. The solid white boxes are digitally enlarged images of the smaller dashed white boxes. (E) The results are rendered as a bar graph generated from data combined from three independent experiments that compare the Pearson's correlation coefficient for Ec-CdtB or Hd-CdtB co-localized with ER in cells treated with Ec-CDT or Hd-CDT, as indicated, in the absence of NH_4Cl (black bars), or cells treated with toxin, as indicated, in the presence of NH_4Cl (gray bars). Error bars represent standard deviations. Statistical significance was calculated for differences in the Pearson's correlation coefficient between cell populations incubated in the presence or absence of NH_4Cl.

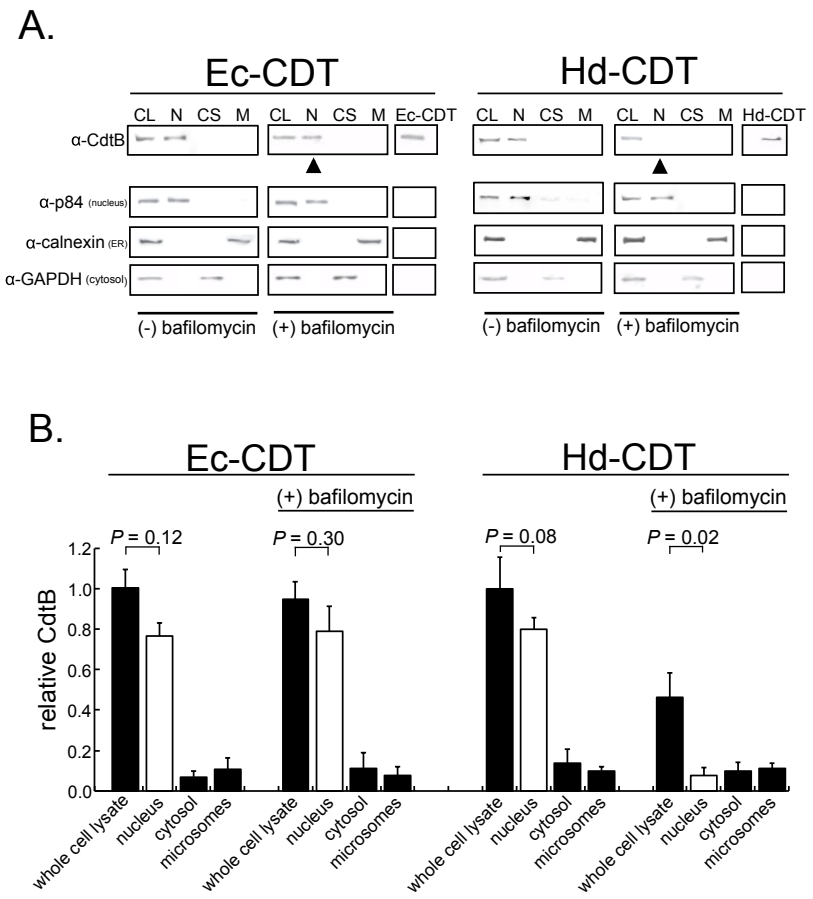

Figure 2.9. Effects of inhibiting acidification of endosomal compartments on Ec-CdtB or Hd-CdtB localization to the nucleus. HeLa cells pretreated with bafilomycin A1 (20 nM) were incubated at 37 °C with either Ec-CDT (100 nM) or Hd-CDT (100 nM). After 30 min, the cells were washed and then further incubated at 37 °C. After another 210 min, the monolayers were lysed and fractionated as described under Experimental Procedures. (A) Western blots are shown, which are representative of three independent experiments. The whole cell lysate (CL), microsomal fraction (M), nuclear fraction (N), and cytosolic fraction (CS) were each analyzed by western blot analysis for CdtB, calnexin (ER marker, representing microsomes), GAPDH (cytosolic marker), and p84 (nuclear matrix marker). Arrowheads indicate CdtB in the nuclear fraction of bafilomycin A1-treated cells. (B) Quantitative rendering of the western blot data for CdtB, as shown in Part (A), using densitometric analysis. For each toxin (Ec-CDT or Hd-CDT) and for each treatment (+/- bafilomycin A1), the data were rendered as bar graphs showing the amount of CdtB in each fraction relative to the pixels for CdtB in the cell lysate normalized to 1.0. The data are combined from 3 independent experiments. Error bars represent standard deviations. Statistical significance was calculated for the difference between amount of CdtB in whole cells lysate (black bar to the left of white), against nuclear fraction (white bar).

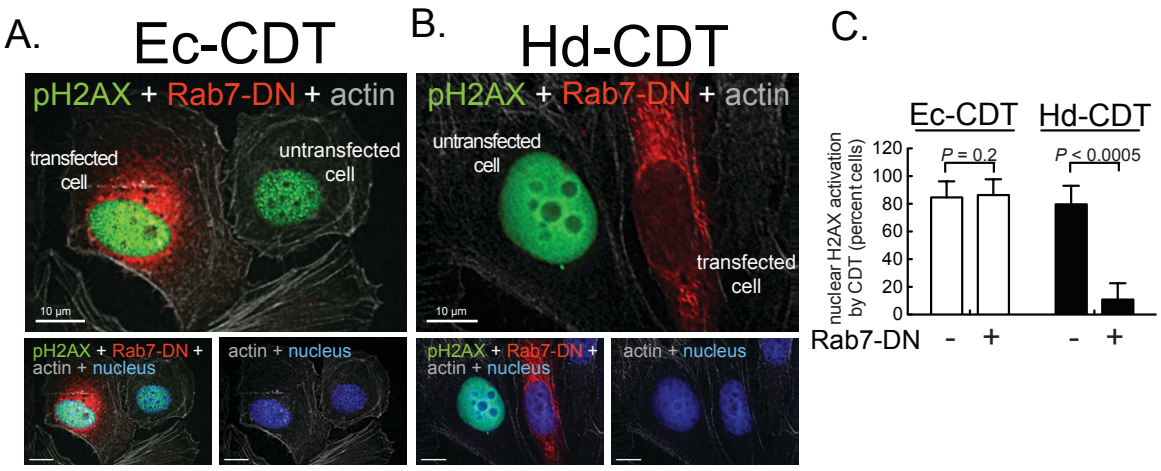

Figure 2.10. Evaluating the effects of ectopic expression of dominant-negative Rab7 (T22N) on Ec-CDT- or Hd-CDT-mediated activation of H2AX. HeLa cells that had been transiently transfected with a plasmid harboring the gene encoding dominant negative DsRed-Rab7 (T22N) (Rab7-DN) were incubated with Ec-CDT (200 nM; A, C) or Hd-CDT (200 nM; B, C) at 37 °C. After 8 h, the monolayers were fixed and imaged using fluorescence microscopy. (A and B) Cellular actin was counterstained with phalloidin conjugated with Alexa Fluor 647. Images were representative of those collected from three independent experiments. The data were rendered as a single z-plane (5 μm depth within each cell). As labeled, green puncta indicate phospho-H2AX (pH2AX), red puncta indicate Rab7-DN, white filaments indicate actin, and the blue staining indicates the nucleus. White bars indicate 10 μm. (C) Quantification of Ec-CDT- or Hd-CDT-mediated activation of H2AX. The data, which were combined from three independent experiments, are rendered as the percentage of cells within the monolayers with activated H2AX, as indicated by presence of green fluorescence within the nucleus, relative to untransfected cells.

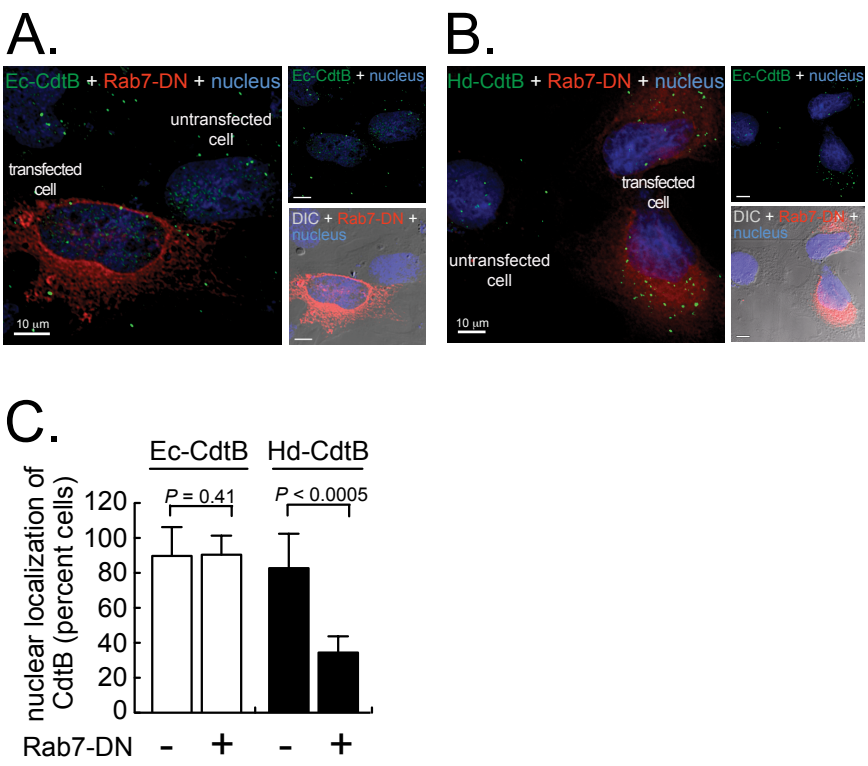

Figure 2.11. Effects of ectopic expression of dominant-negative Rab7 (T22N) on Ec-CdtB or Hd-CdtB localization to the nucleus. HeLa cells that had been transiently transfected with a plasmid harboring the gene encoding dominant negative DsRed-Rab7 (T22N) (Rab7-DN), were chilled to 0 °C on ice for 30 min, and then incubated on ice with either Ec-CDT (200 nM) or Hd-CDT (200 nM), both of which had also been pre-chilled on ice. After 30 min, the cells were washed once with ice-cold PBS pH 7.4, and then further incubated at 37 °C. After 60 min, the monolayers were fixed and evaluated by fluorescence imaging. (A and B) Images were representative of those collected from three independent experiments. The data were rendered as a single z-plane (approximately 5 μm depth within each cell). As labeled, green puncta indicate either Ec-CdtB (A) or Hd-CdtB (B), red puncta indicate cells expressing DsRed-Rab7-DN, and the blue staining indicates the nucleus. White scale bars indicate 10 μm. (C) The results are rendered as a bar graph generated from data combined from three independent experiments that compare the percentage of cells with at least one green puncta (corresponding to either Ec-CdtB (white bars) or Hd-CdtB (black bars)) localized to the nucleus in cells expressing or not expressing Rab7-DN. Error bars represent standard deviations. Statistical significance was calculated for differences in the percentage of nuclear localization of either Ec-CdtB or Hd-CdtB between cell populations expressing or not expressing DsRed-Rab7-DN.

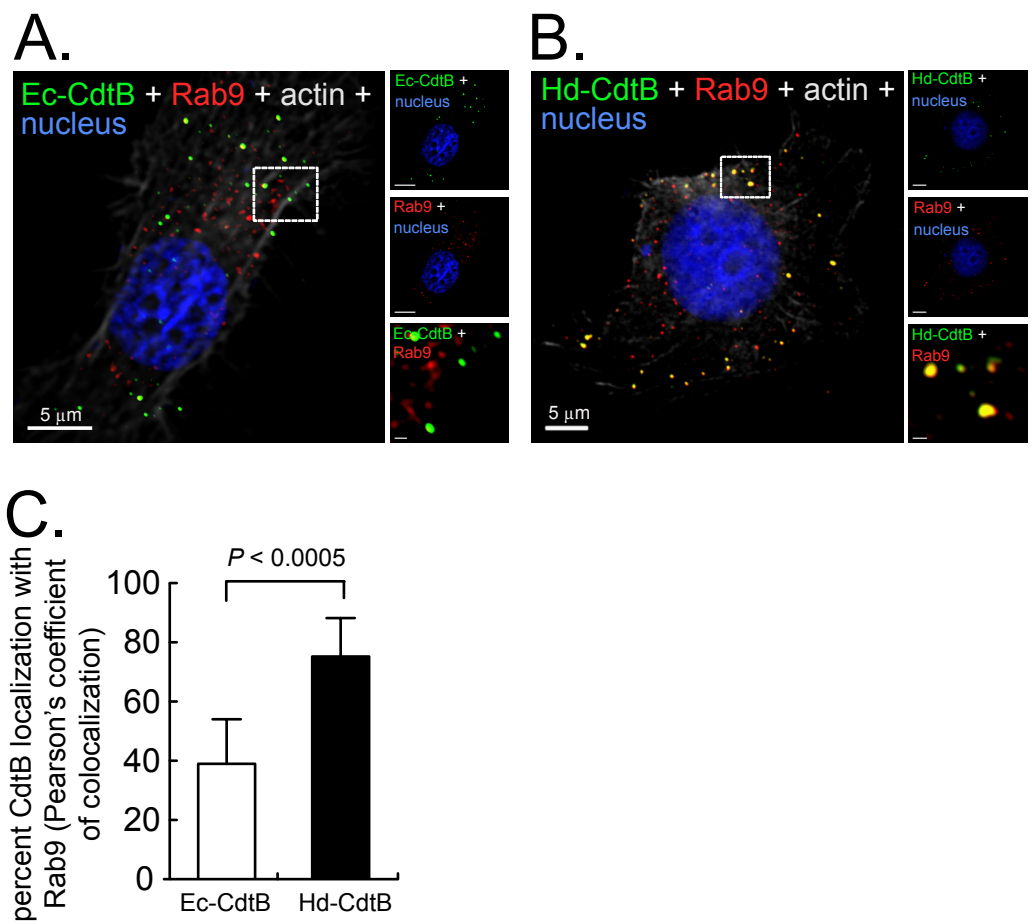

Figure 2.12. Evaluating the co-localization of Ec-CdtB or Hd-CdtB with Rab9. HeLa cells that had been prechilled on ice for 30 min, were incubated on ice with either Ec-CDT (100 nM) or Hd-CDT (100 nM), each of which had also been prechilled on ice. After 30 min, the cells were washed once with PBS pH 7.4, and then further incubated at 37 °C. After 30 min, the cells were fixed and imaged using fluorescence microscopy. (A and B) Images were representative of those collected from three independent experiments. The data were rendered as a single z-plane (approximately 5 μm depth within each cell). As labeled, green puncta indicate either Ec-CdtB or Hd-CdtB, red puncta indicate Rab9, and Ec-CdtB or Hd-CdtB co-localized with Rab9 is indicated by yellow puncta. White bars indicate 10 Mm. The solid white boxes are digitally enlarged images of the smaller dashed white boxes. (C) The results are rendered as a bar graph generated from data combined from three independent experiments that compare the Pearson's correlation coefficient for Ec-CdtB or Hd-CdtB co-localized with Rab9 in cells treated with Ec-CDT or Hd-CDT, as indicated. Error bars represent standard deviations. Statistical significance was calculated for differences in the Pearson's correlation coefficient between cell populations incubated with Ec-CDT or Hd-CDT.

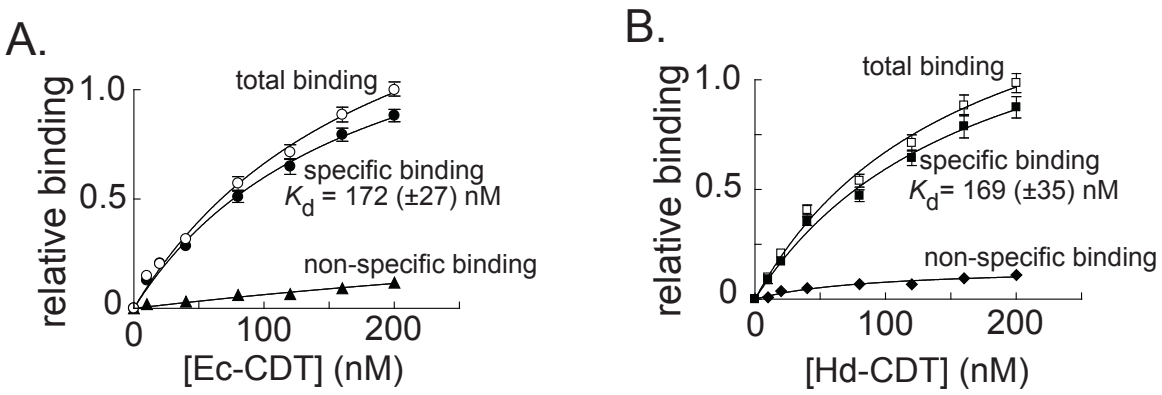

Figure 2.13. Cell surface binding of Ec-CDT and Hd-CDT. The data are rendered as the relative binding after 30 min of biotinylated forms of Ec-CDT (A) or Hd-CDT (B) to HeLa cells as a function of toxin concentration (1-200 nM) in the absence (indicated on the graphs as "total binding," empty circles (A) or squares (B)) or presence (indicated on the graphs as "non-specific binding," filled triangles (A) or diamonds (B)) of 100-fold molar excess of non-biotinylated Ec-CDT (A) or Hd-CDT (B). Specific binding (indicated on the graphs as "specific binding," filled circles (A) or squares (B)) was computationally derived by subtracting the non-specific binding data from the total binding data. The normalized data from three independent experiments, each conducted in triplicate, were combined. K_d values were calculated using non-linear regression, and indicated directly on the graphs, with the error bars indicating standard deviations.

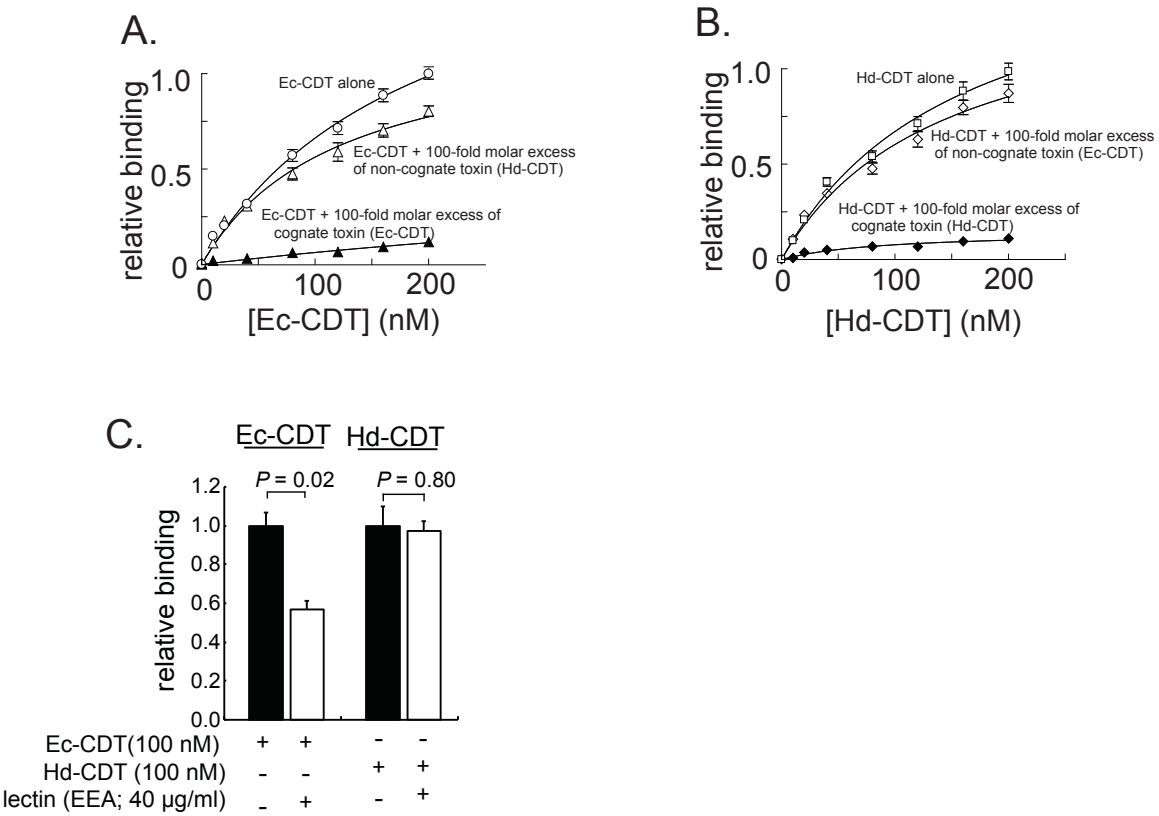

Figure 2.14. Competitive cell surface binding of Ec-CDT and Hd-CDT in the absence or presence of cognate or non-cognate toxins. The data are rendered as the relative binding after 30 min of Ec-CDT (A) or Hd-CDT (B) to HeLa cells as a function of toxin concentration (1-200 nM) in the presence or absence of 100-fold molar excess of non-biotinylated cognate or non-cognate toxins, as indicated. The data were normalized and combined from three independent experiments, each conducted in triplicate, and rendered as line graphs comparing the relative binding of biotinylated Ec-CDT (A) or Hd-CDT (B) in the absence or presence of 100-fold molar excess of unlabeled Ec-CDT or Hd-CDT, as indicated. Error bars are standard deviations. (C) The data are rendered as normalized relative binding of 100 nM of biotinylated Ec-CDT, or Hd-CDT to HeLa cells for 30 minutes, in the absence or presence of the lectin EEA (40 μg/ml). Data are combined from three independent experiments, each conducted in triplicate. Error bars represent standard deviations. Statistical significance was calculated for differences in the cell-surface binding of Ec-CDT or Hd-CDT between cell populations incubated in the absence or presence of the lectin EEA.

2.6. References

1. Abrami, L., Reig, N., & van der Goot, F. G. (2005). Anthrax toxin: the long and winding road that leads to the kill. *Trends Microbiol, 13*(2), 72-78.

2. Aragon, V., Chao, K., & Dreyfus, L. A. (1997). Effect of cytolethal distending toxin on F-actin assembly and cell division in Chinese hamster ovary cells. *Infect Immun, 65*(9), 3774-3780.

3. Bag, P. K., Ramamurthy, T., & Nair, U. B. (1993). Evidence for the presence of a receptor for the cytolethal distending toxin (CLDT) of *Campylobacter jejuni* on CHO and HeLa cell membranes and development of a receptor-based enzyme-linked immunosorbent assay for detection of CLDT. *FEMS Microbiol Lett, 114*(3), 285-291.

4. Blanke, S. R. (2006). Portals and Pathways: Principles of Bacterial Toxin Entry into Host Cells. *Microbe, 1*(1), 26-32.

5. Bouzari, S., & Varghese, A. (1990). Cytolethal distending toxin (CLDT) production by enteropathogenic *Escherichia coli* (EPEC). *FEMS Microbiol Lett, 59*(1-2), 193-198.

6. Bowman, E. J., Siebers, A., & Altendorf, K. (1988). Bafilomycins: a class of inhibitors of membrane ATPases from microorganisms, animal cells, and plant cells. *Proc Natl Acad Sci U S A, 85*(21), 7972-7976.

7. Cao, L., Bandelac, G., Volgina, A., Korostoff, J., & DiRienzo, J. M. (2008). Role of aromatic amino acids in receptor binding activity and subunit assembly of the cytolethal distending toxin of *Aggregatibacter actinomycetemcomitans*. *Infect Immun, 76*(7), 2812-2821.

8. Cao, L., Volgina, A., Huang, C. M., Korostoff, J., & DiRienzo, J. M. (2005). Characterization of point mutations in the cdtA gene of the cytolethal distending toxin of *Actinobacillus actinomycetemcomitans*. *Mol Microbiol, 58*(5), 1303-1321.

9. Cao, L., Volgina, A., Korostoff, J., & DiRienzo, J. M. (2006). Role of intrachain disulfides in the activities of the CdtA and CdtC subunits of the cytolethal distending toxin of *Actinobacillus actinomycetemcomitans*. *Infect Immun, 74*(9), 4990-5002.

10. Carette, J. E., Guimaraes, C. P., Varadarajan, M., Park, A. S., Wuethrich, I., Godarova, A., Kotecki, M., Cochran, B.H., Spooner, E., Ploegh, H.L., & Brummelkamp, T. R. (2009). Haploid genetic screens in human cells identify host factors used by pathogens. *Science, 326*(5957), 1231-1235.

11. Ceelen, L. M., Decostere, A., Ducatelle, R., & Haesebrouck, F. (2006). Cytolethal distending toxin generates cell death by inducing a bottleneck in the cell cycle. *Microbiol Res, 161*(2), 109-120.

12. Cope, L. D., Lumbley, S., Latimer, J. L., Klesney-Tait, J., Stevens, M. K., Johnson, L. S., Purven, M., Munson, R.S., Lagergard,T., Radolf, J.D., & Hansen, E. J. (1997). A diffusible cytotoxin of *Haemophilus ducreyi*. *Proc Natl Acad Sci U S A, 94*(8), 4056-4061.

13. Cortes-Bratti, X., Chaves-Olarte, E., Lagergard, T., & Thelestam, M. (1999). The cytolethal distending toxin from the chancroid bacterium *Haemophilus ducreyi* induces cell-cycle arrest in the G2 phase. *J Clin Invest, 103*(1), 107-115.

14. Cortes-Bratti, X., Chaves-Olarte, E., Lagergard, T., & Thelestam, M. (2000). Cellular internalization of cytolethal distending toxin from *Haemophilus ducreyi*. *Infect Immun, 68*(12), 6903-6911.

15. Damek-Poprawa, M., Jang, J. Y., Volgina, A., Korostoff, J., & DiRienzo, J. M. (2012). Localization of *Aggregatibacter actinomycetemcomitans* cytolethal distending toxin subunits during intoxication of live cells. *Infect Immun, 80*(8), 2761-2770.

16. Daro, E., Sheff, D., Gomez, M., Kreis, T., & Mellman, I. (1997). Inhibition of endosome function in CHO cells bearing a temperature-sensitive defect in the coatomer (COPI) component epsilon-COP. *J Cell Biol, 139*(7), 1747-1759.

17. Dixon, W. (1950). Analysis of extreme values. *Ann Math Stat 21*, 488-506.

18. Elwell, C., Chao, K., Patel, K., & Dreyfus, L. (2001). *Escherichia coli* CdtB mediates cytolethal distending toxin cell cycle arrest. *Infect Immun, 69*(5), 3418-3422.

19. Elwell, C. A., & Dreyfus, L. A. (2000). DNase I homologous residues in CdtB are critical for cytolethal distending toxin-mediated cell cycle arrest. *Mol Microbiol, 37*(4), 952-963.

20. Eshraghi, A., Maldonado-Arocho, F. J., Gargi, A., Cardwell, M. M., Prouty, M. G., Blanke, S. R., & Bradley, K. A. (2010). Cytolethal distending toxin family members are differentially affected by alterations in host glycans and membrane cholesterol. *J Biol Chem, 285*(24), 18199-18207.

21. Frisan, T., Cortes-Bratti, X., Chaves-Olarte, E., Stenerlow, B., & Thelestam, M. (2003). The *Haemophilus ducreyi* cytolethal distending toxin induces DNA double-strand breaks and promotes ATM-dependent activation of RhoA. *Cellular Microbiology, 5*(10), 695-707.

22. Frisk, A., Lebens, M., Johansson, C., Ahmed, H., Svensson, L., Ahlman, K., & Lagergard, T. (2001). The role of different protein components from the *Haemophilus ducreyi* cytolethal distending toxin in the generation of cell toxicity. *Microb Pathog, 30*(6), 313-324.

23. Ganley, I. G., Carroll, K., Bittova, L., & Pfeffer, S. (2004). Rab9 GTPase regulates late endosome size and requires effector interaction for its stability. *Molecular Biology of the Cell, 15*(12), 5420-5430.

24. Gargi, A., Reno, M., & Blanke, S. R. (2012). Bacterial toxin modulation of the eukaryotic cell cycle: are all cytolethal distending toxins created equally? *Front Cell Infect Microbiol, 2*, 124.

25. Ge, Z., Schauer, D. B., & Fox, J. G. (2008). *In vivo* virulence properties of bacterial cytolethal-distending toxin. *Cellular Microbiology, 10*(8), 1599-1607.

26. Gelfanova, V., Hansen, E. J., & Spinola, S. M. (1999). Cytolethal distending toxin of *Haemophilus ducreyi* induces apoptotic death of Jurkat T cells. *Infect Immun, 67*(12), 6394-6402.

27. Guerra, L., Nemec, K. N., Massey, S., Tatulian, S. A., Thelestam, M., Frisan, T., & Teter, K. (2009). A novel mode of translocation for cytolethal distending toxin. *Biochim Biophys Acta, 1793*(3), 489-495.

28. Guerra, L., Teter, K., Lilley, B. N., Stenerlow, B., Holmes, R. K., Ploegh, H. L., Sandvig, K., Thelestam, M., & Frisan, T. (2005). Cellular internalization of cytolethal distending toxin: a new end to a known pathway. *Cellular Microbiology, 7*(7), 921-934.

29. Hassane, D. C., Lee, R. B., & Pickett, C. L. (2003). *Campylobacter jejuni* cytolethal distending toxin promotes DNA repair responses in normal human cells. *Infect Immun, 71*(1), 541-545.

30. Hu, X., Nesic, D., & Stebbins, C. E. (2006). Comparative structure-function analysis of cytolethal distending toxins. *Proteins, 62*(2), 421-434.

31. Hurtado-Lorenzo, A., Skinner, M., El Annan, J., Futai, M., Sun-Wada, G. H., Bourgoin, S., Casanova, J., Wildeman, A., Bechoua, S., Ausiello, D.A., Brown D, & Marshansky, V. (2006). V-ATPase interacts with ARNO and Arf6 in early endosomes and regulates the protein degradative pathway. *Nat Cell Biol, 8*(2), 124-136.

32. Johnson, W. M., & Lior, H. (1988a). A new heat-labile cytolethal distending toxin (CLDT) produced by *Campylobacter spp*. *Microb Pathog, 4*(2), 115-126.

33. Johnson, W. M., & Lior, H. (1988b). A new heat-labile cytolethal distending toxin (CLDT) produced by *Escherichia coli* isolates from clinical material. *Microb Pathog, 4*(2), 103-113.

34. Lara-Tejero, M., & Galan, J. E. (2000). A bacterial toxin that controls cell cycle progression as a deoxyribonuclease I-like protein. *Science, 290*(5490), 354-357.

35. Lee, R. B., Hassane, D. C., Cottle, D. L., & Pickett, C. L. (2003). Interactions of *Campylobacter jejuni* cytolethal distending toxin subunits CdtA and CdtC with HeLa cells. *Infect Immun, 71*(9), 4883-4890.

36. Lencer, W. I., Strohmeier, G., Moe, S., Carlson, S. L., Constable, C. T., & Madara, J. L. (1995). Signal transduction by cholera toxin: processing in vesicular compartments does not require acidification. *Am J Physiol, 269*(4 Pt 1), G548-557.

37. Li, L., Sharipo, A., Chaves-Olarte, E., Masucci, M. G., Levitsky, V., Thelestam, M., & Frisan, T. (2002). The *Haemophilus ducreyi* cytolethal distending toxin activates sensors of DNA damage and repair complexes in proliferating and non-proliferating cells. *Cell Microbiol, 4*(2), 87-99.

38. Lombardi, D., Soldati, T., Riederer, M. A., Goda, Y., Zerial, M., & Pfeffer, S. R. (1993). Rab9 functions in transport between late endosomes and the trans Golgi network. *Embo J, 12*(2), 677-682.

39. Mallard, F., Antony, C., Tenza, D., Salamero, J., Goud, B., & Johannes, L. (1998). Direct pathway from early/recycling endosomes to the Golgi apparatus revealed through the study of shiga toxin B-fragment transport. *Journal of Cell Biology, 143*(4), 973-990.

40. Mayer, M. P., Bueno, L. C., Hansen, E. J., & DiRienzo, J. M. (1999). Identification of a cytolethal distending toxin gene locus and features of a virulence-associated region in *Actinobacillus actinomycetemcomitans*. *Infect Immun, 67*(3), 1227-1237.

41. McSweeney, L. A., & Dreyfus, L. A. (2004). Nuclear localization of the *Escherichia coli* cytolethal distending toxin CdtB subunit. *Cellular Microbiology, 6*(5), 447-458.

42. McSweeney, L. A., & Dreyfus, L. A. (2005). Carbohydrate-binding specificity of the *Escherichia coli* cytolethal distending toxin CdtA-II and CdtC-II subunits. *Infect Immun, 73*(4), 2051-2060.

43. Mellman, I., Fuchs, R., & Helenius, A. (1986). Acidification of the endocytic and exocytic pathways. *Annu Rev Biochem, 55*, 663-700.

44. Mise, K., Akifusa, S., Watarai, S., Ansai, T., Nishihara, T., & Takehara, T. (2005). Involvement of ganglioside GM3 in G_2/M cell cycle arrest of human monocytic cells induced by *Actinobacillus actinomycetemcomitans* cytolethal distending toxin. *Infect Immun, 73*(8), 4846-4852.

45. Mollenhauer, H. H., Morre, D. J., & Rowe, L. D. (1990). Alteration of intracellular traffic by monensin; mechanism, specificity and relationship to toxicity. *Biochim Biophys Acta, 1031*(2), 225-246.

46. Montecucco, C., Papini, E., & Schiavo, G. (1994). Bacterial protein toxins penetrate cells via a four-step mechanism. *FEBS Lett, 346*(1), 92-98.

47. Nesic, D., Hsu, Y., & Stebbins, C. E. (2004). Assembly and function of a bacterial genotoxin. *Nature, 429*(6990), 429-433.

48. Nesic, D., & Stebbins, C. E. (2005). Mechanisms of assembly and cellular interactions for the bacterial genotoxin CDT. *PLoS Pathog, 1*(3), e28.

49. Nishi, T., & Forgac, M. (2002). The vacuolar (H+)-ATPases--nature's most versatile proton pumps. *Nat Rev Mol Cell Biol, 3*(2), 94-103.

50. Nishikubo, S., Ohara, M., Ueno, Y., Ikura, M., Kurihara, H., Komatsuzawa, H., Oswald, E., & Sugai, M. (2003). An N-terminal segment of the active component of the bacterial genotoxin cytolethal distending toxin B (CdtB) directs CdtB into the nucleus. *Journal of Biological Chemistry, 278*(50), 50671-50681.

51. Nougayrede, J. P., Taieb, F., De Rycke, J., & Oswald, E. (2005). Cyclomodulins: bacterial effectors that modulate the eukaryotic cell cycle. *Trends Microbiol, 13*(3), 103-110.

52. Ohara, M., Oswald, E., & Sugai, M. (2004). Cytolethal distending toxin: a bacterial bullet targeted to nucleus. *J Biochem, 136*(4), 409-413.

53. Okuda, J., Kurazono, H., & Takeda, Y. (1995). Distribution of the cytolethal distending toxin A gene (cdtA) among species of *Shigella* and *Vibrio*, and cloning and sequencing of the cdt gene from *Shigella dysenteriae*. *Microb Pathog, 18*(3), 167-172.

54. Orlandi, P. A., Curran, P. K., & Fishman, P. H. (1993). Brefeldin A blocks the response of cultured cells to cholera toxin. Implications for intracellular trafficking in toxin action. *J Biol Chem, 268*(16), 12010-12016.

55. Oswald, E., Nougayrede, J. P., Taieb, F., & Sugai, M. (2005). Bacterial toxins that modulate host cell-cycle progression. *Curr Opin Microbiol, 8*(1), 83-91.

56. Pickett, C. L., & Whitehouse, C. A. (1999). The cytolethal distending toxin family. *Trends Microbiol, 7*(7), 292-297.

57. Riederer, M. A., Soldati, T., Shapiro, A. D., Lin, J., & Pfeffer, S. R. (1994). Lysosome biogenesis requires Rab9 function and receptor recycling from endosomes to the trans-Golgi network. *J Cell Biol, 125*(3), 573-582.

58. Sandvig, K., & van Deurs, B. (2005). Delivery into cells: lessons learned from plant and bacterial toxins. *Gene Ther, 12*(11), 865-872.

59. Simpson, J. C., Dascher, C., Roberts, L. M., Lord, J. M., & Balch, W. E. (1995). Ricin cytotoxicity is sensitive to recycling between the endoplasmic reticulum and the Golgi complex. *J Biol Chem, 270*(34), 20078-20083.

60. Smith, J. L., & Bayles, D. O. (2006). The contribution of cytolethal distending toxin to bacterial pathogenesis. *Crit Rev Microbiol, 32*(4), 227-248.

61. Spinosa, M. R., Progida, C., De Luca, A., Colucci, A. M., Alifano, P., & Bucci, C. (2008). Functional characterization of Rab7 mutant proteins associated with Charcot-Marie-Tooth type 2B disease. *J Neurosci, 28*(7), 1640-1648.

62. Sugai, M., Kawamoto, T., Peres, S. Y., Ueno, Y., Komatsuzawa, H., Fujiwara, T., Kurihara, H., Suginaka, H., & Oswald, E. (1998). The cell cycle-specific growth-inhibitory factor produced by *Actinobacillus actinomycetemcomitans* is a cytolethal distending toxin. *Infect Immun, 66*(10), 5008-5019.

63. Sun-Wada, G. H., Wada, Y., & Futai, M. (2003). Lysosome and lysosome-related organelles responsible for specialized functions in higher organisms, with special emphasis on vacuolar-type proton ATPase. *Cell Struct Funct, 28*(5), 455-463.

64. Sun-Wada, G. H., Wada, Y., & Futai, M. (2004). Diverse and essential roles of mammalian vacuolar-type proton pump ATPase: toward the physiological understanding of inside acidic compartments. *Biochim Biophys Acta, 1658*(1-2), 106-114.

65. Thelestam, M., & Frisan, T. (2004). Cytolethal distending toxins. *Rev Physiol Biochem Pharmacol, 152*, 111-133.

66. Tweten, R. K. (2005). Cholesterol-dependent cytolysins, a family of versatile pore-forming toxins. *Infect Immun, 73*(10), 6199-6209.

67. Vonderheit, A., & Helenius, A. (2005). Rab7 associates with early endosomes to mediate sorting and transport of Semliki forest virus to late endosomes. *PLoS Biol, 3*(7), e233.

68. Wising, C., Magnusson, M., Ahlman, K., Lindholm, L., & Lagergard, T. (2010). Toxic activity of the CdtB component of *Haemophilus ducreyi* cytolethal distending toxin expressed from an adenovirus 5 vector. *APMIS, 118*(2), 143-149.

CHAPTER 3: INTERACTIONS OF CDT WITH THE GOLGI APPARATUS

3.1. Introduction

One of the toxins reported to be secreted by *Campylobacter jejuni*, mammalian pathogen of the intestinal tract, is Cytolethal Distending Toxin (CDT) (Johnson & Lior, 1988; Young, Davis, & Dirita, 2007), member of a larger growing family of exotoxins (Gargi, Reno, & Blanke, 2012). These toxins have a tripartite structure, comprised of three proteins, of which CdtA and CdtC are thought to facilitate the delivery of the catalytically active subunit CdtB to its intracellular target (Lara-Tejero & Galan, 2001; Lee, Hassane, Cottle, & Pickett, 2003). Though there is evidence that CdtB possess phosphodiesterase activity (Jinadasa, Bloom, Weiss, & Duhamel, 2011), structural and functional homology to DNase-I like enzymes suggest CDTs might function within the nucleus by damaging the DNA, thereby arresting the host cell cycle, potentially helping the intestinal pathogen to establish a successful infection (Biswas et al., 2006; Lara-Tejero & Galan, 2000; Nesic, Hsu, & Stebbins, 2004; Pickett & Whitehouse, 1999). To access their intracellular targets in the eukaryotic cells, soluble factors engage with cell surface determinants, followed by uptake into intracellular compartments. Protein transportation between the various membranous compartments is further mediated by cargo vesicles that bud off from the donor organelle and fuse with the target acceptor organelle (Bonifacino & Glick, 2004). Bacterial toxins, including CDTs, exploit these very same pathways where they utilize receptor-mediated endocytosis and vesicular trafficking, eventually to

reach the nucleus. The evidence indicating that CdtB does reach the nucleus are transient transfection, biochemical fractionation, and imaging (Gargi et al., 2013; Lara-Tejero & Galan, 2000; McSweeney & Dreyfus, 2004). However the specific details of how CdtB produced by *C. jejuni*, and other CDT-producing pathogens in general, access their intra-cellular target, are poorly understood.

Although little is known about the exact steps involved in Cj-CDT transport to the nucleus, studies with CDTs released by other pathogens has revealed that CDT subunits localize with GM1-enriched membrane regions which are characteristic of membrane rafts, and cell surface cholesterol depletion reduced the binding activity of Cj-CDT on the cell membrane, leading to impaired toxin uptake, and attenuation of toxin-induced cell cycle arrest (Boesze-Battaglia et al., 2006; Lin et al., 2011). Following cellular uptake, the toxin enters the endolysosomal system (Gillespie et al., 2013; Guerra, Cortes-Bratti, Guidi, & Frisan, 2011). The catalytically active subunit is transported through the endoplasmic reticulum (ER), and the exit from ER is important for the toxin activity, before finally getting into the nucleus (Damek-Poprawa, Jang, Volgina, Korostoff, & DiRienzo, 2012; Eshraghi et al., 2014). Yet very little is known about how the toxin gets to the ER. Studies with CDTs isolated from several other pathogens, including *H. ducreyi*, *E. coli*, and *A. actinomycetemcomitans*, have indicated the importance of an intact Golgi apparatus for the toxin function, and its affect on toxin transport to its target (Cortes-Bratti, Chaves-Olarte, Lagergard, & Thelestam, 2000; Gargi et al., 2013; Guerra et al., 2005). CDT is thought to traffic retrogradely through the Golgi apparatus based on sensitivity of cells to the

disruption of membrane transport by brefeldin A, and in addition Hd-CdtB that had been tagged with a sulfation motif, was sulfated when applied on mammalian cells (Guerra et al., 2005), suggesting that the toxin passes through the Golgi apparatus. However, the details of the mechanism by with Cj-CDT is transported to and engages with the Golgi apparatus, the importance of sub-Golgi compartments, and its implications on toxin's biological activity are poorly understood. Moreover, no Golgi-resident protein associated with CDT-mediated cargo vesicle transport has been identified.

In this study we demonstrate the importance of an intact and functional Golgi apparatus for toxin function, and localization, of active subunit of Cj-CDT to the nucleus. We demonstrate the time dependent and transient localization of Cj-CdtB with the Golgi apparatus, and provide evidence supporting that Cj-CdtB utilizes the cellular machinery from the late-endosomal compartments to the Golgi apparatus. We show that Cj-CDT trafficking and intoxication properties are independent of early endosome to the Golgi apparatus transition, but are sensitive to the endosomal maturation, and the toxin is predominantly trafficked out of vesicles marked by STX10, and rab9, both indicators of transition through the late endosomal compartments, before reaching the Golgi apparatus. Blocking the Golgi apparatus sorting function by small molecule inhibitors abrogated downstream trafficking, and Cj-CDT mediated cell cycle arrest. Moreover, when the Golgi apparatus block was removed, the toxin already present in the cell proceeded to the nucleus, and caused cell cycle arrest, suggesting that Golgi apparatus is a bottleneck in the CDT intoxication of host cells. We also identified

the Golgi-membrane resident protein, COG complex, as the Golgi-receptor for incoming CDT-containing vesicles. Together, our findings suggest an important role of the Golgi apparatus in both function and trafficking of Cj-CdtB to the ER, and ultimately to the nucleus, and identifies specific host cell determinants required for the intracellular transportation, and biological activity of CDT produced by *C. jejuni*.

3.2. Materials and Methods

Cloning of cdt genes and preparation of expression strains. The plasmids used for recombinant expression of Cj-CDT in *E. coli* were constructed as previously described (Gargi et al., 2013).

Expression and purification of recombinant Cj-CDT. Recombinant forms of Cj-CdtA, Cj-CdtB, and Cj-CdtC, were expressed and purified as previously described (Eshraghi et al., 2010). Protein concentrations were quantified using the Bradford Protein Assay (Thermo Scientific, Rockford, IL). Recombinant proteins were used only when purified to at least 95% homogeneity, as estimated by resolving the proteins using sodium-dodecyl sulfate (SDS)-polyacrylamide gel electrophoresis (PAGE), and visualizing after staining the gels with Coomassie Brilliant Blue (Bio-Rad, Hercules, CA). The purified, denatured subunits were stored at -20 °C in HEPES (20 mM, *N*-[2-Hydroxyethyl] piperazine-*N*-[2-ethanesulphonic acid], Calbiochem, La Jolla, CA), pH 7.5 containing urea (8 M, Thermo Scientific) and NaCl (200 mM, Thermo Scientific).

Dialysis retention assay. Cj-CDT holotoxin was prepared as previously described (Gargi et al., 2013). CDT holotoxin was purified to stoichiometric equivalence using gel filtration chromatography, and the holotoxin integrity was evaluated using the dialysis retention assay, as previously described (Cao, Volgina, Huang, Korostoff, & DiRienzo, 2005). Cj-CDT (5-20 μM, 1 ml) was dialyzed (100 kDa molecular mass cut-off tubing; Spectrum Laboratories) at 4 °C against four 250 ml volumes of PBS pH 7.4 containing 5% glycerol. After 24 h, the dialyzed proteins were evaluated using SDS-PAGE followed by staining with Coomassie Brilliant blue. The gels were scanned with a CanonScan 9950F scanner (Canon, Lake Success, NY) using ArcSoft Photo Studio 5.5 software (ArcSoft, Fremont, CA). The integrity of the holotoxins was quantified by comparing the relative intensities of the bands corresponding to CdtA, CdtB, or CdtC before and after dialysis, as determined by using the UN-SCAN-IT program (Silk Scientific, Inc., Orem, UT). Individual CDT subunits, each of which has a molecular mass less than 35 kDa, were used as negative controls to demonstrate that individual subunits diffused out of the dialysis bag.

Mammalian cells. All mammalian cell cultures were maintained at 37°C and under 5% CO_2 within a humidified environment. Human colon colorectal carcinoma (HCT-116) cells (CCL-247, ATCC) were maintained in McCoy's 5A media (ATCC) with 10% fetal bovine serum (FBS, Atlanta Biologicals, Flowery Branch, GA). Human cervical cancer epithelial (HeLa) cells (CCL-2, ATCC) were maintained in Minimal Essential Medium Eagle (MEM, Mediatech, Herndon, VA)

with 10% FBS. Chinese hamster ovary (CHO-K1) cells (CCL-61, ATCC) were maintained in Ham's F-12K (Lonza, Walkersville, MD) with 10% FBS. Complete medium was obtained by supplementing each medium described above with L-glutamine (2 mM, Sigma), penicillin (50 IU/ml, Mediatech), and streptomycin (50 μg/ml, Mediatech).

Flow cytometry. Analytical flow cytometry-based assays were carried out as previously described (Gargi et al, 2013). Briefly, HCT116, HeLa, or CHO-K1 cells were intoxicated with indicated concentrations of Cj-CDT, in the absence or presence of indicated agents in a 12-well plates for 24 h, followed by two washes with Dulbecco's PBS (DPBS, Cellgro), detached with 0.05% trypsin/EDTA (Invitrogen), washed again with DPBS, and fixed with ice-cold 70% ethanol for minimum of 1 h, or maximum of 6 months at -20°C. After hydrating with PBS for 30 minutes, cells were stained with a 10 μg/ml propidium iodide (PI) solution in PBS, containing 0.1% Triton-X100, and 100 μg/ml RNase-A. The fluorescence was quantified for 10^4 cells using a FACSCanto flow cytometer (BD Biosciences, San Jose, CA) with BD FACSDIVA acquisition software (BD Biosciences). Flow cytometry data were subsequently analyzed using FCS4 Express analysis software (De Novo Software, Glendale, CA).

Cell cycle phase determination. The indicated cell lines were seeded (8 x 10^4 cells/800 μl/well) in 12-well plates (Corning Inc., Corning, NY). After 18 h, the cells were further incubated in complete medium in the absence or presence of

Cj-CDT at the indicated concentrations, or mock incubated with PBS pH 7.4. After 24 h, the cells were analyzed for arrest at the G_2/M interface, as previously described (Gargi et al., 2013). From these data, dose response curves were generated by plotting cells in G_2/M as a function of toxin concentration. From the dose response curves, we determined $CCAD_{50}$ (i.e. cell cycle arrest $dose_{50}$) values, which we defined as the toxin concentrations required to induce G_2/M arrest in 50% of the cell population not already in G_2/M.

For Cj-CDT, preliminary studies revealed nearly identical dose response curves for G_2/M arrest in the presence or absence of the hexa-histidine tags. All subsequent studies were conducted with Cj-CDT assembled from subunits that retained their respective hexa-histidine tags.

Some studies were conducted in the presence of the indicated concentrations of brefeldin A (BFA; MP Biomedicals), Exo2 (Sigma), golgicide A (GCA; Sigma) ammonium chloride (NH_4Cl, Sigma), bafilomycin A1 (LC Laboratories, Woburn, MA), monensin (Sigma), nigericin (Sigma), Retro-1 (kind gift from Julien Barbier), or Retro-2 (kind gift from Julien Barbier). These studies were conducted at approximately the $CCAD_{50}$ values determined for Cj-CDT in order to best assess whether each pharmacological agent inhibited, potentiated, or had no effect on toxin activity.

DIC/fluorescence microscopy. Chamber slides were analyzed using a DeltaVision RT microscope (Applied Precision; Issaquah, WA), using an Olympus Plan Apo 40x oil objective with NA 1.42 and working distance of 0.17

mm DIC images were collected using a Photometrics CoolSnap HQ camera; (Photometrics, Tucson; AZ). Images were processed using SoftWoRX Explorer Suite (version 3.5.1, Applied Precision Inc). Deconvolution was carried out using SoftWoRX constrained iterative deconvolution tool (ratio mode), and analyzed using Imaris 5.7 (Bitplane AG, Zurich, Switzerland).

CDT localization inside the cell. HCT116, HeLa, or CHO-K1 cells were pretreated in the absence or presence of BFA (0.2 μg/ml) at 37 °C for 30 min. Cells were chilled for 30 min on ice, washed once with cold media, and replaced with pre-chilled media in the absence or presence of Cj-CDT (100 nM) in complete growth medium. After 30 min binding on ice, toxin containing media was removed, and replaced with pre-warmed media, and incubated at 37 °C At specified time points post internalization, cells were fixed and permeabilized as described above under "*Internalization Assay.*" To monitor Cj-CdtB localization to the Golgi, cells were incubated with rat polyclonal anti-Cj-CdtB antibody (1:500 dilution), and mouse polyclonal anti-Giantin antibody (1:1000 dilution), or mouse polyclonal anti-TGN46 antibody (1:500 dilution) or anti-GM130 rabbit polyclonal antibody (1:1000 dilution), or mouse TOM20 polyclonal antibody (1:500 dilution), at 4 °C overnight, followed by incubation with anti-rat Alexa Fluor 488-labeled goat antibody (1:1000 dilution; Invitrogen) and anti-mouse Alexa Fluor 568-labeled goat antibody (1:1000 dilution; Invitrogen) or anti-rabbit Alexa Fluor 568-labeled goat antibody (1:1000 dilution; Invitrogen) at room temperature for 2 h. The cells were further counter stained for the nucleus by incubating with DAPI (1

ng/200 μl, Invitrogen) for 2 min at room temperature. The slides were mounted with ProLong Gold Antifade Reagent (25 μl/well; Invitrogen). Images were collected using DIC/fluorescence microscopy and deconvolved, as described above. For each cell, images were collected from an average of 30 z-planes, each at a thickness of 0.2 μm. Golgi localization analysis was conducted by using the DeltaVision SoftWoRx 3.5.1 software suite. Percentage of CdtB localization with giantin, TGN46, or GM130 in each group of treated cells were calculated from approximately 30 cells over three independent experiments.

CDT localization to the Golgi apparatus. Mammalian cells were plated in an 8-well chamber slide to 30-40% confluency. After overnight incubation, cells were washed 2 times with PBS pH 7.4, followed by addition of 100 μL OPTI-MEM (Invitrogen, Grand Island, NY), and further incubated for 2 h before transfection. Approximately 30 min prior to addition to cells, the appropriate dilutions of pECFP-Golgi (0.4 μg/200 μl/well), which encodes a fusion protein consisting of enhanced cyan fluorescent protein (ECFP) and a sequence encoding the N-terminal 81 amino acids of human beta 1,4-galactosyltransferase, which contains the membrane-anchoring signal peptide that targets the fusion protein to the trans-medial region of the Golgi apparatus; and Lipofectamine 2000 reagent (1 μl/200 μl/well; Invitrogen) complex were prepared according to the manufacturers instructions, and allowed to incubate at room temperature. After 30 min, OPTI-MEM was removed, and the plasmid DNA-transfection mixture (100 μl) was added to each well in a drop-wise fashion

with gentle agitation, and the cells were immediately incubated at 37 °C and under 5% CO_2. After 4 h, the transfection mixture was removed from the monolayers, and the cells were incubated in complete medium at 37 °C and under 5% CO_2. After overnight incubation, we typically detected 80-90% of the cells within the monolayer to be transfected based on the percentage of cells with ECFP fluorescence, as determined using an Olympus CKX 41 fluorescence microscope (Olympus America Inc., Center Valley, PA).

Images were collected using DIC/fluorescence microscopy and deconvoluted, as described above. For each cell, images were collected from an average of 30 z-planes, each at a thickness of 0.2 μm. Localization analysis was conducted by using the co-localization module of the DeltaVision SoftWoRx 3.5.1 software suite. Results were expressed as the localization index, which was derived from calculating the Pearson's coefficient of correlation values, which in these studies was a measure of localization of the indicated CDT to the Golgi apparatus in each z plane of the cell. In these studies, a localization index value of 1.0 indicates 100% localization of Cj-CDT to the Golgi apparatus, whereas a localization index of 0.0 indicates the absence of Cj-CDT localization to the Golgi apparatus. The localization index was calculated from the analysis of a total of 30 images collected over three independent experiments.

Monitoring nuclear localization of Cj-CdtB within the nuclear fraction of CDT-intoxicated cells. Cells were seeded in 100 mm culture dishes (BD Biosciences, Durham, NC). After overnight incubation, the monolayers were

treated with bafilomycin A1 (20 nM) for 30 min, and further incubated with Cj-CDT (100 nM). After 30 min, the cells were further incubated with fresh medium (not containing toxin) for an additional 210 min. After 240 min total internalization of Cj-CDT, the cells were harvested by scraping, and lysed and fractionated in the presence of protease and phosphatase inhibitors. Briefly, scraped cells were lysed using hypotonic buffer, and fractionated by isolating the nuclear pellet by centrifuging the cell lysate at 600*g* for 5 min. The fractionated samples were evaluated by western blotting, using rabbit polyclonal antibodies against Cj-CdtB (1:20,000 dilution; generated by Thermo Fisher Scientific Inc., Rockford, IL), cytosolic marker GAPDH (1:200; Abcam, Cambridge, MA), nuclear marker p84 (1:2,000; Abcam), and cell lysate loading control actin (1:1,000; NeoMarkers, Fremont, CA). Anti-mouse (1:2,000), and anti-rabbit (1:5,000) secondary antibodies were purchased from Pierce Protein Biology Products (Thermo Fisher Scientific Inc.). Relative amounts of CdtB were determined by densitometric analysis of the blot bands using the UN-SCAN-IT program.

RNA interference. Four synthetic siRNA duplex oligomers (19-mers) targeting human syntaxin 5 (first: CAGAACAUUGAGUCGACAA, second: CAAUCUUGGCAAAGCGCAA, third: GCUCCAGGAUUUCGUGAGA, fourth: GAGCCCAGCUGGACGUUGA), four 19-mers targeting human syntaxin 10 (first: GGAAGAGACCAUCGGUAUA, second: CGACCAAUGAGCUGCGGAA, third: AGGUGUUCGUGGAGCGGAU, fourth: AGGAAGUUGGCCAAAGUAU) were purchased from Dharmacon. Cells were transfected using Lipofectamine

(Invitrogen) according to the manufacturer's protocol. Experiments were carried out 2 days after transfection. Concentrations of 25 nM of siRNA were used for transfection.

Preparing stable cell lines with COG4 and COG8 knock-down. Mission shRNA transduction particles were purchased from Sigma targeting specific genes in the mammalian cells. For COG4, CCGGGTGACCGAGATCCTCGATTACCTCGAGGTAATCGAGGATCTCGGTCACTTTTTTG, COG8: CGGGTGTCCGGAACAGTTATTATGCTCGAGCATAATAACTGTTCCGGACACTTTTTG sequences were targeted. HCT116 cells were seeded overnight for 80% confluency. Lentiviral particles with constructs targeting COG4, or COG8, were added to the cells in growth media containing polybrene. After 24 h incubation, media was removed, and replaced with fresh growth media, and incubated for additional 24 h. Media was removed and replaced with fresh media containing puromycin, and incubated for additional 48 – 72 h, allowing for Puromycin selection. Media with dead cells was replaced every 24 h. Surviving colonies of HCT116 cells were trypsinized, suspended in fresh media, and plated in a 96-well plate, serially diluted by a factor of 2, starting at 1:100 dilution of original cell suspension. Wells with a single cell colony were selected and passaged to expand stable cell line clonality.

H2AX activation assay. Cells were pretreated with BFA (0.2 μg/ml), or transfected with plasmids pDsRed-Rab5 DN, pDsRed-Rab9 DN, pDsRed-Rab11 DN, mChActA, COG4-mChActA, or COG8-mChActA (0.4 μg/200 μl/well), or siRNA 19-mers against STX5 or STX10 (25 nM), using the general transfection procedure as described above under "*CDT localization to the Golgi apparatus."* The treated monolayers, or stable COG4- or COG8-knockdown cell lines, were incubated at 37°C with Cj-CDT (100 nM). After 4 hours, the cells were fixed and permeabilized as described above under "*Internalization Assay*." To monitor activation of H2AX by CDT, samples were stained overnight with a rabbit polyclonal anti-p-H2AX antibody (1:5000 dilution; Invitrogen) at 4 °C, followed by incubation with goat anti-rabbit Alexa Fluor 488 antibody (1:1000 dilution; Invitrogen) at room temperature for 2 h. The cells were further counter stained for nuclei by incubating with DAPI (1 ng/200 μl, Invitrogen) for 30 min. The slides were mounted with ProLong Gold Antifade Reagent (25 μl/well; Invitrogen). Images were collected using DIC/fluorescence microscopy and deconvoluted, as described above. For each cell, images were collected from an average of 30 z-planes, each at a thickness of 0.2 μm. H2AX activation analysis was conducted by using the DeltaVision SoftWoRx 3.5.1 software suite. Percentage of H2AX activated cells in each group of cells were calculated from approximately 50 cells from each group over three independent experiments.

Monitoring nuclear localization of Cj-CdtB using fluorescence microscopy. Cells were pretreated with BFA (0.2 μg/ml), or transfected with pDsRed-Rab5

DN, pDsRed-Rab9 DN, pDsRed-Rab11 DN, mChActA, COG4-mChActA, or COG8-mChActA (0.4 μg/200 μl/well), using the general transfection procedure as described above under "*CDT localization to the ER.*" The transfected monolayers were pre-chilled for 30 min on ice and further incubated with Cj-CDT (100 nM) on ice for 30 min. After 60 min post internalization, the cells were fixed and permeabilized as described above under "*Internalization Assay*" To monitor Cj-CdtB localization to the nucleus, cells were incubated with rat polyclonal anti-Cj-CdtB antibody (1:500 dilution) at 4 °C overnight, followed by incubation with goat anti-rat Alexa Fluor 488-labeled antibody (1:1000 dilution; Invitrogen) at room temperature for 2 h. The cells were further counter stained for the nucleus by incubating with DAPI (1 ng/200 μl, Invitrogen) for 30 min at room temperature. The slides were mounted with ProLong Gold Antifade Reagent (25 μl/well; Invitrogen). Images were collected using DIC/fluorescence microscopy and deconvoluted, as described above. For each cell, images were collected from an average of 30 z-planes, each at a thickness of 0.2 μm. Nuclear localization analysis was conducted by using the DeltaVision SoftWoRx 3.5.1 software suite. Percentage of CdtB localization into nucleus in each group of treated cells were calculated from approximately 30 cells over three independent experiments.

Transmission Electron Microscopy. Samples were treated according to the manufacturer's protocol. In short, HCT116 cells were fixed with cold Karnovsky's EM fixative (2.5% paraformaldehyde, 2% glutaraldehyde in 0.1 M Sorenson's phosphate buffer, pH 7.2) overnight at 4°C. Fixed cells were rinsed with 0.1 M

Sorenson's phosphate buffer pH 7.2 three times. Cells were further fixed with 2% OsO_4 on ice for 20 sec. Samples were microwaved two times for 8 s, with a 20 s break, followed by incubation on ice for 20 s, and on shaker at room temperature for 5 min. This sequence was repeated 5 times, for a total of about 30 min incubation in OsO_4. Retaining OsO_4 on the cells, 3% $K_3[Fe(CN)_6]$ was added and cells were further incubated at room temperature for 15min on shaker. OsO_4 and $K_3[Fe(CN)_6]$ were removed and cells were rinsed with pure water three times. Cells were dehydrated with 25, 50, 75, 95, and 100% ethanol, and a 1:1 mixture of 100% ethanol and acetonitrile. In each dehydration step, cells were microwaved for 40 s and incubated at room temperature for 2 min on shaker. Cells were further microwaved for 30 s in 100% acetonitrile, followed by 2 min incubation at room temperature on shaker twice. For the cell infiltration, 1:1 mixture of acetonitrile and epoxy resin mixture (LX-112 resin, DDSA, NMA, and DMP-30) was added to the cells, and microwaved for 30 s followed by shaking at room temperature for 10min, and repeated two times. The process was further repeated twice with 1:3 mixture of acetonitrile and epoxy resin mixture (30 s microwaving and 20 min incubation at room temperature). Cells were embedded in epoxy resin mixture with 30 s microwaving and shaking for 30 min at room temperature. Epoxy resin mixture was replaced with fresh epoxy resin mixture, and cells were incubated at room temperature one more hour on shaker before polymerizing overnight at 65°C. Epoxy resin embedded cells were trimmed in 0.5 X 0.5 mm squares or trapezoid block face using razor blade. Cells were sectioned 60 nm thin using Diatome diamond knife and Leica Ultracut Uct Ultra

Microtome. Sections were captured on 200-mesh hexagonal copper or nickel grids. Samples were stained with 7% uranly acetate for 1 h and 0.3% lead citrate for 5 min. Stained samples were observed under Phillips CM200 transmission electron microscope.

Statistics. Unless otherwise indicated, each experiment was performed at least three independent times, each time in triplicate. Statistical analyses were performed using Microsoft Excel (Version 11.0, Microsoft, Redmond, WA) or GraphPad Prism (Version 5, La Jolla, CA). The *Q*-test was performed to eliminate data that were statistical outliers. Error bars represent standard deviations. All *P* values were calculated with the Student's *t*-test using paired, two-tailed distribution. A *P* value of less than 0.05 indicated that differences in the specified data were considered statistically significant.

3.3. Results

Effects of brefeldin A (BFA) on Cj-CDT-induced G_2/M cell cycle arrest. Several studies have reported that Hd-CDT-, Aa-CDT-, or Ec-CDT-mediated mammalian cell cycle arrest is blocked in the presence of BFA (Akifusa, Heywood, Nair, Stenbeck, & Henderson, 2005; Cortes-Bratti et al., 2000; Gargi et al., 2013; Guerra et al., 2005), suggesting that an intact Golgi apparatus is required for the cellular action of these toxins. BFA is an antifungal agent that alters Golgi apparatus integrity by inhibiting at least two factors, Golgi brefeldin A

resistance factor 1 (GBF1), which is involved in coordinating coating events within the pre-Golgi to Golgi complex continuum (Lowery et al., 2013) and BFA-inhibited guanine nucleotide exchange factor 1 (BIG1), which is required to maintain the normal morphology of the Golgi (Togawa, Morinaga, Ogasawara, Moss, & Vaughan, 1999). Because the importance of an intact Golgi complex for intoxication of cells with Cj-CDT had not been previously studied, Cj-CDT-mediated cell cycle arrest was evaluated in the presence or absence of BFA. In studies of Cj-CDT cellular activity, we primarily use human-derived HCT116 intestinal cells, which have been widely used as an *in vitro* model for studying *C. jejuni* infection (McAuley et al., 2007). When HCT116 cells incubated with BFA (200 ng/ml) were examined by transmission electron microscopy (TEM), the characteristic Golgi stacks were no longer visibly detectable (data not shown), consistent with the idea that BFA causes the dispersion of the stacked Golgi cisternae so that protein transport through the Golgi apparatus is no longer functional (Nebenfuhr, Ritzenthaler, & Robinson, 2002; Sciaky et al., 1997). Moreover, immunofluorescence microscopy indicated that the giantin stained clusters typical of an intact Golgi apparatus were dispersed in the presence of BFA (200 ng/ml; Figure 3.6). Together, these preliminary experiments supported the idea that the concentration of BFA employed in our subsequent studies of Cj-CDT cellular activity and localization was sufficient to disrupt the intact Golgi apparatus within HCT116 cells.

Monolayers of HCT116 cells were pre-incubated at 37 °C for 30 min in the absence or presence of BFA (200 ng/ml), and then was further incubated in the

absence or presence of Cj-CDT holotoxin (5 nM), which was generated by refolding together the Cj-CdtA, Cj-CdtB, and Cj-CdtC subunits that had been purified as recombinant proteins expressed individually in *Escherichia coli*, as previously described for Ec-CDT and Hd-CDT (Gargi et al., 2012; Gargi et al., 2013). The concentration of Cj-CDT used in these experiments (5 nM) was determined in preliminary studies to induce cell cycle arrest of approximately half the HCT116 cells within a monolayer (Figure 3.1). Because preliminary experiments established that the presence or absence of a hexa-histidine peptide fused to the amino-terminus of all three subunits comprising the CDT holotoxin had no detectable effect on toxin function, His-tagged proteins were used for all the experiments conducted in this study (Figure 3.1). After 24 h, Cj-CDT-intoxicated monolayers were evaluated for cell cycle progression by quantifying DNA content by flow cytometry. These studies revealed that HCT116 cells exposed to Cj-CDT exhibited 60% cell population at the G_2/M interface. In contrast, HCT116 cells, that have been pre-incubated with BFA, demonstrated cell cycle progression at levels similar to those measured in monolayers mock incubated with PBS and not treated either with BFA or Cj-CDT (Figure 3.2). These data indicate that Cj-CDT-mediated cell arrest is inhibited in the presence of BFA. Consistent with these results, we also found that HCT116 cells preincubated with Exo2, which selectively inhibits GBF1 at trans-Golgi network, as a primary target among the ArfGEFs, or Golgicide A (Gol A), a highly specific and reversible inhibitor of the cis-Golgi ArfGEF GBF1 (Saenz et al., 2009), also blocked Cj-CDT mediated cell cycle arrest (Figure 3.2).

To test the intoxication properties of Cj-CDT on the biological systems other than HCT116 cells, HeLa and CHO-K1 cell lines were tested for the capacity of Cj-CDT to induce cell cell arrest. The concentration of Cj-CDT used in these experiments to induce cell cycle arrest in approximately half the HeLa or CHO-K1 cells ($CCAD_{50}$) was determined to be 4.5 nM, or 31 nM, respectively (Figure 3.3). BFA, Exo2, and golgicide A-dependent inhibition of Cj-CDT-mediated cell cycle arrest was recapitulated in HeLa and CHO-K1 cells using the toxin dose close to, or slightly above the $CCAD_{50}$ dose established in HCT116 cells, for the respective cell line (Figure 3.4), which have been widely used to study the mechanism of Cj-CDT intoxication, suggesting that the requirement of an intact and functional Golgi apparatus for Cj-CDT cellular function is not idiosyncratic to HCT116 cell lines. Taken together, these results are consistent with a model that an intact Golgi apparatus is a requirement for Cj-CDT cellular intoxication.

Effects of brefeldin A (BFA) on Cj-CDT-localization to the nucleus. While the demonstration that Cj-CDT-mediated cell cycle arrest is blocked in the presence of BFA is consistent with the idea that an intact Golgi apparatus is important for toxin action, these data do not provide an explanation for why an intact Golgi apparatus is important for Cj-CDT function. Previous studies reported that subsequent to uptake from the cell surface, the catalytic CdtB domain of Cj-CDT (Damek-Poprawa, Korostoff, Gill, & DiRienzo, 2013), as well as Aa-CDT, Ec-CDT, and Hd-CDT, localizes to the nucleus (DiRienzo, 2014; Gargi et al.,

2013), which has been proposed to be the site of toxin action (Lara-Tejero & Galan, 2000). In preliminary immunofluorescence imaging studies, we confirmed that CdtB was visible within nuclei of HCT116 cells within 90 min subsequent to Cj-CDT holotoxin application to the monolayers (Figure 3.5), which was similar to the time frame earlier reported for Ec-CDT and Hd-CDT (Gargi et al., 2013). To evaluate whether an intact and functional Golgi apparatus is important for Cj-CdtB trafficking to the nucleus, we performed a “pulse” type of experiment in which cell entry of Cj-CDT was synchronized so that only pre-bound holotoxin at the cell surface was taken up into cells, allowing for monitoring of the uptake and trafficking of the “front-wave” of toxin into the cell. Monolayers of HCT116 cells were pre-incubated at 37 °C in the absence or presence of BFA (200 ng/ml), cooled to 4 °C, and then further incubated at 4 °C min in the absence or presence of Cj-CDT (100 nM). After 30 min, the monolayers were washed at 4 °C to remove unbound Cj-CDT, and then further incubated at 37 °C. Under these conditions, significantly fewer fluorescent puncta corresponding to immuno-stained Cj-CdtB were detected within the nuclei of HCT116 cells incubated in the presence than absence of BFA (Figure 3.6) indicating that BFA blocked nuclear localization of Cj-CdtB. To validate that BFA was sufficient to block Cj-CDT-mediated activation of the DNA repair response at the same higher toxin concentrations used for fluorescence imaging, HCT116 were pre-incubated in the absence or presence of BFA (200 ng/ml), and then further incubated at 37 °C with Cj-CDT at 100 nM rather than 5 nM, as described earlier. The monolayers were then assayed for both activation of H2AX (4 h) and cell cycle arrest (24 h).

These studies revealed that BFA blocked Cj-CDT-mediated H2AX activation and cell cycle arrest to the same extent in cells incubated with 100 nM Cj-CDT as 5 nM Cj-CDT (data not shown), indicating that an intact functional Golgi apparatus is important for Cj-CDT cellular activity at both low and high toxin concentrations. Taken together, these results are consistent with a model that an intact Golgi apparatus is necessary for both Cj-CdtB arrival at the nucleus, which in turn is required for toxin mediated DNA damage.

Evaluation of Cj-CDT localization with the Golgi apparatus. Our data are consistent with the idea that a functional Golgi apparatus is important for Cj-CDT localization to the nucleus, as well as toxin-dependent activation H2AX and subsequent arrest of cell cycle progression at the G_2/M interface. However, these data do not address a possible functional role of the Golgi apparatus for toxin localization to the nucleus and toxin intracellular activity. The activity of several bacterial toxins, including cholera toxin and shiga toxin, depends on an intact and functional Golgi apparatus (Lauvrak, Torgersen, & Sandvig, 2004b; Lencer, Hirst, & Holmes, 1999). Because the physiological function of the Golgi apparatus is to receive, sort, move, and package macromolecules for delivery to different cellular targets, the Golgi apparatus is thought to play an integral role in trafficking to the endoplasmic reticulum, where the active fragment of these toxins are retro-translocated to the cytosol (Bonifacino & Rojas, 2006). To evaluate the possibility that Cj-CdtB intracellular trafficking might involve the Golgi apparatus, we investigated whether CdtB localizes to the Golgi apparatus. HCT116 cells that

had been pre-chilled on ice, were pre-incubated on ice with Cj-CDT (100 nM) for 30 min, and then further incubated at 37 °C. The cells were analyzed by fluorescence microscopy at several time points to determine the capacity of Cj-CDT to localize to Golgi apparatus. These studies revealed the presence of green puncta, corresponding to Cj-CdtB, co-localized with red puncta, corresponding to giantin, a conserved Golgi membrane marker (Linstedt & Hauri, 1993), indicating that Cj-CdtB co-localizes to the Golgi apparatus. Co-localization of Cj-CdtB with giantin was initially observed at 20 minutes, which decreased significantly at 30 min (Figure 3.5), suggesting that Cj-CdtB trafficks through the Golgi apparatus, preceding trafficking to the nucleus at 90 min. These results were further confirmed from experiments indicating that Cj-CdtB co-localizes with both the trans-Golgi marker TGN46, and cis-Golgi marker GM130 (data not shown). Collectively, these results are consistent with a model that Cj-CDT is transiently and rapidly trafficked to the Golgi apparatus as a requisite step for localization to the nucleus and the toxin's cellular activity.

Evaluation of Cj-CdtB trafficking from early endolysosomal compartments to the Golgi apparatus. The results discussed above are consistent with the idea that toxin trafficking through the Golgi apparatus is important for Cj-CdtB ultimately reaching the nucleus prior to causing DNA damage. However, these data do not address the trafficking of Cj-CDT within host cells prior to arriving at the Golgi apparatus. Previous work had demonstrated that Aa-CDT, Ec-CDT, and Hd-CDT are all taken up into early endolysosomal compartments (Gargi et

al., 2013). Consistent with these studies conducted with CDTs from other pathogen species, preliminary immunofluorescence imaging studies here revealed that Cj-CdtB co-localizes with early endosomal antigen-1 (EEA1) within 10 min of synchronized uptake from the cell surface (data not shown). In addition, Cj-CDT-colocalization with EEA1 was visibly greater at 10 min than at 15 and 20 min (data not shown), suggesting that Cj-CDT-colocalization with the Golgi apparatus is transient. These data are consistent with the idea that subsequent to cell entry, Cj-CDT is trafficked through early endosomal compartments.

To evaluate if Cj-CDT may disembark directly from early endosomal compartments to the Golgi apparatus, we measured the capacity of toxin to produce cell cycle arrest in G_2/M interface in cells incubated in the absence or presence of two inhibitors, Retro-1 and Retro-2, which selectively re-localize SNARE protein syntaxin 5 (STX5), and to some extent STX6, thereby perturbing the early endosomal to Golgi trafficking, without affecting cellular morphology or other trafficking pathways (Stechmann et al., 2010). HCT116 cells that had been pre-incubated at 37 °C in the absence or presence of Retro-1 (10 μM) or Retro-2 (30 μM), were incubated further in the absence or presence of Cj-CDT (5 nM) at 37 ºC under 5% CO_2. After 24 h, the monolayers were evaluated for cell cycle progression by cellular DNA content analysis. These studies revealed that Cj-CDT induced the same degree of HCT116 cell cycle arrest at the G_2/M interface in the absence or presence of Retro-1 or Retro-2 (Figure 3.7), suggesting that Cj-CDT-dependent cell cycle arrest is not sensitive to Retro-1 or Retro-2

perturbation of STX5 mediated vesicular transport from early endosomal compartments to the Golgi apparatus. To further evaluate this idea, we compared the effects of Retro-1 on the Golgi apparatus localization of Cj-CdtB, or cholera toxin B subunit (CTxB), which previously was demonstrated to be transported from early endolysosomal compartments to the Golgi apparatus. These data revealed that in HCT116 cells, Retro-1 blocked the Golgi apparatus localization of CTxB, but not of Cj-CdtB, suggesting while Cj-CDT is not affected by perturbations in STX5, similar perturbations in STX5 affects the trafficking of CTxB to the Golgi apparatus (Figure 3.8).

Further validation of these results were derived from studies in which we evaluated the effects of disrupting the machinery involved in the fusion of vesicles originating from early endosomes destined for the Golgi apparatus on the capacity of Cj-CDT to localize to the Golgi apparatus. Docking and fusion of cargo-containing vesicles with the target organelles is mediated by molecular machines comprised of SNARE [SNAP (Soluble NSF Attachment Protein) Receptor] complex, which are present on the membranes of transport vesicles or target compartments. Syntaxins (STX) are an integral component of a subclass of SNAREs, called Q-SNAREs, which are involved in the trafficking of cargo within specific intracellular compartments. For early endosomal compartments destined to the Golgi transport, we used shRNA to knock down STX5, which is part of the STX5/Ykt6/GS28/GS15 SNARE complex, implicated in early endosome to Golgi apparatus trafficking (Amessou et al., 2007; Tai et al., 2004). HCT116 cells that were transfected with four siRNA constructs targeting different

parts of STX5 mRNA transcript (Dharmacon, Chicago, IL), showing about 90% knock-down of STX5 expression levels (Figure 3.9), were intoxicated with Cj-CDT holotoxin or CTxB, and probed for the localization of Cj-CdtB, or CTxB, with the Golgi apparatus. These data revealed that knocking down STX5, while significantly reduced the localization of CTxB with giantin, had minimal effect on Cj-CdtB localization with giantin (data not shown). Furthermore, STX5-knock down cells treated with Cj-CDT demonstrated H2AX activation similar to wild-type HCT116 cells (Figure 3.10). Taken together, these results suggest that Cj-CdtB might traffic to the Golgi apparatus utilizing a pathway independent of early endosome to Golgi trafficking, which prompted us to explore alternate pathways Cj-CdtB might employ to disembark from the endolysosomal system.

Evaluation of Cj-CdtB enrichment in late endolysosomal compartments. Our results above is consistent with a model that although Cj-CDT localizes to early endosomal vesicles subsequent to uptake from the cell surface, direct trafficking from these compartments to the Golgi apparatus is neither required for toxin cellular activity or Cj-CdtB arrival at the nucleus. However, these data do not address whether Cj-CdtB trafficking beyond early endosomal compartments is important for Cj-CDT cellular activity. To evaluate this possibility, we examined the effects of perturbing maturation of early endolysosomal compartments on the downstream trafficking of Cj-CDT and cellular activity of Cj-CdtB. To evaluate the effects of endosomal pH perturbing lysosomotropic agents on the biological activity of Cj-CDT, we first tested the correlation of late endosomal maturation on

the cytotoxic activity of Cj-CDT. HCT116 cells preincubated with ammonium chloride (20 mM), were intoxicated with Cj-CDT (5 nM), and analyzed for cell cycle progression 24 hours post-intoxication. These studies revealed that cell incubated in the presence of ammonium chloride demonstrated resistance to Cj-CDT-mediated cell cycle arrest (Figure 3.11). Moreover, cells pretreated with bafilomycin A1 (20 nM), which inhibits the action of vacuolar ATPase, thus blocking the acidification of intracellular vacuoles, also demonstrated resistance to Cj-CDT-mediated cell cycle arrest (Figure 3.11). These data indicate that the transport of Cj-CdtB to the Golgi apparatus is sensitive to pH-neutralizing drugs that affect vesicular transport at the late endosomal compartments. These findings were confirmed by the effect of polyether ionophore monensin, which is known to block intracellular protein transport by collapsing proton gradients as a sodium/proton antiporter, and, the potassium/proton carboxylic ionophore, nigericin, both of which significantly reduced the levels of cells arrested in G_2/M interface in response to Cj-CDT intoxication (Figure 3.12). Taken together, these results suggest late endosomal biogenesis might be important for the capacity of Cj-CDT to produce cell cycle arrest, and the Cj-CdtB might be targeted to the Golgi compartments from the late endosomes.

Our results above are consistent with a model that normal maturation of early to late endosomal vesicles is important for Cj-CDT cellular activity. However, these data do not address whether Cj-CDT is trafficked beyond early compartments to late endolysosomal vesicles. To evaluate this possibility, we used fluorescence imaging to visualize the localization of Cj-CdtB with the small

GTPase Rab9, which contributes to the generation and maintenance of late endosomal compartments (Ganley, Carroll, Bittova, & Pfeffer, 2004). HCT116 cells that were pre-chilled on ice, and then pre-incubated with Cj-CDT (100 nM) at 4 °C. After 30 min, the monolayers were washed to removed unbound Cj-CDT, and then further incubated at 37 °C, which are conditions that are permissive for uptake of surface-bound Cj-CDT. At 0, 10, and 20 min, HCT116 cells were analyzed for localization of Cj-CdtB with Rab9 using immunofluorescence microscopy. Our data revealed that green puncta, indicating Cj-CdtB, and red puncta, indicating Rab9, demonstrate significant co-localization, indicated by yellow puncta, within 10 min of Cj-CDT internalization (data not shown). Because we demonstrated above that Cj-CdtB localization to the Golgi apparatus is not detectable until 20 min after altering medium conditions to allow Cj-CDT uptake, these results are consistent with the model that the toxin is trafficked through late endolysosomal compartments prior to reaching the Golgi apparatus.

Evaluation of Cj-CdtB trafficking from late endolysosomal compartment to the Golgi apparatus. The results above are consistent with a model that subsequent to uptake from the plasma membrane, Cj-CDT trafficking within the endolysosomal system from early to late endosomal compartments is important for the toxin's cellular activity. However, these data did not address whether toxin egress from late to endosomal compartment is required for the toxin's cellular activity. To evaluate the importance of Cj-CDT trafficking out of late endosomal compartments, we compared Cj-CDT-dependent phosphorylation of H2AX (as an

early marker of DNA-damage response, (Kuo & Yang, 2008; Sharma, Singh, & Almasan, 2012)) in untransfected HCT116 cells versus HCT116 cells that had been transiently transfected with a plasmid expressing a gene encoding and dominant-negative form of Rab9 (DN-Rab9 (S21N)) fused to DsRed, (DN-DsRed-Rab9 (S21N)), which is defective in nucleotide exchange and has a reduced affinity for GTP (Choudhury et al., 2002). The GTPase Rab9, component of the late endosome-to-TGN pathway, is required for efficient trafficking of cargo, like furin, from late endosomes to the Golgi apparatus (Chia, Gasnereau, Lieu, & Gleeson, 2011; Pfeffer, 2009). We evaluated the importance of a functional Rab9 in the retrograde trafficking of Cj-CDT in HCT116 cells. Monolayers of HCT116 cells that contained cells expressing and not expressing DN-DsRed-Rab9 (S21N) were incubated at 37 °C in the absence or presence of Cj-CDT (100 nM), and then scored after 4 h for the percentage of cells with visible H2AX phosphorylation. Because not all cells within HCT116 monolayers were successfully transfected (as indicated by the lack of red fluorescence corresponding to the expression of DN-DsRed-Rab9 (S21N), we scored pDN-DsRed-Rab9 transfected and non-transfected cells simultaneously within individual wells for H2AX phosphorylation. These studies revealed significantly fewer cells with nuclear-localized green fluorescence corresponding to phosphorylated H2AX in cells expressing DN-DsRed-Rab9 (Figure 3.13). These data indicate that Cj-CDT-mediated activation of the host cell's DNA repair response is inhibited in cells in which egress from late endosomal vesicles is

impaired, which is consistent with the idea that Cj-CDT trafficking through late endolysosomal compartments is important for toxin mediated cellular activity.

Although the above results support a model that Cj-CDT trafficking through late endolysosomal compartments is required for toxin cellular activity, these data do not address whether egress of Cj-CDT from late endosomal vesicles is important for toxin localization to the Golgi apparatus or the nucleus, both of which we have demonstrated are required for toxin activity. To evaluate this idea, we determined the extent to which Cj-CdtB is localized to the Golgi apparatus and nucleus in cells in which egress from late endolysosomal vesicles was impaired. Monolayers of HCT116 cells that contained cells expressing and not expressing DN-DsRed-Rab9 (S21N) were pre-chilled on ice to prevent the internalization of cell surface membrane components, and then further incubated on ice in the presence or absence of Cj-CDT (100 nM). After 30 min, the monolayers were washed to removed unbound Cj-CDT, and then further incubated at 37 °C to allow for uptake and intracellular trafficking of plasma membrane-bound toxin. After 20 and 90, the cells were monitored for Cj-CDT localization to the Golgi apparatus and nucleus, respectively, using immunofluorescence microscopy. These studies revealed that Cj-CdtB colocalization with giantin, and DAPI-stained nuclei, were significantly reduced in cells expressing DN-Rab9 versus untransfected cells (data not shown), indicating that functional Rab9 GTPase is important for the downstream trafficking of Cj-CdtB to the Golgi apparatus, and the nucleus. Taken together, these results suggest that toxin egress from late endolysosomal vesicles is important for

subsequent localization of the Golgi apparatus and nucleus, which is consistent with a model that Cj-CDT trafficking through late-endolysosomal compartments is required for toxin localization and function within the nucleus.

Although the results described above support the idea that Cj-CdtB trafficking through the late endosomes is important for toxin localization to the Golgi apparatus and nucleus, these data don't address whether Cj-CDT is trafficked directly from late-endolysosomal compartments to the Golgi apparatus. To evaluate this possibility, we investigated the effects of disrupting a known pathway for the trafficking of membrane-associated cargo from late-endosomal vesicles to the Golgi apparatus. Specifically, steady-state levels of syntaxin10 (STX10) were knocked-down using STX10-specific siRNAs. STX10 is part of the STX10/STX16/Vti1A/VAMP3-containing SNARE complex, which is important for trafficking of the mannose phosphate receptor from late endosomal compartments to the TGN (Amessou et al., 2007; Ganley, Espinosa, & Pfeffer, 2008; Saint-Pol et al., 2004). Western blot analysis indicated significantly less STX10 in cells transfected with STX10-specific siRNAs than in untransfected cells, or in cells transfected with a scrambled siRNA (Figure 3.14), and quantification indicated that cellular STX10 in STX10-knockdown cells was less than 10% in cells transfected with the scrambled siRNA (Figure 3.14). Untransfected HCT116 cells or HCT116 cells transfected with either STX10-specific siRNA or scrambled siRNA were incubated at 37 °C with Cj-CDT (100 nM). The monolayers were visualized using immuno-fluorescence microscopy for phosphorylated H2AX within the nucleus of host cells at 4 h, a time at which we

detected a significantly great number of cells with activated H2AX in cells incubated in the presence than absence of Cj-CDT. These experiments revealed significantly less green fluorescence, corresponding to nuclear localized phosphorylated H2AX, in HCT116 cells transfected with STX10-specific siRNA than in HCT116 cells transfected with scrambled siRNA or untransfected HCT116 cells (Figure 3.15), indicating that Cj-CDT-dependent H2AX activation was inhibited in cells which STX10 was knocked down. These data suggest that a functional STX10-dependent late-endosomal to Golgi apparatus trafficking pathway is important for Cj-CDT cellular function, which is consistent with the idea that Cj-CDT trafficking from late endolysosomal compartments to the Golgi apparatus is important for toxin-mediated cellular activity.

Although the results described above support a model that a functional STX10-dependent late-endosomal to Golgi apparatus trafficking pathway is required for Cj-CDT cellular activity, these data do not address whether this same pathway is important for toxin transit from late endosomal compartments to the Golgi apparatus, and ultimately the nucleus. To evaluate this possibility, untransfected HCT116 cells, or, HCT116 cells transfected with either STX10-specific siRNA or scrambled siRNA were prechilled on ice, and then further incubated on ice with Cj-CDT (100 nM). After 30 min, the monolayers were washed to remove unbound Cj-CDT, and then further incubated at 37 °C to allow the internalization and trafficking of surface bound toxin, and the cells were examined by fluorescence microscopy for Cd-CdtB co-localization with giantin, as a marker for localization to the Golgi apparatus, and, DAPI, as a marker for

localization to the nucleus. These experiments revealed significantly less green fluorescence associated with giantin-enriched structures, corresponding to the Golgi apparatus at 20 min in HCT116 cells transfected with STX10-specific siRNA than in HCT116 cells transfected with scrambled siRNA or untransfected HCT116 cells (data not shown), indicating that Cj-CDT localization to the Golgi apparatus was inhibited in cells which STX10 was knocked down. In addition, there was significantly less green fluorescence associated with the DAPI stain, corresponding to the nucleus at 90 min in HCT116 cells transfected with STX10-specific siRNA than in HCT116 cells transfected with scrambled siRNA or untransfected HCT116 cells (data not shown), indicating that Cj-CDT localization to the nucleus was inhibited in cells which STX10 was knocked down. Taken together, these data suggest that a functional STX10-dependent late-endosomal to Golgi apparatus trafficking pathway is important for Cj-CDT localization to the Golgi apparatus and subsequently to the nucleus, consistent with the idea that Cj-CDT transitions from late endolysosomal compartments to the Golgi apparatus by a vesicular-mediated pathway involving the STX10/STX16/Vti1A/VAMP3-containing SNARE complex.

Evaluation of the importance of tethering of Cj-CDT-containing vesicles to the Golgi complex.The results described above are consistent with a model that a functional STX10-dependent late-endosome to Golgi apparatus trafficking pathway is important for the transition of endolysosomal-localized Cj-CDT to the Golgi apparatus. However, these data do not address whether Golgi-specific

targeting of Cj-CDT-containing vesicles (CCVs) is important for toxin localization to the nucleus and cellular activity. Golgi specific tethering of vesicular targeting and fusion machinery (Willett et al., 2013) is mediated by the conserved oligomeric Golgi (COG) complex, a Golgi membrane resident hetero-octamer composed of 8 subunits (COG1 to COG8), which is required for tethering and docking vesicles targeting the Golgi apparatus. To evaluate the importance of the Golgi tethering machinery for Cj-CDT mediated cellular activity, we compared the toxin-dependent DNA damage response in the parental HCT116 cell line versus two HCT116 cell lines where two components of the COG complex, COG4 and COG8, had been stably knocked down using COG4- specific or COG8-specific shRNAs (data not shown). Stable HCT116 cell lines with either COG4 or COG8 knocked down, or, HCT116 cells stably transfected with a scrambled shRNA, were incubated at 37 °C in the absence or presence of Cj-CDT (100 nM). After 4 h, the monolayers were visualized using immuno-fluorescence microscopy for phosphorylated H2AX within the nucleus. These experiments revealed significantly less green fluorescence, corresponding to nuclear localized phosphorylated H2AX, in HCT116 cells stably transfected with COG4- specific or COG8-specific shRNAs than in HCT116 cells transfected with scrambled shRNA or untransfected HCT116 cells (Figure 3.16), indicating that Cj-CDT-dependent H2AX activation was inhibited in cells which COG4 or COG8 was knocked down. These data suggest that a functional COG complex is important for Cj-CDT cellular function, which is consistent with the idea that CCV-specific targeting of the Golgi apparatus is important for toxin-mediated cellular activity.

Although the results described above support a model that a functional COG complex is required for Cj-CDT cellular activity, these data do not address whether a functional COG complex is important for toxin transit from late endosomal compartments to the Golgi apparatus, and ultimately the nucleus. To evaluate this possibility, stable HCT116 cell lines with either COG4 or COG8 knocked down, or, HCT116 cells stably transfected with a scrambled shRNA, were pre-chilled on ice, and then further incubated on ice in the absence or presence of Cj-CDT (100 nM) that had also been pre-chilled on ice. After 30 min, the monolayers were washed with ice-cold PBS pH 7.4 to remove unbound toxin, and then further incubated at 37 °C in order to allow for the uptake and intracellular trafficking of plasma membrane bound Cj-CDT. After 20 min, the cells were examined by fluorescence microscopy for Cd-CdtB co-localization with giantin, as a marker for toxin localization to the Golgi apparatus, and, after 90 min, were examined for co-localization with DAPI, as a marker for toxin localization to the nucleus. These experiments revealed significantly less green fluorescence associated with giantin-enriched structures, corresponding to the Golgi apparatus at 20 min, in HCT116 cells stably transfected with COG4- or COG8- specific shRNA than in HCT116 cells transfected with scrambled shRNA or untransfected HCT116 cells (data not shown), indicating that Cj-CDT localization to the Golgi apparatus was inhibited in cells which COG4 or COG8 had been knocked down. In addition, there was significantly less green fluorescence associated with the DAPI stain, corresponding to the nucleus at 90 min, in HCT116 cells transfected with COG4- or COG8-specific shRNA than in

HCT116 cells transfected with scrambled shRNA or untransfected HCT116 cells (Figure 3.17), indicating that Cj-CDT localization to the nucleus was inhibited in cells which COG4 or COG8 was knocked down. Taken together, these data suggest that a functional COG complex-dependent tethering of CCVs is important for localization of Cj-CdtB to the Golgi apparatus and nucleus, which is consistent with the hypothesis that tethering of vesicles originating from late endolysosomal compartments to the Golgi apparatus is a critical step for trafficking of Cj-CdtB to the nucleus and toxin-mediated activation of the DNA repair response.

Evaluation of the effects of mis-targeting Cj-CDT-containing vesicles. The results described above are consistent with the idea that a functional COG complex is important for localization of Cj-CdtB to the Golgi apparatus and nucleus, as well as toxin-dependent activation of the host cell DNA repair response. These findings suggest that the COG complex is critical for tethering CCVs to the Golgi apparatus as a requisite step for the transition of Cj-CdtB from CCVs to the lumen of the trans-Golgi network, and provides an opportunity to definitively establish a causal link between Cj-CdtB localization to the Golgi apparatus as step that is essential for the toxin's cellular activity. Specifically, we adopted an approach to determine the effects of mis-targeting CCVs away from the Golgi apparatus on toxin function. HCT116 cells were co-transfected with a plasmid overexpressing either the gene encoding siRNA-resistant COG4 or COG8, each fused to mCherry (mCh) fluorescent protein and the mitochondrial-

targeting ActA sequence from *Listeria*, which were called COG4-mChActA or COG8-mChActA, respectively (Willett et al., 2013), and COG4- and COG8-specific siRNA. Preliminary studies validated that in HCT116 cells expressing either COG4-mChActA or COG8-mChActA, red puncta corresponding to either COG4-mChActA or COG8-mChActA were significantly more co-localized with TOM20, a mitochondrial resident protein, than cells expressing mChActA alone, indicating that mislocalized COG proteins do in fact localize to mitochondria (data not shown).

To evaluate the consequences of mis-targeting CCVs to mitochondria on Cj-CDT cellular activity, HCT116 cells transiently co-transfected with siRNA against COG4, and a plasmid expressing siRNA-resistant COG4-mChActA, or with siRNA against COG8, and a plasmid expressing siRNA-resistant COG8-mChActA, were incubated at 37 °C in the absence or presence of Cj-CDT (100 nM). After 4 h, the monolayers were visualized using immuno-fluorescence microscopy for phosphorylated H2AX within the nucleus. These experiments revealed significantly less green fluorescence, corresponding to nuclear localized phosphorylated H2AX, in HCT116 cells transiently co-transfected with siRNA against COG4, and a plasmid expressing siRNA-resistant COG4-mChActA, or with siRNA against COG8, and a plasmid expressing siRNA-resistant COG8-mChActA than in HCT116 cells transfected with scrambled siRNA or untransfected HCT116 cells (Figure 3.18). These data indicate that mistargeting of COG4-mChActA or COG8-mChActA inhibits Cj-CdtB-mediated activation of

H2AX, further validating the importance of the COG complex for targeting of cytolethal distending toxin-containing vesicles (CCVs) within the cell.

Although the results described above further validate the requirement for a functional COG complex for Cj-CDT cellular activity, these data do not address whether mis-targeting COG complexes to mitochondria results in mis-targeting of CdtB to mitochondria. HCT116 cells transiently co-transfected with siRNA against COG4, and a plasmid expressing siRNA-resistant COG4-mChActA, or with siRNA against COG8, and a plasmid expressing siRNA-resistant COG8-mChActA, HCT116 cells transfected with scrambled siRNA, or untransfected HCT116 cells, were pre-chilled on ice, and then further incubated on ice with Cj-CDT (100 nM) that had also been pre-chilled on ice. After 30 min, the monolayers were washed with pre-chilled PBS pH 7.4 to remove unbound Cj-CDT, and then further incubated at 37 °C to allow for the uptake and intracellular trafficking of plasma membrane Cj-CDT. After 20 min, the cells were examined by fluorescence microscopy for Cd-CdtB co-localization with giantin, as a marker for toxin localization to the Golgi apparatus, and, after 90 min, were examined for co-localization with DAPI, as a marker for toxin localization to the nucleus. These experiments revealed significantly less green fluorescence associated with giantin-enriched structures, corresponding to the Golgi apparatus at 20 min, in HCT116 cells expressing COG4-mChActA or COG8-mChActA, than in the HCT116 parental cells (data not shown), indicating that Cj-CDT localization to the nucleus was inhibited in cells which COG4 or COG8 was mis-targeted to mitochondria. In addition, there was significantly less green fluorescence

associated with the DAPI stain, corresponding to the nucleus at 90 min, in HCT116 cells expressing COG4-mChActA or COG8-mChActA than in the HCT116 parental cells (data not shown), indicating that Cj-CDT localization to the nucleus was inhibited in the cells in which COG4 or COG8 was targeted to the mitochondria.

Finally, because we had already demonstrated that COG4-mChActA or COG8-mChActA are retargeted to mitochondria in HCT116 cells, we evaluated whether CdtB is localized to mitochondria in these same cells. HCT116 cells transiently co-transfected with siRNA against COG4, and a plasmid expressing siRNA-resistant COG4-mChActA, or with siRNA against COG8, and a plasmid expressing siRNA-resistant COG8-mChActA, HCT116 cells transfected with scrambled siRNA, or untransfected HCT116 cells, were pre-chilled on ice, and then further incubated on ice with Cj-CDT (100 nM) that had also been pre-chilled on ice. After 30 min, the monolayers were washed with pre-chilled PBS pH 7.4 to remove unbound Cj-CDT, and then further incubated at 37 °C to allow for the uptake and intracellular trafficking of plasma membrane Cj-CDT. After 20 min, the cells were examined by fluorescence microscopy for Cd-CdtB co-localization with TOM20, as a marker for toxin localization to mitochondria. These experiments revealed significantly greater green fluorescence associated with TOM20-enriched structures, corresponding to mitochondria, in HCT116 cells expressing COG4-mChActA or COG8-mChActA, than in the HCT116 parental cells (Figure 3.19), indicating that Cj-CdtB localized to mitochondria in cells in which COG4 or COG8 was targeted to mitochondria. Taken together, these data

provide strong causal evidence that the correct targeting of Cj-CDT from late endolysosomal system to the Golgi apparatus is an essential step for subsequent toxin localization to the nucleus and toxin-mediated DNA damage.

3.4. Discussion

There is substantial evidence that CDTs localize to the nuclei of host cells, whereby the active Cj-CdtB induces the activation of the DNA repair response, presumably through this subunit's DNAse I-like enzymatic activity (DiRienzo, 2014; Gargi et al., 2012). However, the mechanistic details by which members of the CDT family transition from the surface of the host cell cells to the nucleus remain poorly understood. Several lines of evidence suggest that, similar to cholera, Shiga, and pertussis toxins, CDTs usurp retrograde trafficking pathways, in which protein cargo are moved through the cell to the endoplasmic reticulum (ER), where the active subunits are translocated from the ER lumen to the cytosol. Retro-translocation is thought to be absolutely required for access to the host target molecule to the toxin's active subunit. A major gap in knowledge has been the mechanism of how Cj-CDT is trafficked from the cell surface to the nucleus, which previous studies have strongly implicated as the site of Cj-CdtB action. Here, we provide evidence supporting a model that subsequent to uptake from the cell surface into the endolysosomal system, Cj-CDT is trafficked from early to late endolysosomal compartments. Localization of Cj-CdtB to the nucleus requires egress of the toxin from the endolysosomal system, and for Cj-CdtB. Although our data revealed an association between transient Cj-CdtB localization

to the TGN, and, toxin mediated cellular activity, these data did not definitively establish that Cj-CdtB trafficking through the Golgi apparatus is essential for the toxin's cellular activity. To do so, we demonstrated that an approach involving the mistargeting of CDT-containing vesicles, originating from late endosomal compartments, to mitochondria rather than the Golgi apparatus, was sufficient to completely block Cj-CDT mediated DNA damage. To our knowledge, this is the first evidence that CDT targeting to the Golgi apparatus is essential for the toxin to reach its ultimate site of action.

An intact and functional Golgi apparatus was found to be critical for Cj-CDT trafficking to the nucleus as a requisite step for toxin mediated DNA damage. Bacterial exotoxins that access intracellular targets via retrograde trafficking are taken up into the endolysosomal system, from where they must move to the ER for retro-translocation of their active subunits to the cytosol. Many studies have revealed two overall intracellular routes by which toxins move from the endolysosomal system to the ER. Several toxins have been demonstrated to move directly from the endolysosomal system to the ER, by a mechanism requiring vesicular trafficking. Alternatively, some bacterial toxins, including cholera-, shiga-, and pertussis toxins are trafficked through the Golgi apparatus as a requisite step preceding toxin action were based primarily on the requirement for an intact Golgi apparatus (Falnes & Sandvig, 2000). The exact mechanism that differentiates toxins that undergoes direct trafficking to the ER, from toxins that must transit through the Golgi apparatus along the way, is still not known.

The discovery that Cj-CdtB localization to the nucleus, and, toxin-dependent activation of the DNA repair response requires the presence of the conserved oligomeric Golgi (COG) complex, not only extended our understanding of the host machinery required for toxin association with the Golgi apparatus, but also provided an opportunity to evaluate the requirement of Golgi-specific targeting of cytolethal distending toxin-containing vesicles (CCVs) for toxin activity.

Previous work demonstrated that some bacterial toxins, including cholera (Lencer et al., 1999) and shiga toxins (Lauvrak, Torgersen, & Sandvig, 2004a), are trafficked to the Golgi apparatus from early compartments within the endolysosomal system. Here, we demonstrate a different scenario, where Cj-CDT does not exit the endolysosomal system from early compartments, but rather is trafficked to late endolysosomal compartments. Our studies demonstrating that Cj-CDT-mediated cellular intoxication and Cj-CdtB localization to the nucleus occur in a syntaxin10-dependent manner were consistent with a model that Cj-CDT is trafficked from late endolysosomal compartments to the Golgi apparatus. The studies here revealed the importance of an intact Golgi apparatus for the trafficking of Cj-CdtB to the nucleus as a requisite step for Cj-CdtB-mediated DNA damage. How might the requirement for an intact Golgi apparatus relate to the cellular activity of Cj-CDT? Typically, studies that have reported the blocking of bacterial toxin cellular activities with BFA have interpreted these results to indicate the requirement for toxin trafficking through the Golgi apparatus. The pathway from TGN to ER in almost all cells is,

however, sensitive to Brefeldin A, a fungal metabolite known to induce tubulation of the TGN and subsequent dispersion into endosomes and ER membranes (Nambiar, Oda, Chen, Kuwazuru, & Wu, 1993). The effects of Exo2 are different, in that this small molecule inhibitor collapses the Golgi stacks, but does not affect the TGN (Feng et al., 2004). Retrograde transport of cholera toxin from the plasma membrane to the endoplasmic reticulum requires the trans-Golgi network but not the Golgi apparatus in Exo2-treated cells (Feng et al., 2004). In contrast to Cj-CDT, cholera toxin is not sensitive to Exo2, suggesting that this toxin might bypass the Golgi cisternae trafficking directly to the ER (Feng et al., 2004). The demonstration that Cj-CdtB localization to the nucleus as well as Cj-CdtB-dependent activation of H2AX were inhibited not only by BFA, by also by Exo2, is consistent with the idea that, unlike for cholera toxin, trans-Golgi apparatus is involved in the vesicular trafficking of Cj-CdtB.

In conclusion, this study has demonstrated that Golgi-specific targeting of Cj-CDT to the Golgi apparatus is essential for toxin to reach nucleus and elaborate its cytotoxic activity. This study will impact our understanding on the role of host's molecular machinery in pathogenesis.

3.5. Figures

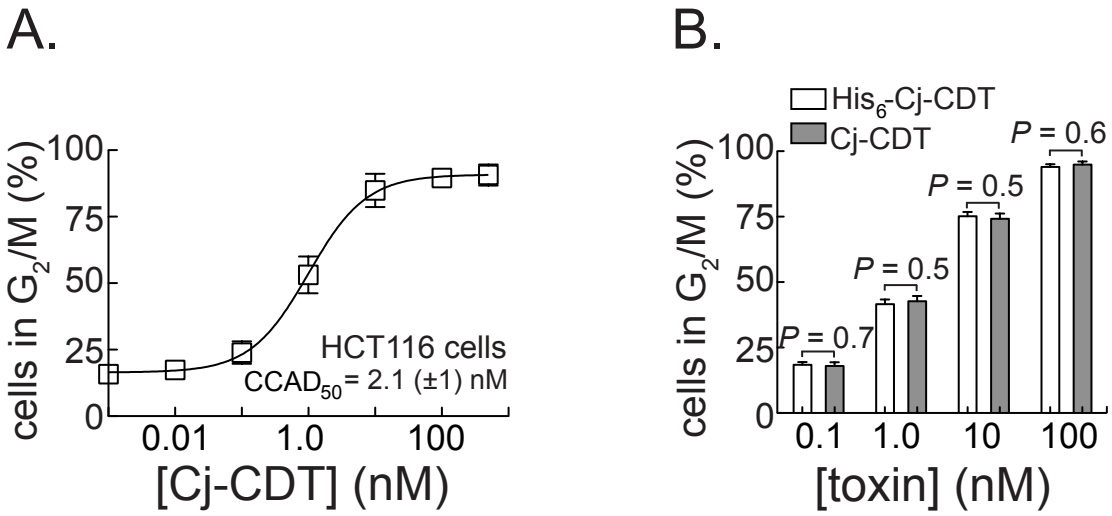

Figure 3.1. Cj-CDT mediated cell cycle arrest in HCT116 cells. (A) Dose response curve of Cj-CDT mediated cell cycle arrest. Monolayers of HCT116 cells were incubated in the presence of Cj-CDT (0.01 -100 nM). After 24 h, the cells were analyzed for G_2/M arrest using flow cytometry, as described under "Experimental Procedures." The data were rendered as the percentage of cells detected in G_2/M arrest as a function of toxin concentration. Data were collected from 3 independent experiments. Error bars represent standard deviations. (B) Effect of His-tag on the cell cycle arrest properties of Cj-CDT. Monolayers of HCT116 cells were incubated in presence of Cj-CDT (0.1 - 100 nM), without, or with, N-terminal His-tag. After 24 h, the cells were analyzed for arrest in G_2/M using flow cytometry. The results are rendered as bar graphs generated from data combined from three independent experiments that compare the percentage of cells arrested in G_2/M in Cj-CDT with N-terminal Hist-tag (while bars), or without His-tag (black bars). Error bars represent standard deviations. Statistical significance was calculated for the differences between cell populations incubated in the presence of Cj-CDT with, or without N-terminal His-tag.

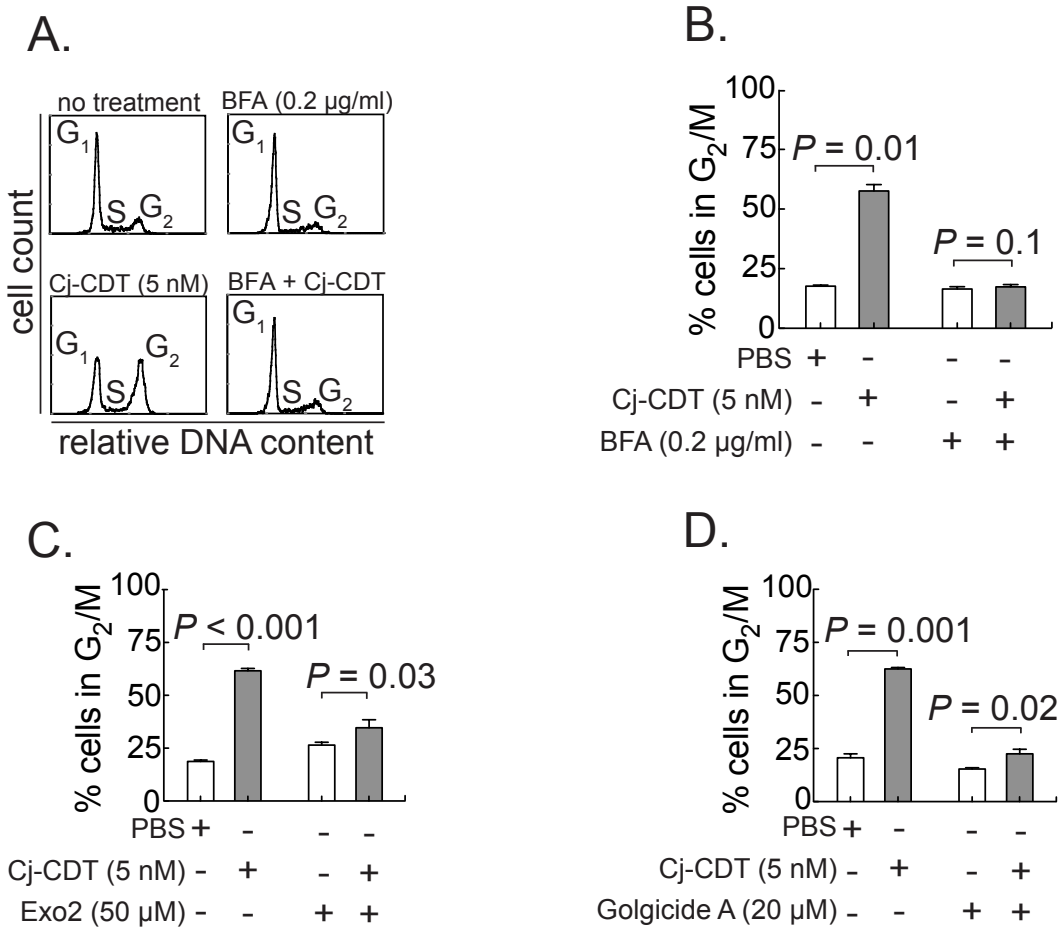

Figure 3.2. Importance of the Golgi apparatus for Cj-CDT activity in HCT116 cells. Cj-CDT (5 nM)-mediated arrest of HCT116 cells in G_2/M was determined in the absence or presence of BFA (0.2 μg/ml; A - B), Exo2 (50 μM; C), or Golgicide A (20 μM; D). (A) The data are rendered as individual histograms representative of those collected during three independent experiments. Histograms indicate the number of cells (y axis, same scale for each histogram) at a given PI fluorescence intensity (x axis, same scale for each histogram), with, as indicated in the top left histogram, the left peak representing cells in G_0/G_1 phase (designated as G_1) of the cell cycle, the right peak representing cells in G_2/M (designated as G_2), and the area between the peaks representing cells in S phase (designated as S). (B – D) The results are rendered as bar graphs generated from data combined from three independent experiments that compare the percentage of cells arrested in G_2/M in untreated cells (white bars), cells treated with Cj-CDT, in the absence of drug (black bars) or cells treated with the drug in the absence or presence of Cj-CDT, as indicated by gray bars (BFA, B; Exo2, C; or GCA, D). Error bars represent standard deviations. Statistical significance was calculated for the differences between cell populations incubated in the absence or presence of the pharmacological agents.

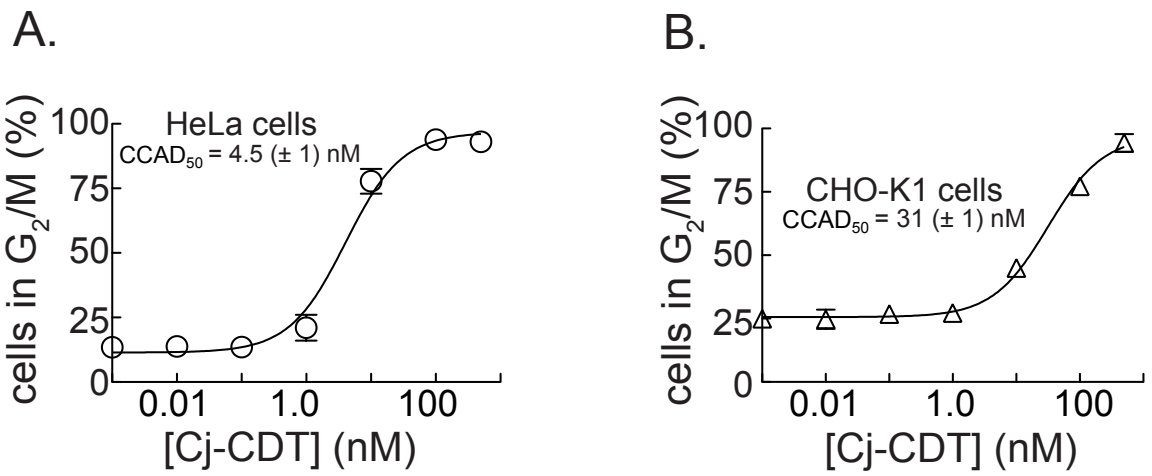

Figure 3.3. Dose response curve of Cj-CDT mediated G_2/M arrest in HeLa, and CHO-K1 cells. Monolayers of HeLa (A), and CHO-K1 (B) cells were incubated in the presence of Cj-CDT (0.01 -100 nM). After 24 h, the cells were analyzed for G_2/M arrest using flow cytometry, as described under "Experimental Procedures." The data were rendered as the percentage of cells detected in G_2/M arrest as a function of toxin concentration. Data were collected from 3 independent experiments. Error bars represent standard deviations.

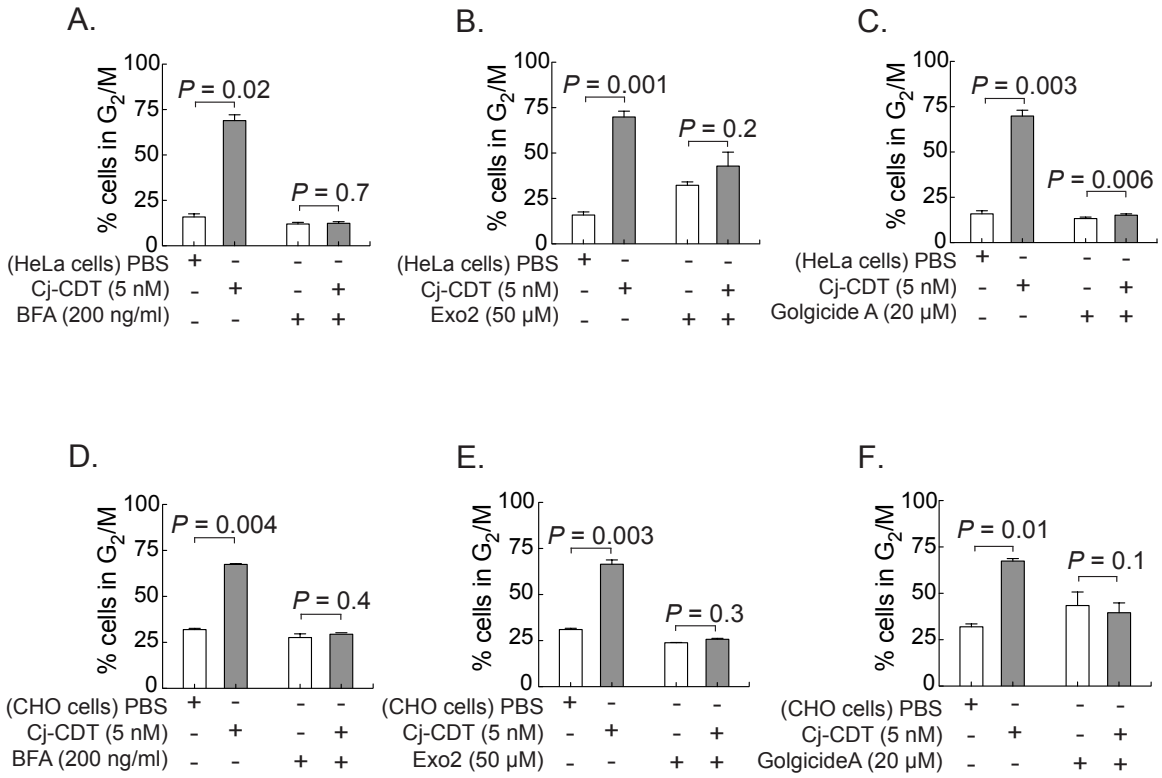

Figure 3.4. Importance of the Golgi apparatus for Cj-CDT activity in HeLa and CHO-K1 cells. Monolayers of HeLa (A – C), or CHO-K1 (D – F) cells, were intoxicated with Cj-CDT close their respective $CCAD_{50}$ values (5 nM Cj-CDT for HeLa cells, and 100 nM Cj-CDT CHO-K1 cells) that were pre-incubated in the absence or presence of BFA (0.2 μg/ml; A, D), Exo2 (50 μM; B, E), or Golgicide A (20 μM; C, F). After 24 h, the cells were analyzed for arrest in G_2/M using flow cytometry. The data were rendered as the percentage of cells in G_2/M as a function of Cj-CDT intoxication and presence of small molecule inhibitor. Error bars represent standard deviations. Statistical significance was calculated for the differences between cell populations incubated in the absence or presence of indicated pharmacological agents.

A.

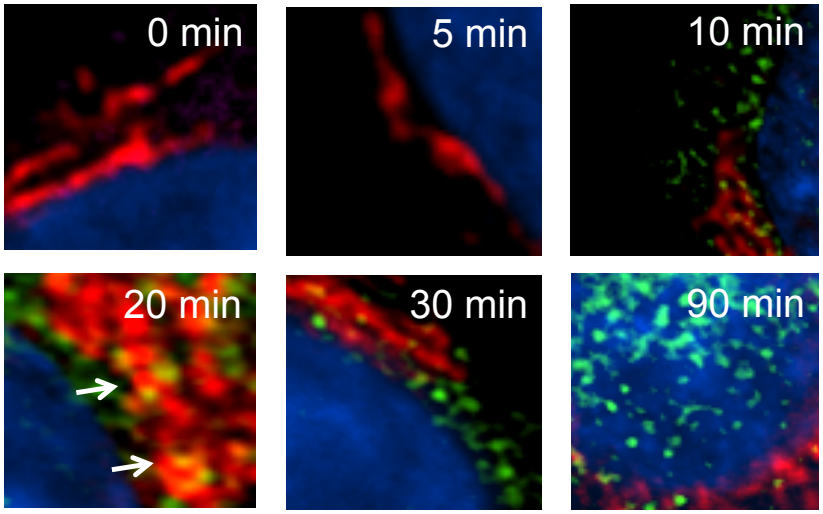

B.

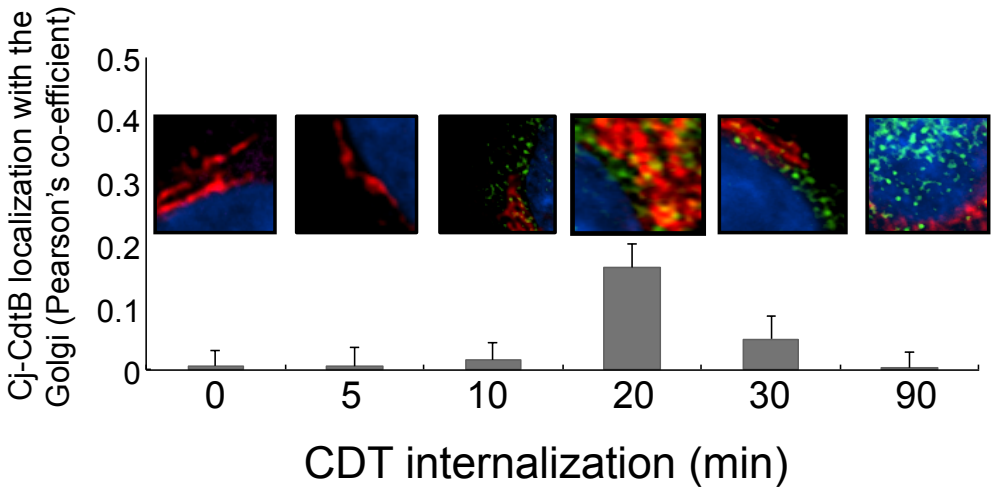

Figure 3.5. Cj-CdtB co-localization with the Golgi apparatus. HCT116 cells that had been prechilled on ice for 30 min, were incubated with prechilled Cj-CDT (100 nM). After 30 min, the cells were washed once with PBS pH 7.4, and then further incubated at 37 °C. (A) After 0, 5, 10, 20, 30, or 90 mins, the cells were fixed, and probed for Cj-CdtB and giantin, using fluorescence microscopy. Images are representative of those collected from three independent experiments. The data were rendered as a single z-plane (approximately 5 μm depth within each cell). As labeled, green puncta indicate Cj-CdtB, red puncta indicate giantin, and Cj-CdtB co-localized with giantin is indicated by yellow puncta. (B) The results are rendered as bar graphs generated from data combined from three independent experiments. Error bars represent standard deviations.

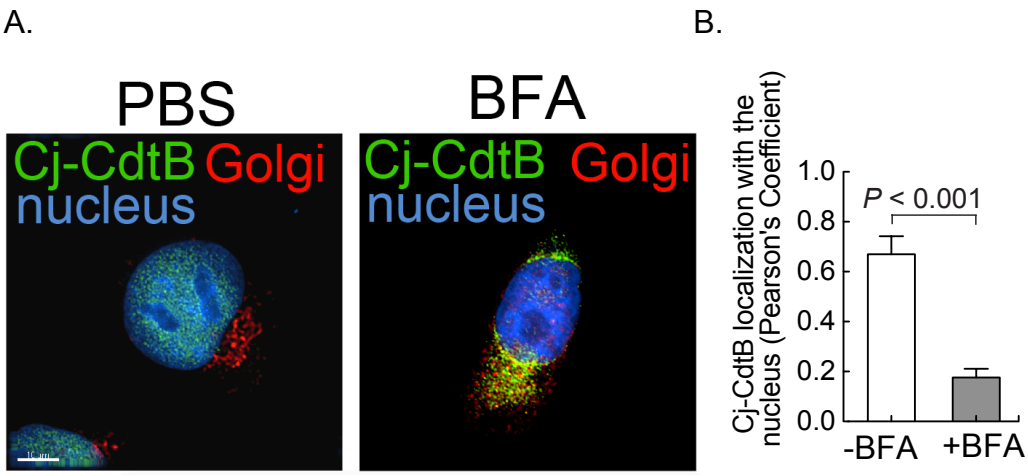

Figure 3.6. Effects of Golgi dysfunction on Cj-CdtB localization to the nucleus. HCT116 cells were incubated with 100 nM Cj-CDT at 37 °C for 90 min in the absence or presence of BFA (0.2 μg/ml), and were imaged using fluorescence microscopy. (A) Images were representative of those collected from three independent experiments. The data were rendered as a single z-plane (5 μm depth within each cell). As labeled, green puncta indicate Cj-CdtB, and blue fluorescence indicate nucleus. White bars indicate 10 μm. (B) The results are rendered as a bar graph generated from data combined from three independent experiments that compare the Pearson's correlation coefficient for Cj-CdtB co-localized with nucleus in cells treated with Cj-CDT, in the absence (black bars), or presence (gray bars) of BFA. Error bars represent standard deviations. Statistical significance was calculated for differences in the Pearson's correlation coefficient between cell populations incubated in the presence or absence of BFA.

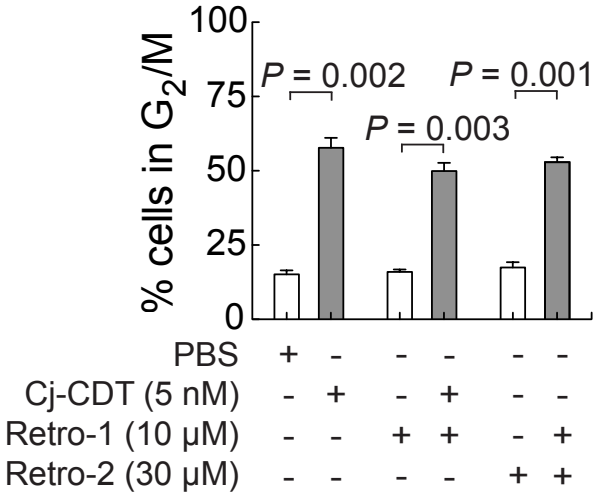

Figure 3.7. Effect of inhibiting cargo transition from early endosome to the Golgi apparatus, on Cj-CDT mediated cell cycle arrest. Monolayers of HCT116 cells were exposed to Retro-1 (10 μM) or Retro-2 (30 μM) for 30 min at 37 °C. After 30 min, cells were intoxicated by Cj-CDT (5 nM), and further incubated at 37 °C. After 24 h, holotoxin mediated arrest of HCT116 cells in G_2/M was determined in the absence or presence of Retro-1 or Retro-2. The results are rendered as bar graphs generated from data combined from three independent experiments that compare the percentage of cells arrested in G_2/M in untreated cells (white bars), cells treated with Cj-CDT, or cells treated with Retro-1 or Retro-2 in the absence or presence of Cj-CDT, as indicated (gray bars). Error bars represent standard deviations. Statistical significance was calculated for the differences between cell populations incubated in the absence or presence of Retro-1 or Retro-2. Error bars represent standard deviations.

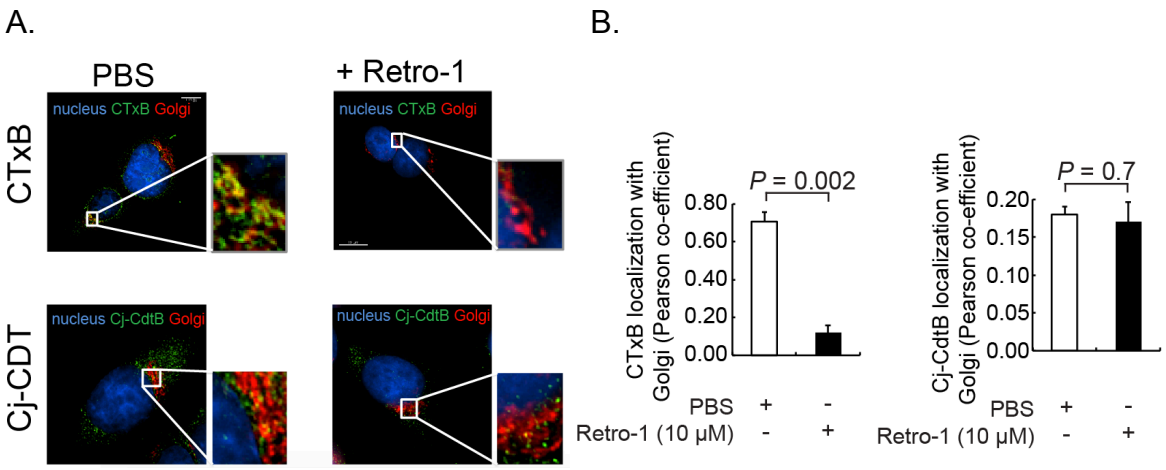

Figure 3.8. Effect of inhibiting cargo transition from early endosome to the Golgi apparatus, on the localization of CTxB, or Cj-CdtB, with the Golgi apparatus. Monolayer of HCT116 cells were treated with Retro-1 (10 μM) at 37 °C. After 30 minutes, cells were chilled on ice for additional 30 minutes, and treated with prechilled alexa-488 labeled Cholera Toxin B-subunit (CTxB-488; 100 nM), or Cj-CDT (100 nM). After 30 min, the cells were washed once with PBS pH 7.4, and incubated at 37 °C. After 60 min, the cells were fixed, probed with the antibodies against specified antigens, and imaged using fluorescence microscopy. Images are representative of those collected from three independent experiments. The data were rendered as a single z-plane (approximately 5 μm depth within each cell). As labeled, green puncta indicate CTxB-488 or Cj-CdtB, red puncta indicate giantin, and toxin co-localized with giantin is indicated by yellow puncta. (B) The results are rendered as bar graphs generated from data combined from three independent experiments that compare the localization of the toxin with the Golgi apparatus in the absence (white bars), or presence (black bars), of Retro-1. Error bars represent standard deviations. Statistical significance was calculated for the differences between cell populations incubated in the absence or presence of the Retro-1.

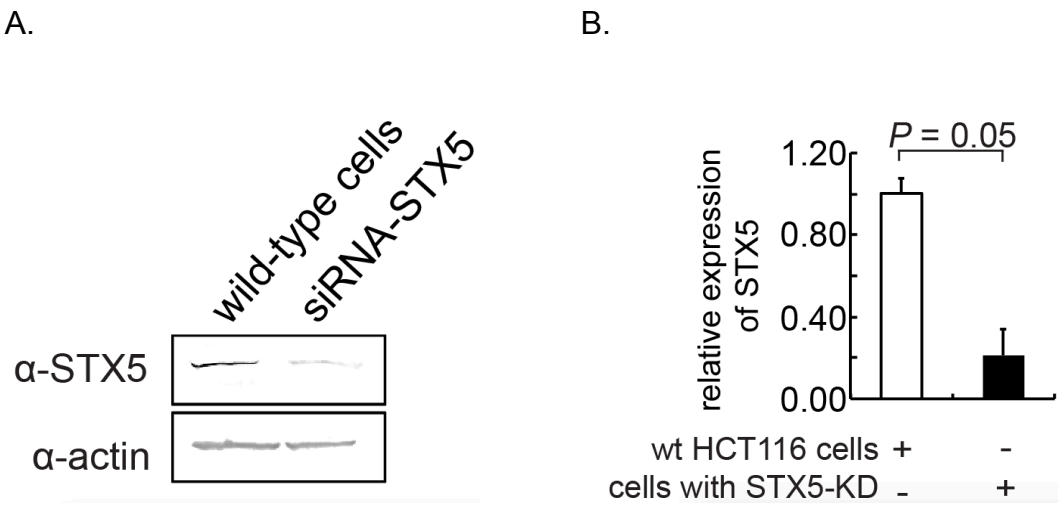

Figure 3.9. Western Blot analysis of STX5 expression in HCT116 cells treated with siRNA for STX5. HCT116 cells were transfected with a mixture of four different STX5-siRNAs, as detailed in Materials and Methods, and tested for the levels of STX5 expression using Western Blot analysis, compared to the control untreated cells. Actin was used as the loading control. STX5 expression was normalized against the actin expression in the respective cell line, and quantified to compare the expression levels of STX5. The results are rendered as bar graphs generated from data combined from three independent experiments that compare the relative expression of STX5 in cells treated with siRNA, compared to the untreated control. Error bars represent standard deviations.

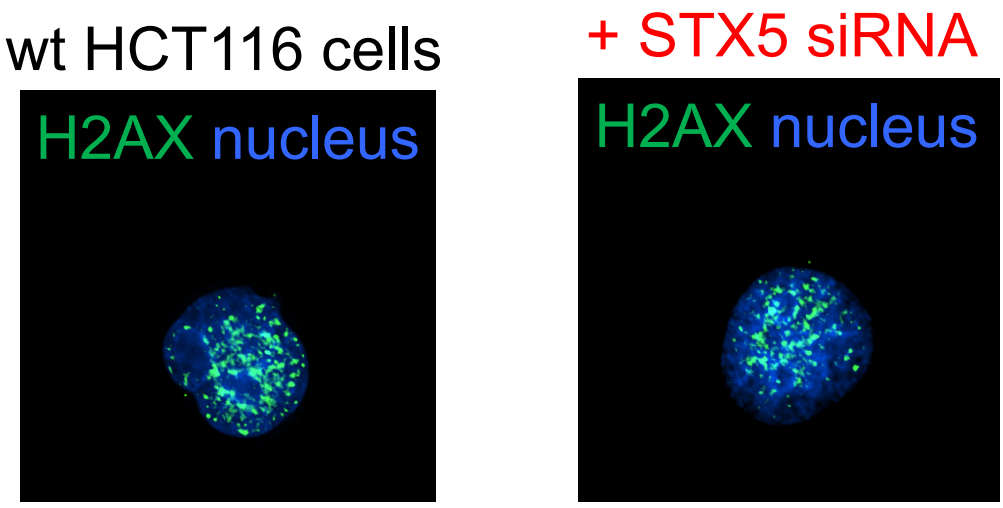

Figure 3.10. Cj-CDT activates H2AX in cells with knocked-down STX5. HCT116 cells that had been transiently transfected with siRNA targeting STX5, were incubated with Cj-CDT (100 nM) at 37 °C. After 4 h, the monolayers were fixed and imaged using fluorescence microscopy. Cells were probed for H2AX activation in response to CDT-mediated DNA damage. Green puncta indicates phosphorylated H2AX, with nucleus counter stained blue with DAPI. Images are representative of three experiments.

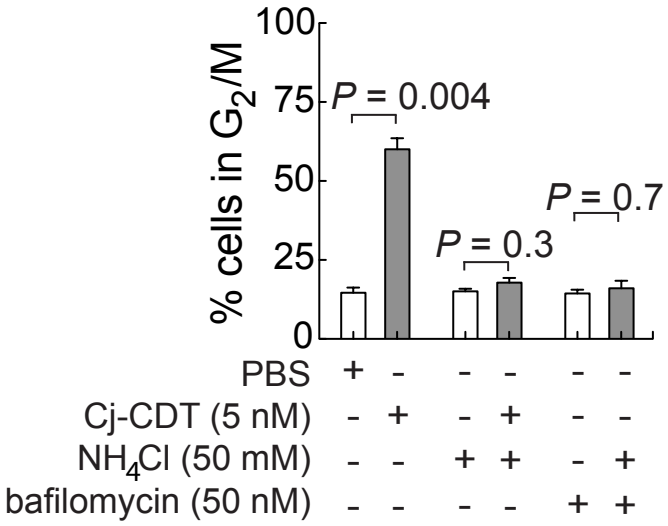

Figure 3.11. Effect of late-endosomes transport block on Cj-CDT mediated cell cycle arrest. (A) Cj-CDT (5 nM)-mediated arrest of HCT116 cells in G_2/M was determined, as indicated in the absence or presence of NH_4Cl (20 mM), or bafilomycin A1 (20 nM). The results are rendered as bar graphs generated from data combined from three independent experiments that compare the percentage of cells arrested in G_2/M phase in untreated cells (white bars), cells treated with Cj-CDT, cells treated with pharmacological agents (black bars), or cells treated with Cj-CDT in the presence of pharmacological agents (gray bars). Error bars represent standard deviations. Statistical significance was calculated for the differences between cell populations incubated in the absence or presence of the indicated agent.

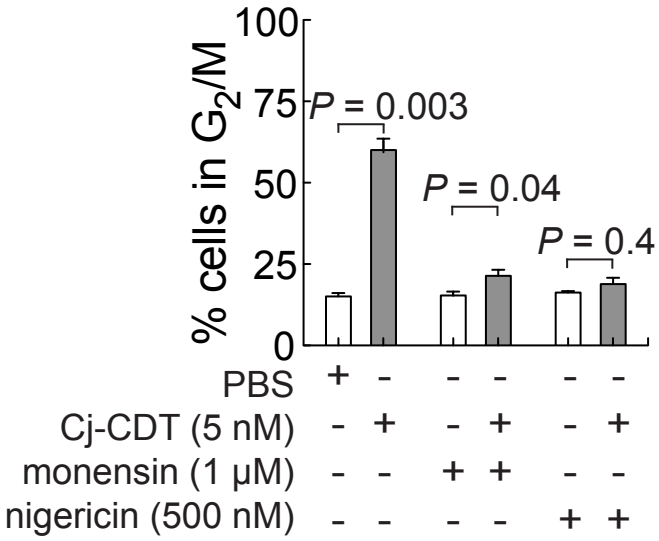

Figure 3.12. Cj-CDT activity is blocked in cells treated with monensin, and nigericin. Cj-CDT (5 nM)-mediated arrest of HCT116 cells in G_2/M was determined, as indicated in the absence or presence of monensin (50 nM), or nigericin (200 nM). The results are rendered as bar graphs generated from data combined from three independent experiments that compare the percentage of cells arrested in G_2/M phase in untreated cells (white bars), cells treated with Cj-CDT, cells treated with pharmacological agents (black bars), or cells treated with Cj-CDT in the presence of pharmacological agents (gray bars). Error bars represent standard deviations. Statistical significance was calculated for the differences between cell populations incubated in the absence or presence of the indicated agents.

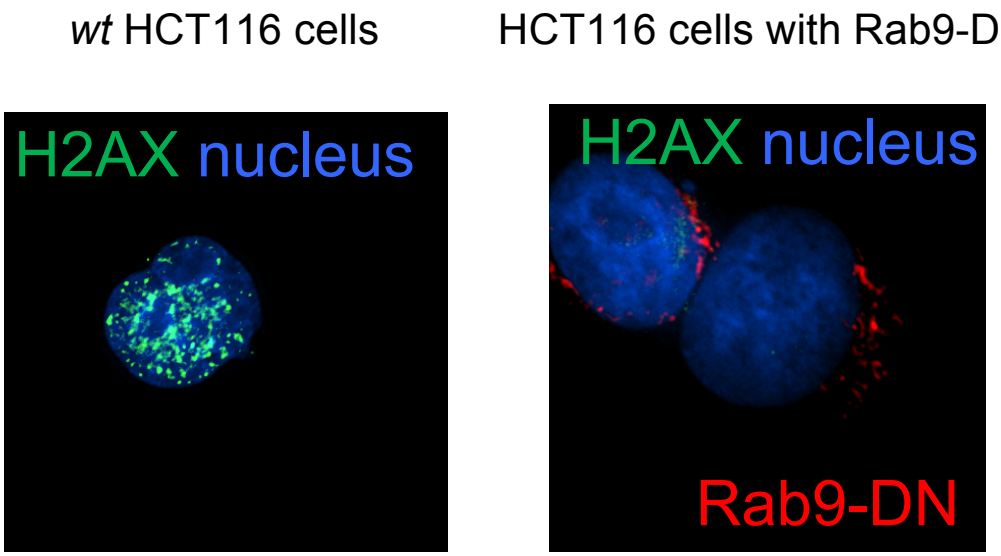

Figure 3.13. Effect of dominant-negative isoform of Rab9 on Cj-CDT mediated H2AX activation. HCT116 cells that had been transfected with the plasmid expressing the dominant negative isoform of Rab9, DN-DsRed-Rab9 (S21N), were incubated at 37 °C in the absence or presence of Cj-CDT (100 nM), and then scored for the percentage of cells with visible H2AX phosphorylation. After 4 h, the monolayers were fixed and imaged using fluorescence microscopy. Images were representative of those collected from three independent experiments. The data were rendered as a single z-plane (5 μm depth within each cell). As labeled, green puncta indicate phospho-H2AX (pH2AX), red puncta indicate the dominant-negative isoform of Rab9, and the blue staining indicates the nucleus.

A. B.

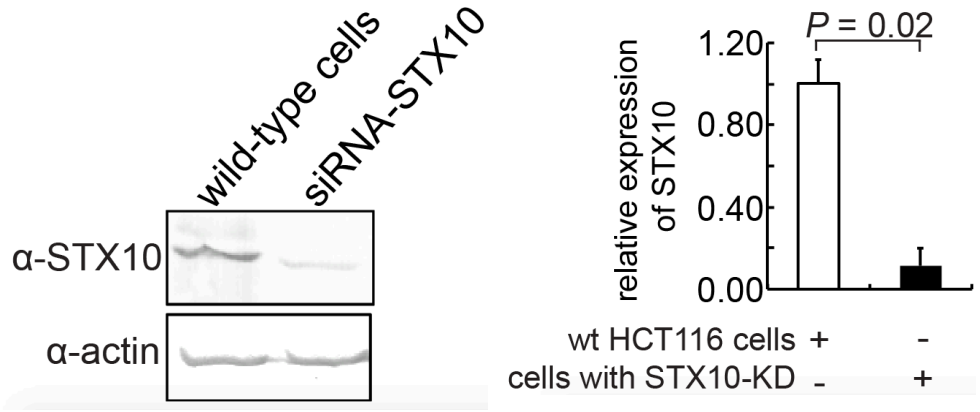

Figure 3.14. Western Blot analysis of STX10 expression in HCT116 cells treated with siRNA for STX10. HCT116 cells were transfected with a mixture of four different STX10-siRNAs, as detailed in Materials and Methods, and tested for the levels of STX10 expression using Western Blot analysis, compared to the control untreated cells. Actin was used as the loading control. (A) Western Blot analysis of STX10 expression. Data is representative of three independent experiments. (B) STX10 expression was normalized against the actin expression in the respective cell line, and quantified to compare the expression levels of STX10. The results are rendered as bar graphs generated from data combined from three independent experiments that compare the relative expression of STX10 in cells treated with siRNA, compared to the untreated control. Error bars represent standard deviations.

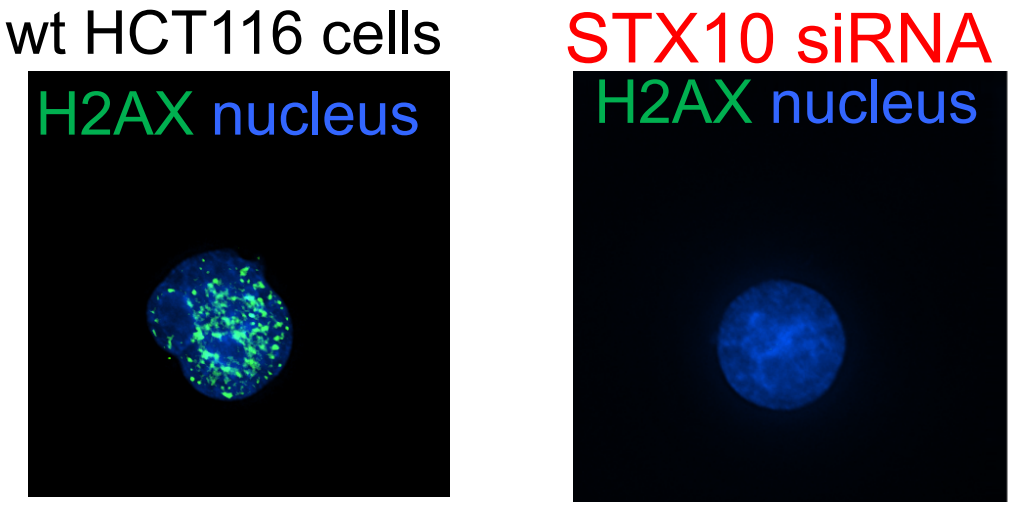

Figure 3.15. Effect of STX10 knock-down on Cj-CDT mediated H2AX activation. HCT116 cells that had been transiently transfected siRNA targeting STX10 were incubated with Cj-CDT at 37 °C. After 4 h, the monolayers were fixed and imaged using fluorescence microscopy. Images were representative of those collected from three independent experiments. The data were rendered as a single z-plane (5 μm depth within each cell). As labeled, green puncta indicate phospho-H2AX (pH2AX), and the blue staining indicates the nucleus.

A.

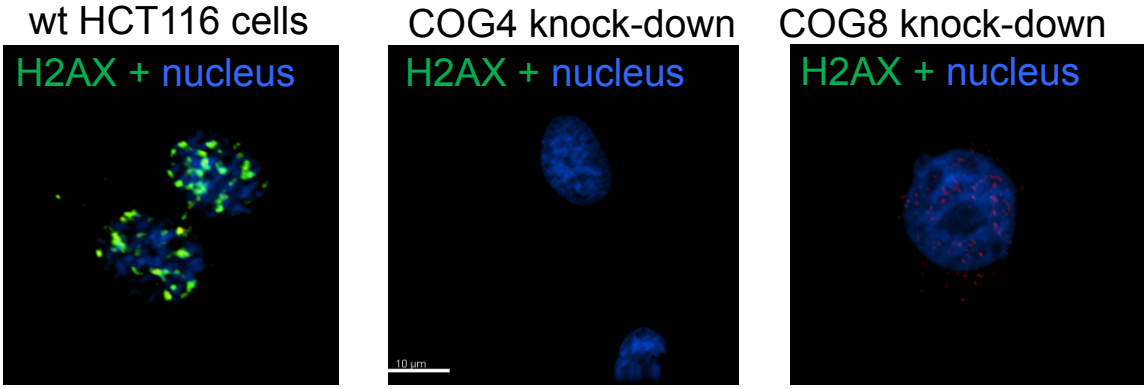

B.

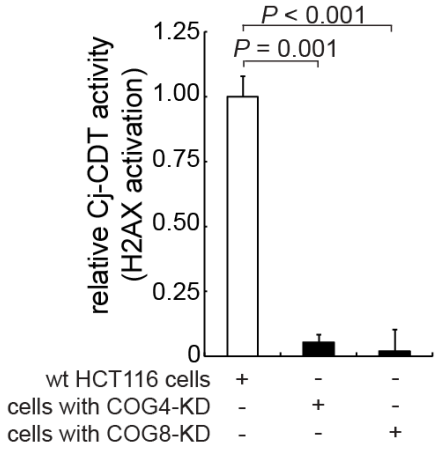

Figure 3.16. Effect of COG4 and COG8 knockdown on Cj-CDT activity. Monolayer of HCT116 cells with COG4 or COG8 knockdown, were incubated with Cj-CDT (100 nM) at 37 °C against wildtype HCT116 cells. After 4 h, the monolayers were fixed and probed for the activation of H2AX. (A) Data is representative of three independent experiments. Green puncta indicate phospho-H2AX, nucleus is stained blue. (B) The results are rendered as bar graphs generated from data combined from three independent experiments that compare the Cj-CDT mediated H2AX activation in wildtype cells (white bars), against the cells with COG knock-down (black bars). Error bars represent standard deviations.

A.

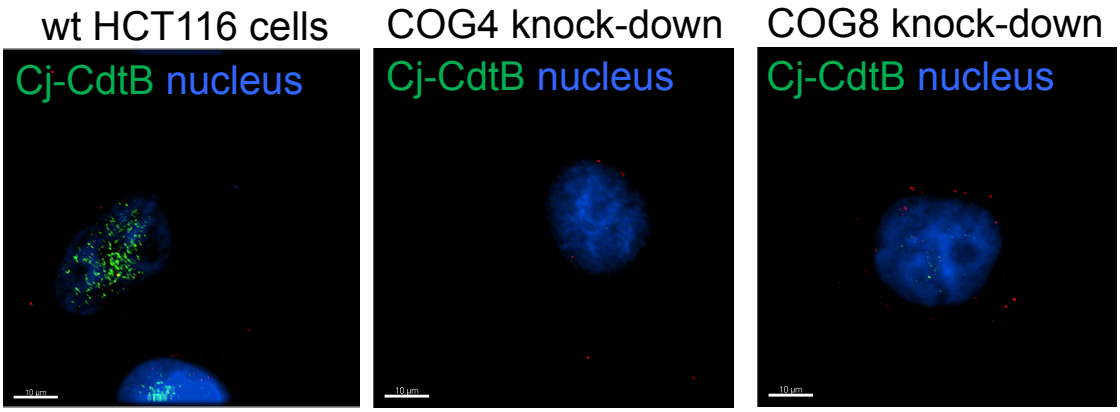

B.

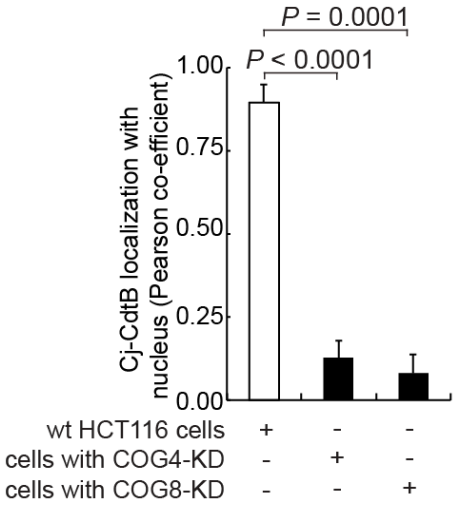

Figure 3.17. Effect of COG4 and COG8 knockdown on Cj-CdtB transport to the nucleus. Monolayer of HCT116 cells, without or with COG4 or COG8 knockdown, were incubated on ice for 30 minute, followed by incubation with prechilled Cj-CDT (100 nM). After 30 min, the cells were washed once with PBS pH 7.4, and incubated at 37 °C. After 90 min, the cells were fixed, probed for Cj-CdtB, and imaged using fluorescence microscopy. (A) Data is representative of three independent experiments. Green puncta indicate Cj-CdtB, with nucleus counterstained blue. (B) The results are rendered as bar graphs generated from data combined from three independent experiments that compare the localization of Cj-CdtB in the nucleus of wildtype cells (white bars), against the cells with COG knock-down (black bars). Error bars represent standard deviations.

A.

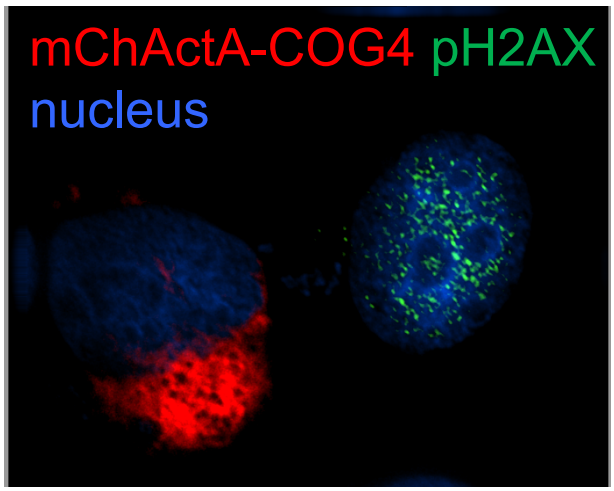

B.

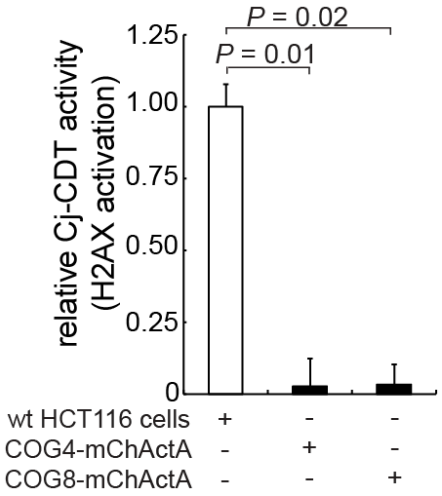

Figure 3.18. Effect of misdirecting COGs on Cj-CDT mediated H2AX activation. HCT116 cells that had been transiently transfected with a plasmid harboring the gene encoding siRNA resistant isoform of COG4, fused with mCherry gene, and mitochondrial localization signal, ActA (COG4-mChActA), were incubated with Cj-CDT (100 nM) at 37 °C. After 4 h, the monolayers were fixed and imaged using fluorescence microscopy. The data were analyzed for level of phospho-H2AX (pH2AX) in response of Cj-CDT intoxication in untreated, or transfected cells. (A) The data, which is representative of three independent experiments, shows activated H2AX, as indicated by presence of green fluorescence within the nucleus, and cells expressing mis-localized COG4 are represented by red fluorescence. (B) The results are rendered as bar graphs generated from data combined from three independent experiments that compare the Cj-CDT mediated activation levels of H2AX in wildtype HCT116 cells (white bars), or cells with mis-directed COG4 or COG8 (black bars). Error bars represent standard deviations. Statistical significance was calculated for the differences between Cj-CDT treated cell populations without or with COG mislocalization.

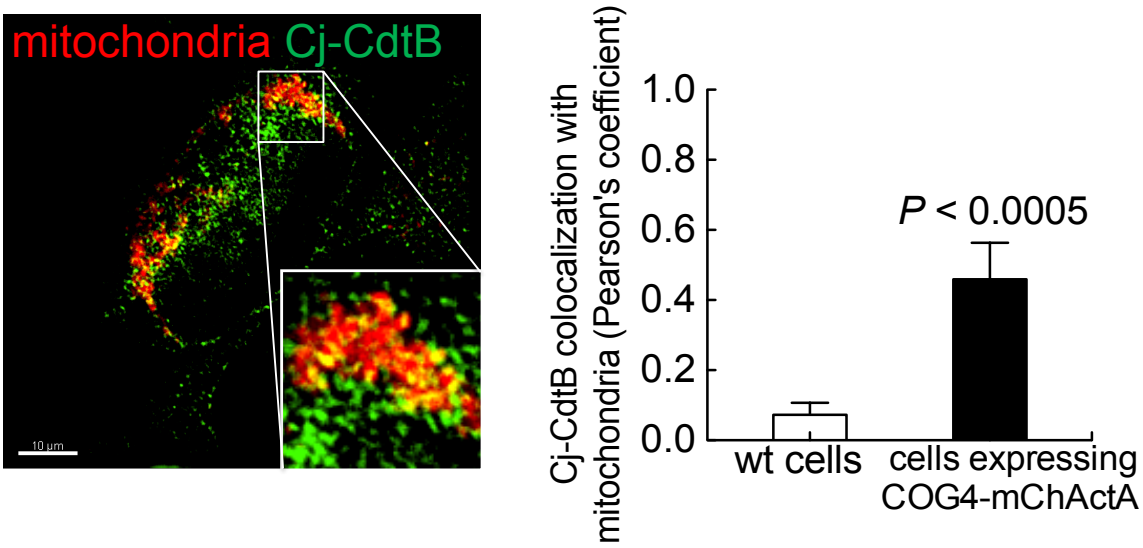

Figure 3.19. Cj-CdtB co-localize with the mitochondria in cells expressing COG4-mChActA. HCT116 cells that had been transiently transfected with a plasmid harboring the gene encoding siRNA resistant isoform of COG4, fused with mCherry gene, and mitochondrial localization signal, ActA (COG4-mChActA), were incubated with Cj-CDT (100 nM) at 37 °C. After 1 h, the monolayers were fixed and imaged using fluorescence microscopy. The data were analyzed for the localization of Cj-CdtB with TOM20, a mitochondrial marker. The data, which is representative of three independent experiments, shows Cj-CdtB indicated in green fluorescence, TOM20 in red fluorescence, and Cj-CdtB localization on the mitochondria, in yellow fluorescence, which was quantified against the wild-type cells with unperturbed COG4.

3.6. References

1. Akifusa, S., Heywood, W., Nair, S. P., Stenbeck, G., & Henderson, B. (2005). Mechanism of internalization of the cytolethal distending toxin of *Actinobacillus actinomycetemcomitans*. *Microbiology, 151*(Pt 5), 1395-1402.

2. Amessou, M., Fradagrada, A., Falguieres, T., Lord, J. M., Smith, D. C., Roberts, L. M., Lamaze, C., & Johannes, L. (2007). Syntaxin 16 and syntaxin 5 are required for efficient retrograde transport of several exogenous and endogenous cargo proteins. *Journal of Cell Science, 120*(Pt 8), 1457-1468.

3. Biswas, D., Fernando, U., Reiman, C., Willson, P., Potter, A., & Allan, B. (2006). Effect of cytolethal distending toxin of *Campylobacter jejuni* on adhesion and internalization in cultured cells and in colonization of the chicken gut. *Avian Dis, 50*(4), 586-593.

4. Boesze-Battaglia, K., Besack, D., McKay, T., Zekavat, A., Otis, L., Jordan-Sciutto, K., & Shenker, B. J. (2006). Cholesterol-rich membrane microdomains mediate cell cycle arrest induced by *Actinobacillus actinomycetemcomitans* cytolethal-distending toxin. *Cellular Microbiology, 8*(5), 823-836.

5. Bonifacino, J. S., & Glick, B. S. (2004). The mechanisms of vesicle budding and fusion. *Cell, 116*(2), 153-166.

6. Bonifacino, J. S., & Rojas, R. (2006). Retrograde transport from endosomes to the trans-Golgi network. *Nat Rev Mol Cell Biol, 7*(8), 568-579.

7. Cao, L., Volgina, A., Huang, C. M., Korostoff, J., & DiRienzo, J. M. (2005). Characterization of point mutations in the cdtA gene of the cytolethal distending toxin of *Actinobacillus actinomycetemcomitans*. *Mol Microbiol, 58*(5), 1303-1321.

8. Chia, P. Z., Gasnereau, I., Lieu, Z. Z., & Gleeson, P. A. (2011). Rab9-dependent retrograde transport and endosomal sorting of the endopeptidase furin. *Journal of Cell Science, 124*(Pt 14), 2401-2413.

9. Choudhury, A., Dominguez, M., Puri, V., Sharma, D. K., Narita, K., Wheatley, C.L., Marks, D.L., & Pagano, R. E. (2002). Rab proteins mediate Golgi transport of caveola-internalized glycosphingolipids and correct lipid trafficking in Niemann-Pick C cells. *J Clin Invest, 109*(12), 1541-1550.

10. Cortes-Bratti, X., Chaves-Olarte, E., Lagergard, T., & Thelestam, M. (2000). Cellular internalization of cytolethal distending toxin from *Haemophilus ducreyi*. *Infect Immun, 68*(12), 6903-6911.

11. Damek-Poprawa, M., Jang, J. Y., Volgina, A., Korostoff, J., & DiRienzo, J. M. (2012). Localization of *Aggregatibacter actinomycetemcomitans* cytolethal distending toxin subunits during intoxication of live cells. *Infect Immun, 80*(8), 2761-2770.

12. Damek-Poprawa, M., Korostoff, J., Gill, R., & DiRienzo, J. M. (2013). Cell junction remodeling in gingival tissue exposed to a microbial toxin. *J Dent Res, 92*(6), 518-523.

13. DiRienzo, J. M. (2014). Breaking the Gingival Epithelial Barrier: Role of the *Aggregatibacter actinomycetemcomitans* Cytolethal Distending Toxin in Oral Infectious Disease. *Cells, 3*(2), 476-499.

14. Eshraghi, A., Dixon, S. D., Tamilselvam, B., Kim, E. J., Gargi, A., Kulik, J. C., Damoiseaux, R., Blanke, S.R., & Bradley, K. A. (2014). Cytolethal distending toxins require components of the ER-associated degradation pathway for host cell entry. *PLoS Pathog, 10*(7), e1004295.

15. Eshraghi, A., Maldonado-Arocho, F. J., Gargi, A., Cardwell, M. M., Prouty, M. G., Blanke, S. R., & Bradley, K. A. (2010). Cytolethal distending toxin family members are differentially affected by alterations in host glycans and membrane cholesterol. *Journal of Biological Chemistry, 285*(24), 18199-18207.

16. Falnes, P. O., & Sandvig, K. (2000). Penetration of protein toxins into cells. *Current Opinion in Cell Biology, 12*(4), 407-413.

17. Feng, Y., Jadhav, A. P., Rodighiero, C., Fujinaga, Y., Kirchhausen, T., & Lencer, W. I. (2004). Retrograde transport of cholera toxin from the plasma membrane to the endoplasmic reticulum requires the trans-Golgi network but not the Golgi apparatus in Exo2-treated cells. *EMBO Rep, 5*(6), 596-601.

18. Ganley, I. G., Carroll, K., Bittova, L., & Pfeffer, S. (2004). Rab9 GTPase regulates late endosome size and requires effector interaction for its stability. *Molecular Biology of the Cell, 15*(12), 5420-5430.

19. Ganley, I. G., Espinosa, E., & Pfeffer, S. R. (2008). A syntaxin 10-SNARE complex distinguishes two distinct transport routes from endosomes to the trans-Golgi in human cells. *Journal of Cell Biology, 180*(1), 159-172.

20. Gargi, A., Reno, M., & Blanke, S. R. (2012). Bacterial toxin modulation of the eukaryotic cell cycle: are all cytolethal distending toxins created equally? *Front Cell Infect Microbiol, 2*, 124.

21. Gargi, A., Tamilselvam, B., Powers, B., Prouty, M. G., Lincecum, T., Eshraghi, A., Maldonado-Arocho, F.J., Wilson, B.A., Bradley, K.A., & Blanke, S. R. (2013). Cellular interactions of the cytolethal distending toxins from *Escherichia coli* and *Haemophilus ducreyi*. *Journal of Biological Chemistry, 288*(11), 7492-7505.

22. Gillespie, E. J., Ho, C. L., Balaji, K., Clemens, D. L., Deng, G., Wang, Y. E., Elsaesser, H.J., Tamilselvam, B., Gargi, A., Dixon, S.D., France, B., Chamberlain, B.T., Blanke, S.R., Cheng, G., de la Torre, J..C, Brooks, D.G., Jung, M..E, Colicelli, J., Damoiseaux, R., & Bradley, K. A. (2013). Selective inhibitor of endosomal trafficking pathways exploited by multiple toxins and viruses. *Proceedings of the National Academy of Sciences of the United States of America, 110*(50), E4904-4912.

23. Guerra, L., Cortes-Bratti, X., Guidi, R., & Frisan, T. (2011). The biology of the cytolethal distending toxins. *Toxins, 3*(3), 172-190.

24. Guerra, L., Teter, K., Lilley, B. N., Stenerlow, B., Holmes, R. K., Ploegh, H. L., Sandvig, K., Thelestam, M., & Frisan, T. (2005). Cellular internalization of cytolethal distending toxin: a new end to a known pathway. *Cellular Microbiology, 7*(7), 921-934.

25. Jinadasa, R. N., Bloom, S. E., Weiss, R. S., & Duhamel, G. E. (2011). Cytolethal distending toxin: a conserved bacterial genotoxin that blocks cell cycle progression, leading to apoptosis of a broad range of mammalian cell lineages. *Microbiology, 157*(Pt 7), 1851-1875.

26. Johnson, W. M., & Lior, H. (1988). A new heat-labile cytolethal distending toxin (CLDT) produced by Campylobacter spp. *Microbial Pathogenesis, 4*(2), 115-126.

27. Kuo, L. J., & Yang, L. X. (2008). Gamma-H2AX - a novel biomarker for DNA double-strand breaks. *In Vivo, 22*(3), 305-309.

28. Lara-Tejero, M., & Galan, J. E. (2000). A bacterial toxin that controls cell cycle progression as a deoxyribonuclease I-like protein. *Science, 290*(5490), 354-357.

29. Lara-Tejero, M., & Galan, J. E. (2001). CdtA, CdtB, and CdtC form a tripartite complex that is required for cytolethal distending toxin activity. *Infect Immun, 69*(7), 4358-4365.

30. Lauvrak, S. U., Torgersen, M. L., & Sandvig, K. (2004a). Efficient endosome-to-Golgi transport of Shiga toxin is dependent on dynamin and clathrin. *Journal of Cell Science, 117*(Pt 11), 2321-2331.

31. Lauvrak, S. U., Torgersen, M. L., & Sandvig, K. (2004b). Efficient endosome-to-Golgi transport of Shiga toxin is dependent on dynamin and clathrin. *Journal of Cell Science, 117*(Pt 11), 2321-2331.

32. Lee, R. B., Hassane, D. C., Cottle, D. L., & Pickett, C. L. (2003). Interactions of *Campylobacter jejuni* cytolethal distending toxin subunits CdtA and CdtC with HeLa cells. *Infect Immun, 71*(9), 4883-4890.

33. Lencer, W. I., Hirst, T. R., & Holmes, R. K. (1999). Membrane traffic and the cellular uptake of cholera toxin. *Biochim Biophys Acta, 1450*(3), 177-190.

34. Lin, C. D., Lai, C. K., Lin, Y. H., Hsieh, J. T., Sing, Y. T., Chang, Y. C., Chen, K., Wang, W., Su, H., & Lai, C. H. (2011). Cholesterol depletion reduces entry of *Campylobacter jejuni* cytolethal distending toxin and attenuates intoxication of host cells. *Infect Immun, 79*(9), 3563-3575.

35. Linstedt, A. D., & Hauri, H. P. (1993). Giantin, a novel conserved Golgi membrane protein containing a cytoplasmic domain of at least 350 kDa. *Molecular Biology of the Cell, 4*(7), 679-693.

36. Lowery, J., Szul, T., Styers, M., Holloway, Z., Oorschot, V., Klumperman, J., & Sztul, E. (2013). The Sec7 guanine nucleotide exchange factor GBF1 regulates membrane recruitment of BIG1 and BIG2 guanine nucleotide exchange factors to the trans-Golgi network (TGN). *Journal of Biological Chemistry, 288*(16), 11532-11545.

37. McAuley, J. L., Linden, S. K., Png, C. W., King, R. M., Pennington, H. L., Gendler, S. J., Florin, T.H., Hill, G.R., Korolik, V., & McGuckin, M. A. (2007). MUC1 cell surface mucin is a critical element of the mucosal barrier to infection. *J Clin Invest, 117*(8), 2313-2324.

38. McSweeney, L. A., & Dreyfus, L. A. (2004). Nuclear localization of the *Escherichia coli* cytolethal distending toxin CdtB subunit. *Cellular Microbiology, 6*(5), 447-458.

39. Nambiar, M. P., Oda, T., Chen, C., Kuwazuru, Y., & Wu, H. C. (1993). Involvement of the Golgi region in the intracellular trafficking of cholera toxin. *Journal of Cellular Physiology, 154*(2), 222-228.

40. Nebenfuhr, A., Ritzenthaler, C., & Robinson, D. G. (2002). Brefeldin A: deciphering an enigmatic inhibitor of secretion. *Plant Physiol, 130*(3), 1102-1108.

41. Nesic, D., Hsu, Y., & Stebbins, C. E. (2004). Assembly and function of a bacterial genotoxin. *Nature, 429*(6990), 429-433.

42. Pfeffer, S. R. (2009). Multiple routes of protein transport from endosomes to the trans Golgi network. *FEBS Letters, 583*(23), 3811-3816.

43. Pickett, C. L., & Whitehouse, C. A. (1999). The cytolethal distending toxin family. *Trends Microbiol, 7*(7), 292-297.

44. Saenz, J. B., Sun, W. J., Chang, J. W., Li, J., Bursulaya, B., Gray, N. S., & Haslam, D. B. (2009). Golgicide A reveals essential roles for GBF1 in Golgi assembly and function. *Nat Chem Biol, 5*(3), 157-165.

45. Saint-Pol, A., Yelamos, B., Amessou, M., Mills, I. G., Dugast, M., Tenza, D., Schu, P., Antony, C., McMahon, H.T., Lamaze, C., & Johannes, L. (2004). Clathrin adaptor epsinR is required for retrograde sorting on early endosomal membranes. *Developmental Cell, 6*(4), 525-538.

46. Sciaky, N., Presley, J., Smith, C., Zaal, K. J., Cole, N., Moreira, J. E., Terasaki, M., Siggia, E., & Lippincott-Schwartz, J. (1997). Golgi tubule traffic and the effects of brefeldin A visualized in living cells. *Journal of Cell Biology, 139*(5), 1137-1155.

47. Sharma, A., Singh, K., & Almasan, A. (2012). Histone H2AX phosphorylation: a marker for DNA damage. *Methods Mol Biol, 920*, 613-626.

48. Stechmann, B., Bai, S. K., Gobbo, E., Lopez, R., Merer, G., Pinchard, S., Panigai, L., Tenza, D., Raposo, G., Beaumelle, B., Sauvaire, D., Gillet, D., Johannes, L., & Barbier, J. (2010). Inhibition of retrograde transport protects mice from lethal ricin challenge. *Cell, 141*(2), 231-242.

49. Tai, G., Lu, L., Wang, T. L., Tang, B. L., Goud, B., Johannes, L., & Hong, W. (2004). Participation of the syntaxin 5/Ykt6/GS28/GS15 SNARE complex in transport from the early/recycling endosome to the trans-Golgi network. *Molecular Biology of the Cell, 15*(9), 4011-4022.

50. Togawa, A., Morinaga, N., Ogasawara, M., Moss, J., & Vaughan, M. (1999). Purification and cloning of a brefeldin A-inhibited guanine nucleotide-exchange protein for ADP-ribosylation factors. *Journal of Biological Chemistry, 274*(18), 12308-12315.

51. Willett, R., Kudlyk, T., Pokrovskaya, I., Schonherr, R., Ungar, D., Duden, R., & Lupashin, V. (2013). COG complexes form spatial landmarks for distinct SNARE complexes. *Nat Commun, 4*, 1553.

52. Young, K. T., Davis, L. M., & Dirita, V. J. (2007). *Campylobacter jejuni*: molecular biology and pathogenesis. *Nat Rev Microbiol, 5*(9), 665-679.

CHAPTER 4: CHARACTERIZING THE BINDING PROPERTIES OF HD-CDT

4.1. Introduction

Cytolethal Distending Toxins (CDTs) are AB toxins where B-moiety, comprised of CdtA and CdtC, is required to facilitate the delivery of A-moiety, CdtB, inside the cell (Sandvig et al., 2004). It is understood that CdtA and CdtC aid in the binding of holotoxin to the host cell, leading to the toxin uptake, eventually guiding CdtB through the retrograde pathway to help reach nucleus (Gargi, Reno, & Blanke, 2012). But the molecular details of how CdtA and CdtC deliver CdtB inside the cell, is not known.

Since the seminal paper that published first crystal structure of a CDT holotoxin (Nesic, Hsu, & Stebbins, 2004), numerous studies have attempted to evaluate the functional roles of distinct domains present on the toxin, aiming to characterize its potential role in cell surface receptor engagement. Studying the domains on the toxin has also paralleled the study of host cell determinants that might engage with the toxins, but the understanding of toxin's determinants required for host cell binding, is still emerging (Eshraghi et al., 2010).

Not surprisingly, different groups have reported differing views on the relative importance of CdtA against CdtC in cell binding. Based on multiple structure-activity studies, it is understood that CdtA and, to a lesser extent, CdtC subunit proteins bind to cells in culture (Cao, Volgina, Huang, Korostoff, & DiRienzo, 2005; Kanno, Korostoff, Volgina, & DiRienzo, 2005; McSweeney & Dreyfus, 2005). Yet in other studies it has been suggested that CdtC may aid the

entry of CdtB into the cell (Akifusa, Heywood, Nair, Stenbeck, & Henderson, 2005), with CdtA having much less significant role to play. While investigating the cell surface binding of CDT produced by *A. actinomycetemcomitans*, a group reported that while Aa-CdtA bound to HEp-2 cells both at 4 ºC and 37 ºC, Aa-CdtC bound to cell surface only at 37ºC, while Aa-CdtB did not bind to HEp-2 cells at either temperature, indicating that the availability of Aa-CdtC-binding sites may be dependent on normal physiologic conditions (Akifusa et al., 2005). *In vitro* studies report that both CdtA and CdtC recognize gangliosides, such as GM1 and GM3 (Mise et al., 2005), or N-linked fucose-containing glycoproteins (McSweeney & Dreyfus, 2005). It has become quite clear that the nature of CDT-receptor is not the same for all CDTs, and further characterization is required to find a co-relation between the toxin receptor and the species-specific CDT. Another problem that needs to be solved, which I have partially addressed in this chapter, is to characterize the residues present on CDT subunits that engage with the host cell receptor, thus initiating first step towards cellular intoxication by the CDTs. Understanding CDT determinants that interact with host receptor will not only impart better understanding in the molecular pathogenesis of CDTs, but will also help in developing strategies to block such interactions, and help fight infectious diseases.

It is not clear how CdtA or CdtC interact with the cell receptor, or with each other, and possibly contribute towards cytotoxic properties of the holotoxin. I started out by characterizing the residues on CdtA and CdtC, beyond the ones reported by earlier studies (Nesic et al., 2004). An aromatic patch on Hd-CdtA,

composed of three tryptophans and a tyrosine residue (W91, W98, W100, and Y102), is shown to be important for toxin binding and cellular activity of Hd-CDT (Nesic et al., 2004). My findings expand the involvement of aromatic residues on the surface of CdtA, which are responsible for the toxin interactions with the cell surface. I also evaluated potential microdomains on the surface of CdtC, specifically around the putative receptor-binding groove on the toxin subunit, which might be important for engaging with the host cell surface. My findings contribute towards refining the role of molecular determinants involved in the B-moiety of the AB toxin, CDT.

4.2. Materials and Methods

Cloning of cdt genes and preparation of expression strains. The cloning of the genes encoding Hd-CDT subunits in plasmids for recombinant expression in *E. coli* was previously described (Eshraghi et al., 2010).

Site-directed mutagenesis. Mutagenesis was performed using the QuikChange mutagenesis kit from Stratagene (La Jolla, CA). First, complementary mutagenic primers were engineered with the desired mutation in the center of the primer and 10 to 15 bases of correct sequence on either side. Reaction mixtures were prepared as described in the QuikChange protocol with pET15b-Hd-CdtA or pET15b-CdtC as the plasmid template for generation of various CdtA or CdtC mutants. After cycling of the reaction mixture 18 times in a

thermal cycler, the resulting mixture was digested with DpnI, and the resulting DNA was transformed into chemically competent *E. coli* DH5α cells. The resulting mutant plasmids were isolated, and the entire gene was sequenced to ensure that the appropriate mutations were introduced, while the rest of the gene sequences remained unchanged.

Expression and purification of recombinant Hd-CDT. Each recombinant protein was expressed and purified as previously described (Eshraghi et al., 2010). Protein concentrations were quantified using the Bradford Protein Assay (Thermo Scientific, Rockford, IL). Recombinant proteins were used only when purified to at least 95% homogeneity, as estimated by resolving the proteins using sodium-dodecyl sulfate (SDS)-polyacrylamide gel electrophoresis (PAGE), and visualizing after staining the gels with Coomassie Brilliant Blue (Bio-Rad, Hercules, CA; data not shown). The purified, denatured subunits were stored at -20 °C in HEPES (20 mM, *N*-[2-Hydroxyethyl] piperazine-*N*-[2-ethanesulphonic acid], Calbiochem, La Jolla, CA), pH 7.5 containing urea (8 M) and NaCl (200 mM).

Hd-CDT holotoxins were prepared as previously described (Nesic et al., 2004). Toxin integrity was evaluated using the dialysis retention assay, as previously described (Cao et al., 2005). Hd-CDT holotoxin (5-20 μM, 1 ml) was dialyzed (100 kDa molecular mass cut-off tubing; Spectrum Laboratories) at 4 °C against four 250 ml volumes of PBS pH 7.4 containing 5% glycerol. After 24 h, the dialyzed proteins were evaluated using SDS-PAGE followed by staining with

Coomassie Brilliant blue. The gels were scanned with a CanonScan 9950F scanner (Canon, Lake Success, NY) using ArcSoft Photo Studio 5.5 software (ArcSoft, Fremont, CA). The integrity of the holotoxins was quantified by comparing the relative intensities of the bands corresponding to CdtA, CdtB, or CdtC before and after dialysis, as determined by using the UN-SCAN-IT program (Silk Scientific, Inc., Orem, UT). Individual CDT subunits, each of which has a molecular mass less than 35 kDa, were used as negative controls.

Mammalian cells. Mammalian cell cultures were maintained at 37 °C and under 5% CO_2 within a humidified environment. Human cervical cancer epithelial (HeLa) cells (CCL-2, ATCC) were maintained in Minimal Essential Medium Eagle (MEM, Mediatech, Herndon, VA) with 10% fetal bovine serum (FBS, Mediatech). Complete medium was obtained by supplementing MEM with L-glutamine (2 mM, Sigma), penicillin (50 IU/ml, Mediatech), and streptomycin (50 μg/ml, Mediatech).

Cell cycle phase determination. The indicated cell lines were seeded (1.5 x 10^5 cells per well) in 6-well plates (Corning Inc., Corning, NY). After 18 h, the cells were further incubated in complete medium with or without Ec-CDT or Hd-CDT at the indicated concentrations, or mock incubated with PBS pH 7.4. After 48 h, the cells were analyzed for arrest at the G_2/M interface, as previously described (Eshraghi et al., 2010). From these data, dose response curves were generated by plotting cells in G_2/M as a function of toxin concentration. From the dose response curves, we determined $CCAD_{50}$ (i.e. cell cycle arrest $dose_{50}$)

values, which we defined as the toxin concentrations required to induce G_2/M arrest in 50% of the cell population not already in G_2/M.

Preliminary intoxication studies with Hd-CDT revealed nearly identical dose response curves for G_2/M arrest in the presence or absence of the hexa-histidine tags. All subsequent studies were conducted with toxin assembled from subunits that retained their respective hexa-histidine tags.

Molecular modeling. Molecular modeling of CDT holotoxin, or subunits, was performed using UCSF Chimera, an extensible molecular modeling system (Pettersen et al., 2004). Protein structure of Hd-CDT was fetched using PDF code “1SR4” for the holotoxin (Nesic et al., 2004), and surface topology was studied using Chimera software. Residues with peculiar properties, like charged residues or aromatic, were marked for this study. Information collected from molecular modeling was used to target the residues on CdtA and CdtC to be investigated for their role in toxin binding and activity.

Flow cytometry. Analytical flow cytometry-based assays were carried out as previously described (Eshraghi et al., 2010). Briefly, 8 x 10^4 HeLa cells were seeded in a 12-well plate. After overnight incubation, cells were intoxicated for additional 24 h, then washed with PBS (pH = 7.4), detached with 0.05% trypsin/EDTA (Invitrogen), and harvested in 1 ml PBS containing 10% FBS. Cells were spun down at 600*g* for 5 minutes, and permeabilized with 70% ethanol at least for one hour at -20ºC. Cells were hydrated by incubating in PBS for 30

minutes, and stained with 10 µg/ml propidium iodide (PI) solution containing 0.1% Triton X-100, and 100 µg/ml RNase-A. After incubating for one hour at room temperature, samples were analyzed for DNA content using FACS Canto Flow Cytometry Analyser (BD Biosciences) with CellQuest acquisition software (BD Biosciences). Flow cytometry data were subsequently analyzed using FACS analysis software.

Protease sensitivity assays. Wild-type Hd-CDT, or respective mutants were incubated in a Tris buffer (50 mM Tris-HCl, 100 mM NaCl, 2 mM DTT; pH 8.0) with various concentrations of trypsin (0, 53, 213, and 640 µg/ml) at 4°C. After 1 h, reaction was stopped by adding sodium dodecyl sulfate (SDS) sample buffer (4% SDS, 100 mM Tris, 0.4 mg bromophenol blue/ml, 0.2 M DTT, 20% glycerol). The samples were boiled for 3 min and resolved by SDS-polyacrylamide gel electrophoresis (PAGE) (16% acrylamide; 70 V for 25 min and then 200 V for an additional 100 min). The gels were soaked in fixing solution (25% isopropanol, 10% acetic acid) for 15 min and then placed in Coomassie blue stain (10% acetic acid, 0.06 mg/ml Coomassie brilliant blue G-250). After 10 h, the gels were rinsed twice with H_2O, preserved by soaking in water with 3% glycerol for 10 h, and dried between gel drying films.

Cell binding assay. Mammalian cell binding assays were conducted as previously described (Cao et al., 2005; Lee, Hassane, Cottle, & Pickett, 2003). Cells were seeded (2×10^4/well) in 96-well plates (Fisher). After 18 h, the plates

were incubated on ice. After 30 min, the cells were washed two times with ice-cold PBS pH 7.4, and then further incubated on ice with or without biotinylated toxin (at the indicated concentrations) and BSA (3%) in PBS pH 7.4, or mock incubated with BSA (3%) in PBS pH 7.4. After 30 min on ice, the cells were washed three times with ice-cold PBS pH 7.4, and then fixed by adding ice-cold 2% formaldehyde and 0.2% glutaraldehyde, and then further incubated at room temperature. Preliminary studies indicated that maximal binding occurred between 30 and 60 min (not shown). After 15 min, the plate was washed three times with PBS pH 7.4 at room temperature, and then incubated at room temperature with streptavidin-HRP conjugate (1:15,000, GE Healthcare, Little Chalfont, Buckinghamshire, UK) in PBS pH 7.4. After 30 min, the cells were washed five times with PBS pH 7.4, and then incubated at room temperature with TMB Ultra (100 μl, Thermo Scientific). After 30 min, the supernatant from each well was removed and added to an equal volume of sulfuric acid (2 N, Mallinckrodt Baker Inc., Paris, KY) at room temperature. The optical density at 450 nm ($O.D._{450nm}$) was measured using a Biotek Synergy 2 plate reader (Biotek Instruments Inc., Winooski, VT). The $O.D._{450nm}$ measured for supernatants collected from wells containing cells incubated with PBS pH 7.4 alone (background absorbance) was subtracted from the $O.D._{450nm}$ measured for supernatants collected from wells containing cells that had been incubated with the toxin. Relative binding was determined by dividing the $O.D._{450nm}$ minus background at each toxin concentration by the $O.D._{450\ nm}$ minus background at the highest concentration of toxin used in these studies (200 nM). The

dissociation constants (K_d) were calculated by non-linear regression of the curve generated from plotting relative binding as a function of toxin concentration, using GraphPad Prism (Version 4.03, GraphPad Software, La Jolla, CA). Competitive binding assays were conducted as described above, except in the absence or presence of 100-fold molar excess of the specified non-biotinylated proteins.

Statistics. Unless otherwise indicated, each experiment was performed at least three independent times, each time in triplicate. Statistical analyses were performed using Microsoft Excel (Version 11.0, Microsoft, Redmond, WA) or GraphPad. The *Q*-test was performed to eliminate data that were statistical outliers (Dixon, 1950). Error bars represent standard deviations. All *P* values were calculated with the Student's *t*-test using paired, two-tailed distribution. A *P* value of less than 0.05 indicated that differences in the specified data were considered statistically significant.

4.3. Results

Targeting residues on CdtA. There are only a handful studies that explored the topology of CDT to study the contribution of surface-exposed residues towards toxin's binding to the host cell surface, the first step in the process of cellular intoxication. To evaluate the role of distinct microdomains on the surface of CDT, and their contribution towards cell binding, residues on the CdtA were mapped based on their spatial information and chemical nature. Either aromatic or basic residues were selected, and based on their vicinity in the

folded protein, were grouped into distinct microdomains for further studies (modeled in Figure 4.1). Because no difference was observed between the binding and activity of holotoxin with or without N-terminus His-tag, studies were conducted with recombinant protein with His-tag (data not shown). Site directed mutagenesis was carried out for individual regions, testing their impact on the toxin binding to the host cell surface. Protein stability of the mutant toxin was tested by limited proteolysis, using trypsin digestion assay. All mutants showed protein digestion pattern similar to the wild-type control, suggesting the mutants made a stable holotoxin (data not shown).

Effect of CdtA mutations on the cytotoxic activity of Hd-CDT. To evaluate the importance of specific surface-exposed residues on Hd-CdtA, cell cycle analysis was conducted to compare the cytotoxic activity of respective mutants against the wild-type control. Mutant holotoxin was prepared using mutated CdtA along with wild-type CdtB and CdtC. HeLa cells were exposed to a range of indicated concentrations of mutant holotoxin, and compared against the wild-type isoform. Cells were harvested 24 h post intoxication, and evaluated for DNA content. Our studies revealed that while wild-type Hd-CDT produced cell cycle arrest in 50% cell population at around 3 pM, toxin containing mutated forms of CdtA demonstrated differing potencies, ranging from 5 pM to 42 pM. Region 1 mutation (Y119A/Y168A) had CCA_{50} value of 42 pM (Figure 4.2). Regions 2 through 6 gave attenuations between 1.5 to 3 fold, and were considered not significant biologically. These data indicate that not all residues contribute equally

towards the activity of the holotoxin, and some are dispensable. The mechanism of activity attenuation in not known, but we propose that owing to its aromatic nature, and presence on the surface of holotoxin, Y119 and Y168 might contribute towards the binding of holotoxin to the cell surface.

Relative binding of Hd-CDT with the cell surface. Of the surface exposed residues on Hd-CdtA, there are two tyrosine residues, Y119 and Y168, flanking either side of the tetra-aromatic patch, that were hypothesized to be involved in toxin binding to the cell surface (Figure 4.3). To investigate the importance of surface exposed Y119 and Y168, alanine was substituted for tyrosine, and the effects of alanine substitution were evaluated on the cell binding properties of the holotoxin. Wild-type holotoxin was used as the positive control.

Cell based ELISA (CELISA) was used to investigate cell surface binding of the mutant toxin against the wild-type. After binding the toxin for 30 minutes, with the cells under conditions non-permissive of cellular uptake, cells were fixed and probed for the presence of toxin on the cell surface. Wild-type CDT demonstrated saturation binding kinetics with HeLa cells. In contrast, holotoxin with CdtA containing Y119A and Y168A substitutions exhibited a statistically significant reduction in binding (Figure 4.4). These data suggest Y119 and Y168 residues are required for the interactions of CDT with the host cell surface. These results indicate that aromatic patch is not restricted to the tetra-aromatic residues W91, W98, W100, and Y102, but extends beyond and includes the neighboring aromatic residues. These findings will help define the role of CdtA as the B-

moiety of the holotoxin, while aiding in the characterization of specific residues on the toxin surface and their role towards overall intoxication properties of the holotoxin.

Targeting residues on CdtC. To evaluate the role of distinct microdomains on the surface of CDT, and their contribution towards cell binding, residues on the CdtC subunit were mapped based on their spatial information and chemical nature. Either aromatic or basic residues were selected, and based on their vicinity in the folded protein, were grouped into distinct microdomains for further studies (Figure 4.5). Protein stability of the mutant toxin was tested by limited proteolysis, using trypsin digestion assay. All mutants showed protein digestion pattern similar to the wild-type control, suggesting the mutants made a stable holotoxin (data not shown).

Cytotoxic activity of Hd-CDT with mutant CdtC. To evaluate the importance of specific surface-exposed residues on Hd-CdtC, cell cycle analysis was conducted to compare the cytotoxic activity of respective mutants against the wild-type control. Mutant holotoxin was prepared using mutated CdtC along with wild-type CdtA and CdtB. HeLa cells were exposed to a range of indicated concentrations of mutant holotoxin, and compared against the wild-type isoform. Cells were harvested 24 h post intoxication, and evaluated for DNA content. Our studies revealed that while wild-type Hd-CDT produced cell cycle arrest in 50% cell population at around 3 pM, CdtC-tetramutant demonstrated a CCA_{50} value of

5 pM (Figure 4.6). These data indicate that the tetramutant (K82E/F79K/V31K/F121K) might not be critical for toxin activity. Extrapolating it back, owing to its failure to attenuate toxin activity, residues in tetramutant might not contribute towards holotoxin binding either, as any interference in the binding would have reflected in the cytotoxic activity of the holotoxin. Because the CdtC mutant did not attenuate the activity of holotoxin, binding studies for the toxin with mutant CdtC were not performed.

4.4. Discussion

Owing to their distinct chemical nature, most aromatic residues are buried in the core of a protein or peptide. If surface exposed, it is believed that the residues have an important role to play, involving interacting with a specific receptor or enzyme. CdtA protein of CDTs also have certain surface exposed residues that are distinct for an otherwise exposed residues that come in contact with hydrophilic environment. There are at least eight surface-exposed aromatic on CdtA, four of which have already been shown important for toxin binding to the cell surface. Extending the aromatic patch region, I mutated a tyrosine residue on either side of the aromatic patch, to examine the precise contribution of these amino acids to the binding of the subunits to the receptor and effect on holotoxin's activity (Figure 4.1). Mutating Y119 and Y168, the activity was attenuated by approximately 15-fold, suggesting the residues are important for full-activity of the holotoxin. Further, The data obtained extend the initial findings

of Nesic et al. implicating primarily residues W91, W98, W100, and Y102 in Hd-CdtA aid in CDT binding to the receptor.

While my studies mapped the surface exposed residues on Hd-CDT, another study later carried out similar study on Aa-CDT, addressing the aromatic residues on CdtA that might be involved in cell binding. In this report, Cao and co-workers found that aromatic residues at the periphery of the binding domain (Y105 and Y140) of Aa-CdtA were reported to make a weaker contribution to binding than those closer to the middle of the domain (Y188 and Y189). Taken together, these studies have enhanced the understanding of the residues involved on the toxin that are important for engaging with the host cell receptor, potentially as the first step towards cellular intoxication.

Our studies are preliminary as they address only certain residues on CDT that might be involved in receptor recognition and cell binding. It doesn't fully characterize the binding determinants present on the toxin in its entirety. It also doesn't address the molecular details of the receptor that might be involved in CDT recognition and binding. Future studies should not only firm up a model for toxin binding to the cell, but also investigate the applicability of this model across other members of the CDT-family. Though surface-exposed residues are conserved through most members of the family, studies reporting differing views on cell surface binding properties argue the applicability of a uniform model of CDT and host cell binding. We think that a combination of conserved residues, along with non-conserved, give CDTs host tissue specificity, setting up the CDT-family as a non-uniform model for cellular interactions.

In summary, analysis of the binding properties of the *H. ducreyi* CdtA and CdtC proteins, having substitutions for surface-exposed molecular determinants, improved our understanding of the CDT receptor-binding domain. It also provided evidence that the CdtC subunit most likely plays a relatively minor role in cell binding. These findings have important implications for studying the specificity of the receptor for CDTs in general, and for developing strategies designed to block the activity of CDTs, which is part of the arsenal of several Gram-negative pathogens.

4.5. Figures

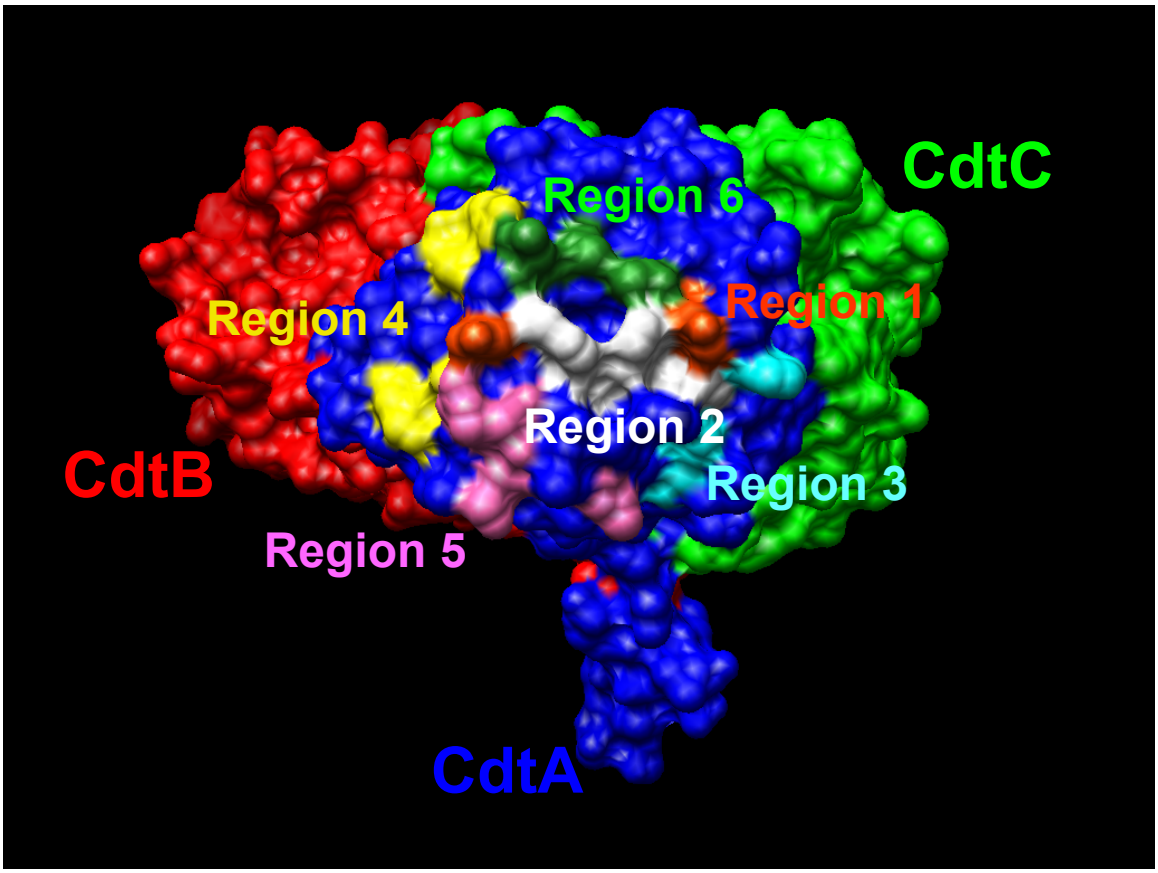

Figure 4.1. Microdomains mutated on Hd-CdtA. Hd-CDT holotoxin protein was modeled using UCSF Chimera, and distinct residues were zoned into small patches based on their side chain (aromatic or basic). In this model, CdtA is colored blue, CdtB is red, and CdtC green, with mutants given distinct colors to identify their location on the surface. Total 6 regions on Hd-CdtA were investigated, and grouped mutants were created to study their binding and intoxication properties. Region 1: Y119A and Y168A, region 2: W76G, W78G, andY80A, region 3: F88A, F167A, region 4: E117A, K132A, Q154A, and R156A, region5: L71E, K73E, and R74E, and region 6: N121A, T170A, and T172A

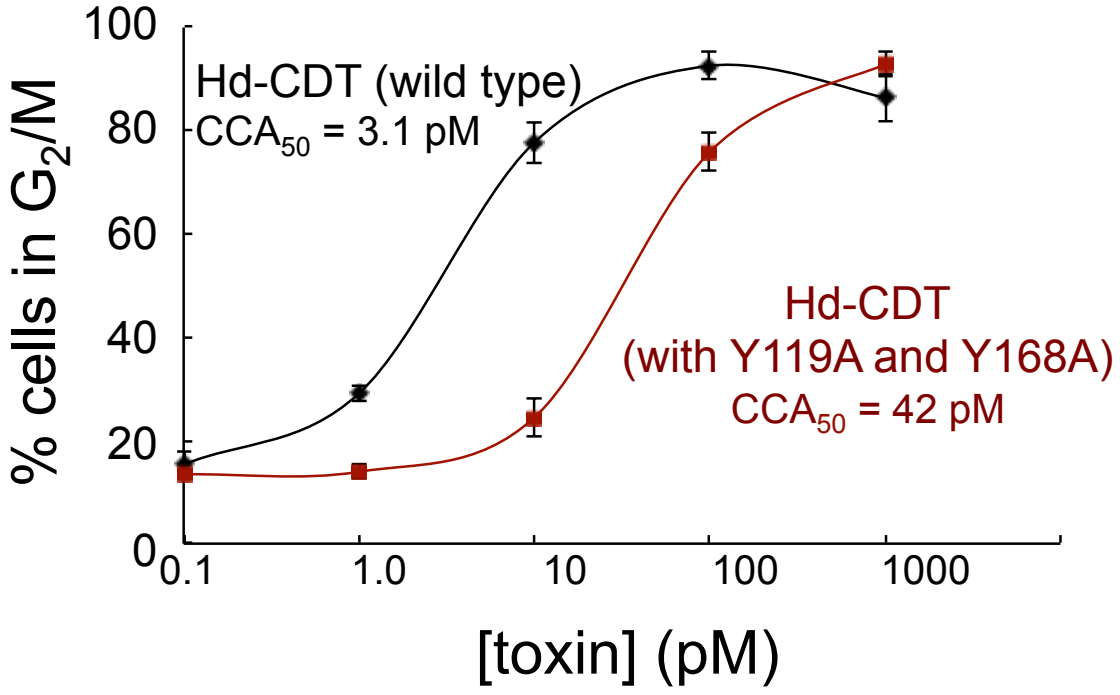

Figure 4.2. Dose response curve of wildtype and mutant Hd-CDT holotoxin. Monolayers of HeLa cells were exposed to indicated concentration of toxin, and evaluated for cell cycle phase at 24 h. Data is collected from three independent experiments. Error bars denote standard deviation.

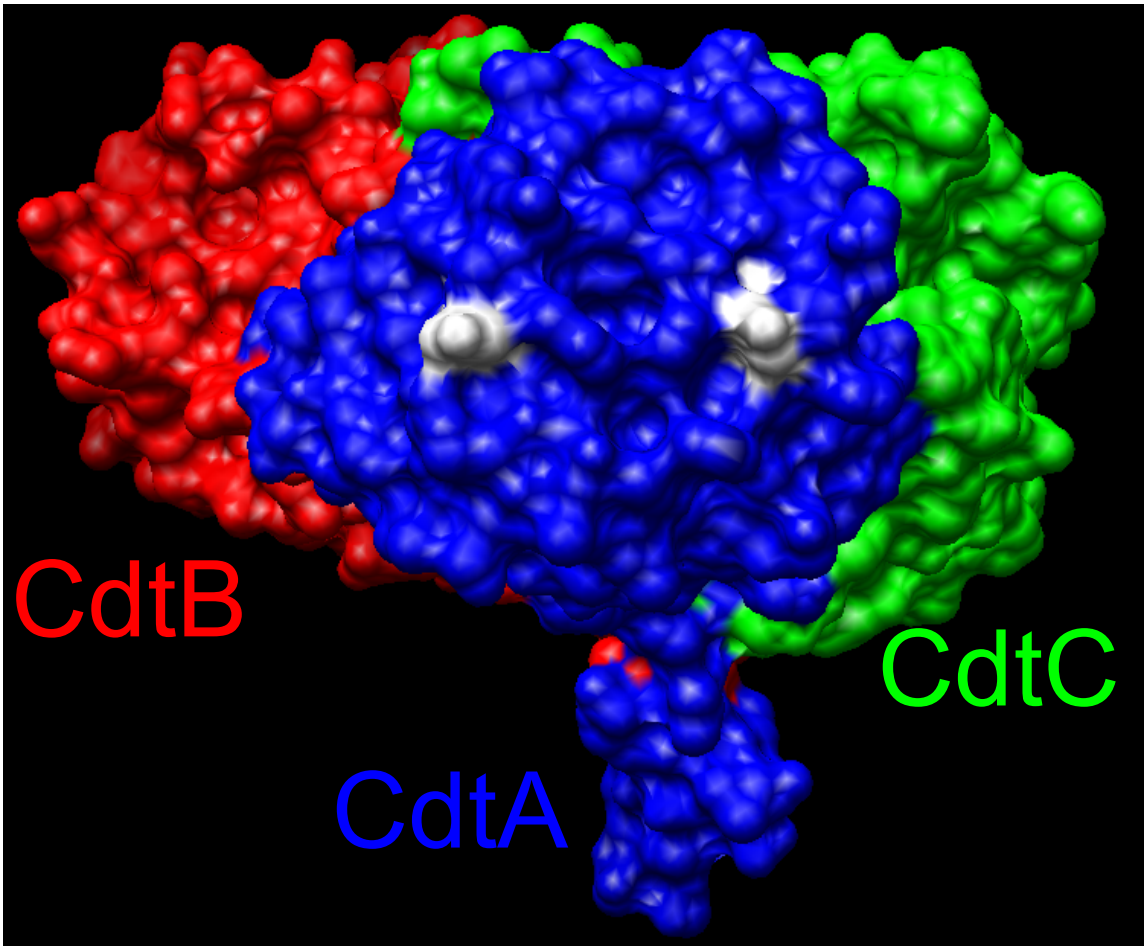

Figure 4.3. Y119 and Y168 residues on Hd-CdtA. Hd-CDT holotoxin protein was modeled using UCSF Chimera, with CdtA colored in blue, CdtB in red, and CdtC green. Y119 and Y168 are colored white. The patch between Y119 and Y168 is the tetra-amino acid aromatic patch, consisting of W91, W98, W100, and Y102.

A.

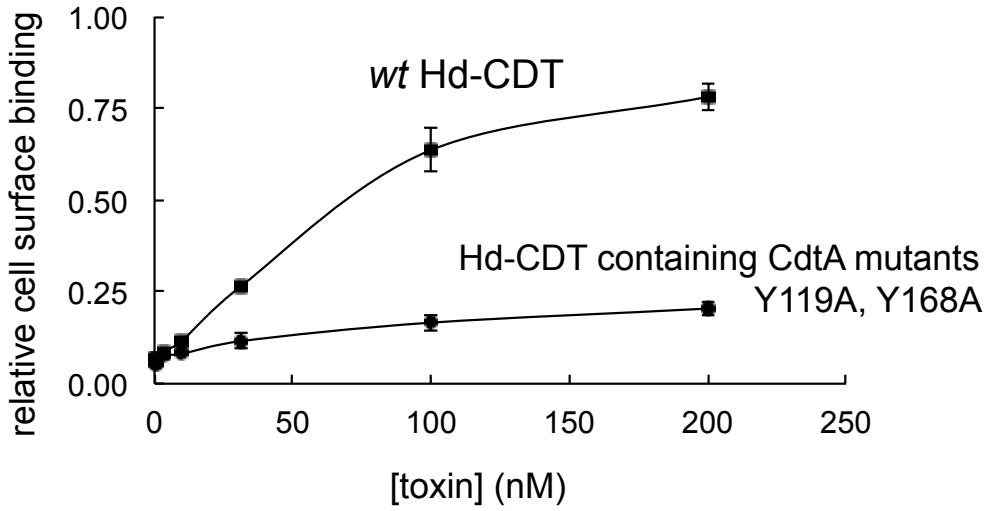

B.

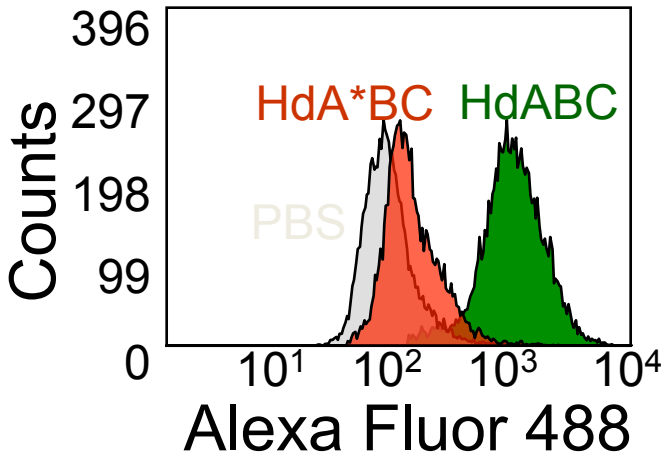

Figure 4.4. Cell surface binding of Hd-CDT against holotoxin with mutant CdtA. (A) Monolayers of HeLa cells were exposed to indicated concentrations of holotoxin under conditions non-permissive of cellular uptake, as detailed in Material and Methods. The data are rendered as the relative binding after 30 min of biotinylated forms of toxin to HeLa cells as a function of toxin concentration (1-200 nM). Total binding curves were fitted with non-linear regression. Data is representative of three independent experiments, each done in triplicate. Error bars indicate standard deviation. (B) HeLa cells in suspension were exposed to 100 nM wildtype or mutated toxin, and bound for 30 minutes before being fixed and probed for holotoxin. Cells were analyzed by flow-cytometry with wildtype holotoxin labeled in green, mutant in red, and PBS control in gray. Data is representative of three independent experiments.

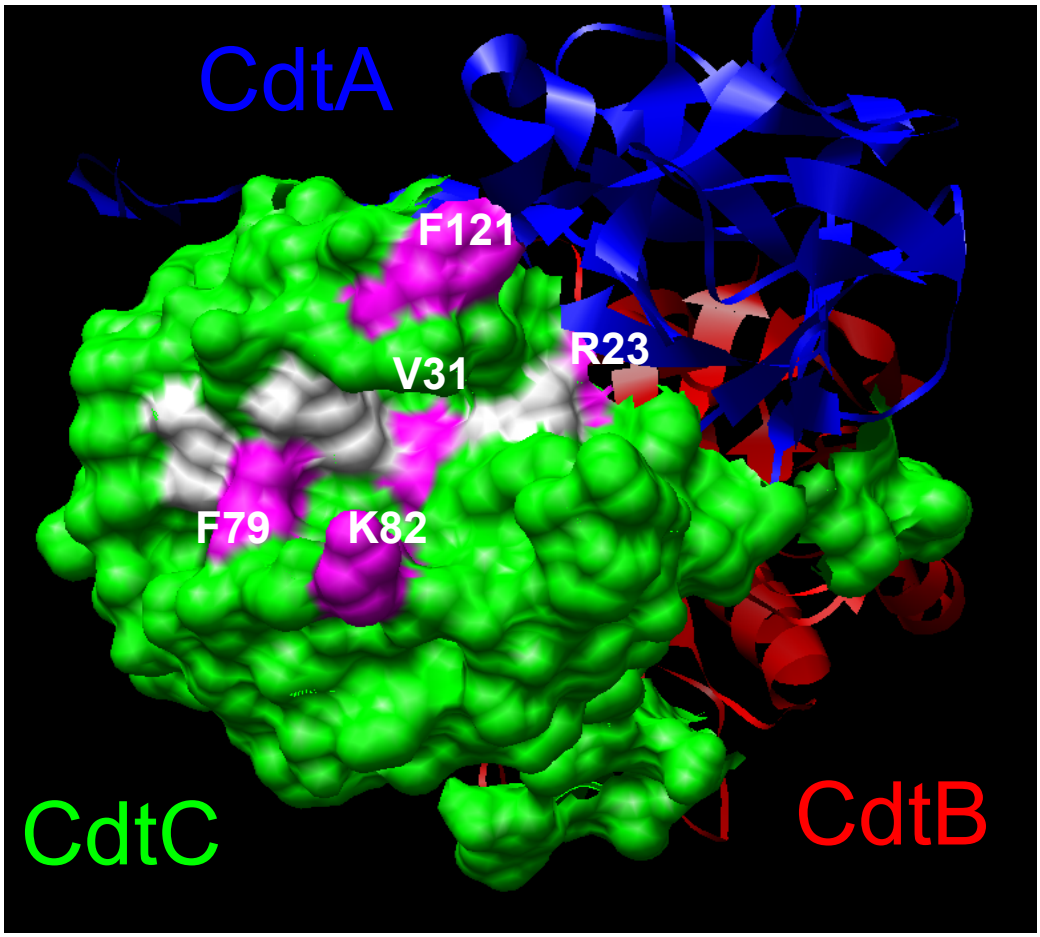

Figure 4.5. Microdomains mutated on Hd-CdtC. Hd-CDT holotoxin protein was modeled using UCSF Chimera, and distinct residues, either hydrophobic or basic, were identified around the putative binding groove. In this model, CdtA is colored blue, CdtB is red, and CdtC green, with residues earmarked for mutation in pink. Total 5 residues on CdtC were investigated: R23, V31, F79, K82, and F121.

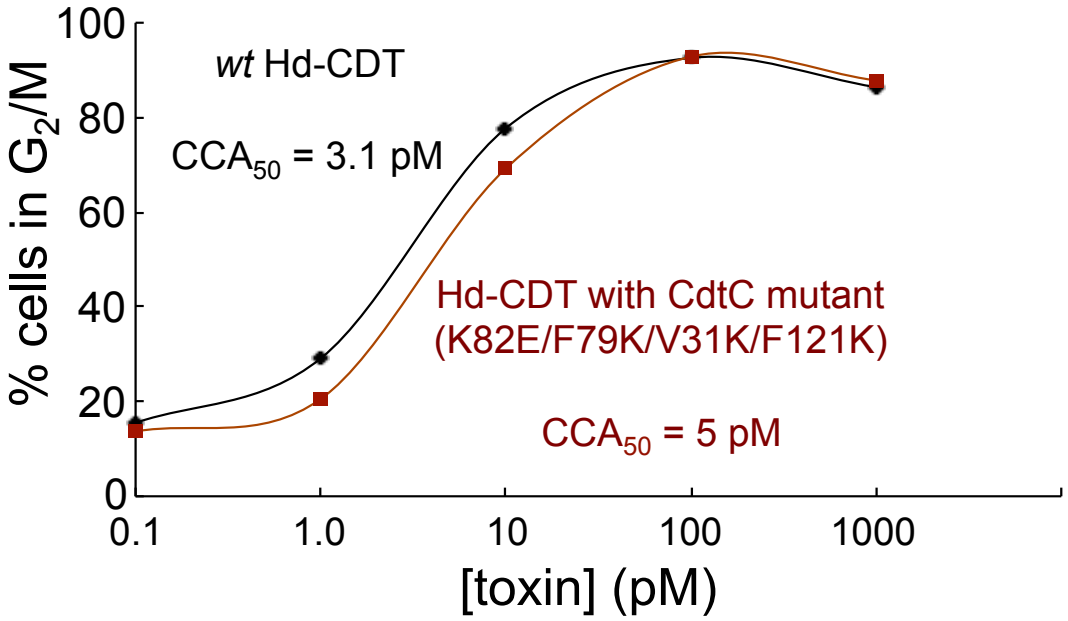

Figure 4.6. Dose response curve of wildtype and mutant Hd-CDT holotoxin. Monolayers of HeLa cells were exposed to indicated concentration of toxin, and evaluated for cell cycle phase at 24 h. Data is representative of three independent experiments.

4.6. References

1. Akifusa, S., Heywood, W., Nair, S. P., Stenbeck, G., & Henderson, B. (2005). Mechanism of internalization of the cytolethal distending toxin of *Actinobacillus actinomycetemcomitans*. *Microbiology, 151*(Pt 5), 1395-1402.

2. Cao, L., Volgina, A., Huang, C. M., Korostoff, J., & DiRienzo, J. M. (2005). Characterization of point mutations in the cdtA gene of the cytolethal distending toxin of *Actinobacillus actinomycetemcomitans*. *Mol Microbiol, 58*(5), 1303-1321.

3. Dixon, W. (1950). Analysis of extreme values. *Ann Math Stat 21*, 488-506.

4. Eshraghi, A., Maldonado-Arocho, F. J., Gargi, A., Cardwell, M. M., Prouty, M. G., Blanke, S. R., & Bradley, K. A. (2010). Cytolethal distending toxin family members are differentially affected by alterations in host glycans and membrane cholesterol. *Journal of Biological Chemistry, 285*(24), 18199-18207.

5. Gargi, A., Reno, M., & Blanke, S. R. (2012). Bacterial toxin modulation of the eukaryotic cell cycle: are all cytolethal distending toxins created equally? *Front Cell Infect Microbiol, 2*, 124.

6. Kanno, F., Korostoff, J., Volgina, A., & DiRienzo, J. M. (2005). Resistance of human periodontal ligament fibroblasts to the cytolethal distending toxin of *Actinobacillus actinomycetemcomitans*. *J Periodontol, 76*(7), 1189-1201.

7. Lee, R. B., Hassane, D. C., Cottle, D. L., & Pickett, C. L. (2003). Interactions of *Campylobacter jejuni* cytolethal distending toxin subunits CdtA and CdtC with HeLa cells. *Infect Immun, 71*(9), 4883-4890.

8. McSweeney, L. A., & Dreyfus, L. A. (2005). Carbohydrate-binding specificity of the *Escherichia coli* cytolethal distending toxin CdtA-II and CdtC-II subunits. *Infect Immun, 73*(4), 2051-2060.

9. Mise, K., Akifusa, S., Watarai, S., Ansai, T., Nishihara, T., & Takehara, T. (2005). Involvement of ganglioside GM3 in G_2/M cell cycle arrest of human monocytic cells induced by *Actinobacillus actinomycetemcomitans* cytolethal distending toxin. *Infect Immun, 73*(8), 4846-4852.

10. Nesic, D., Hsu, Y., & Stebbins, C. E. (2004). Assembly and function of a bacterial genotoxin. *Nature, 429*(6990), 429-433.

11. Pettersen, E. F., Goddard, T. D., Huang, C. C., Couch, G. S., Greenblatt, D. M., Meng, E. C., & Ferrin, T. E. (2004). UCSF Chimera--a visualization system for exploratory research and analysis. *J Comput Chem, 25*(13), 1605-1612.

12. Sandvig, K., Spilsberg, B., Lauvrak, S. U., Torgersen, M. L., Iversen, T. G., & van Deurs, B. (2004). Pathways followed by protein toxins into cells. *Ijmm International Journal of Medical Microbiology, 293*(7-8), 483-490.

CHAPTER 5: CONCLUSIONS AND FUTURE WORK

5.1. Introduction

The major objective of this dissertation was to understand the molecular mechanisms underlying toxin trafficking inside mammalian cells, which is an important requisite for toxins to access its intracellular target and to modulate host cell functions (Blanke, 2006). Of various subcellular systems and organelles, owing to its control on the genetic information and cell homeostasis, nucleus presents itself as an attractive, yet infrequent target for pathogens (Nougayrede, Taieb, De Rycke, & Oswald, 2005). In this work, we used CDT as the model to study the mechanism how toxins destined to reach nucleus are trafficked through specific compartments within the host cell.

When considering the CDT family, most of work that has been conducted thus far, to identify and characterize the structure-function relationships and intoxication properties has appropriately focused on just several CDTs (Aa-CDT, Cj-CDT, Ec-CDT, and Hd-CDT) (Eshraghi et al., 2010; Gargi, Reno, & Blanke, 2012). The conclusions from studying this small subset of the CDT family have been extended rather generically across the broader family of CDTs. Yet, neither the structure-function relationships nor cellular intoxication mechanisms of the vast majority of CDTs have been examined. In fact, the striking diversity in the sequences of CDT subunits identified in an increasing number of genomes of bacterial species from the γ-Proteobacteria and ε-Proteobacteria suggest that the

extent to which individual CDTs function in a similar fashion should be reexamined (Gargi et al., 2012).

Since its initial discovery in 1988 (Johnson & Lior, 1988a, 1988b), CDT has been reported to be produced by over two dozen Gram-negative pathogens, contributing towards the virulence properties of the bacteria (Gargi et al., 2012). Because of similarities or divergences in primary sequences of the holotoxin, for my present study, I investigated CDTs produced by four pathogens: *A. actinomycetemcomitans, E. coli, C. jejuni*, and *H. ducreyi*. The current state of field also aided my selection, in which recent advancements, due to information available on the protein crystal structure or structure-activity studies (Nesic, Hsu, & Stebbins, 2004; Yamada, Komoto, Saiki, Konishi, & Takusagawa, 2006), or the widespread occurrence of infection by certain infecting pathogens (Gargi et al., 2012; Smith & Bayles, 2006; Young, Davis, & Dirita, 2007), rendered studying CDT produced by above mentioned pathogens, critical to understanding the molecular pathogenesis model of the CDT-family.

5.2. Major Findings

Addressing CDT trafficking and intoxication properties is important not only to understand the molecular basis of pathogenesis of CDT-producing bacteria, but also to understand the model in which exogenous molecules successfully target the host cell nucleus. In my doctoral work, parts in collaboration with Ken Bradley's group, I have addressed the events spanning

from cell-surface binding, to the trafficking of CDT through the subcellular compartments of the host cell, as a prerequisite for toxin to reach nucleus to exert its cytotoxic effects. Multiple cell lines, and CDT produced from divergent pathogens were tested, and sometimes directly compared, to validate the findings across different species and biological systems. Based on my work, I have constructed a model of CDT-trafficking through the eukaryotic cell, which reflects our work and current understanding of the field (Figure 5.1). My findings enhanced the understanding of CDT intoxication mechanism and its potential role in the virulence properties of CDT-producing pathogens. Moreover, my studies will also aid in the design of novel tools to target specific subcellular compartments and host cell functions.

5.2.1. Cell surface binding

Despite several attempts to resolve the identity of host cell surface determinants that engage with CDTs, there is only suggestive evidence elaborating on the chemical nature of putative CDT-receptor. Moreover, information on the domains present on CDT, which are critical for host cell surface binding, is limited. While my studies did not make an aggressive attempt to identify the nature of CDT-receptor, I explored the general chemical nature and the specificity of the toxin receptor. I further investigated subdomains on one of the CDT holotoxins (Hd-CDT), mapping residues critical for cell surface binding, and intoxication of the mammalian cells.

Recent reports have suggested the biochemical nature of the putative CDT receptor, with plasma membrane cholesterol, cell surface glycoproteins, and glycosphingolipids playing a major role in aiding cell surface binding of different CDTs (Eshraghi et al., 2010; Lin et al., 2011). While testing the ability of cholesterol supplementation to increase host cell sensitivity, it was found that increasing plasma cholesterol resulted in increased sensitivity to some CDTs, but not to Cj-CDT (Eshraghi et al., 2010), which suggested that cholesterol might be an important component for binding of most CDTs, but Cj-CDT. Contrarily, another group later showed that cholesterol depletion results in resistance to Cj-CDT (Lin et al., 2011). These results, and further studies that identified a cholesterol recognition amino acid consensus (CRAC) sequence in Aa-CdtC and a non-traditional CRAC sequence in CdtC from *Haemophilus parasuis* suggests that cholesterol may play a role in the binding of most, if not all, CDTs to the host cell surface (Boesze-Battaglia et al., 2009; Zhou, Zhang, Zhao, & Jin, 2012). A genetic screen using the KBM7 chronic myeloid leukemia cell line revealed that a putative G protein–coupled receptor, TMEM181, contributes to cellular binding and sensitivity to Ec-CDT (Carette et al., 2009), thus proposing TMEM181 as the potential CDT-receptor. Later studies questioned the presence of TMEM181 on the cell surface, refuting its claim as a toxin-receptor. Further studies will be required to fully characterize the CDT-receptor, but so far we do know that the receptor is rich in cholesterol and might involve the lipid rafts.

Receptor recognition and binding is critical for the function of intracellular-acting toxins because the receptor, in part, functions as a molecular carrier

whose normal uptake and trafficking through the cell directly impacts the final cellular destination of the toxin. Based on the inability of Ec-CDT or Hd-CDT to competitively bind to the surface of cells, we believe that the two toxins might utilize distinct cell surface receptors (Gargi et al., 2013). This idea was further supported by studies in which I observed lectin EEA inhibited the cell surface binding of Ec-CDT, but not Hd-CDT (Gargi et al., 2013). The highly dissimilar protein sequences of the CdtA and CdtC subunits of Ec-CDT and Hd-CDT are consistent with the idea that these two toxins may interact with and intoxicate cells by disparate mechanisms. Consistent with the idea that Ec-CDT and Hd-CDT may bind to different receptors on the surface of sensitive cells, in collaboration with Bradley group, we reported that a mutant CHO cell line, characterized by abbreviated glycan sequences on membrane glycoproteins and glycolipids, was hypersensitive to Hd-CDT, but demonstrated the same sensitivity as the parental CHO cells to Ec-CDT (Eshraghi et al., 2010), which further supports the idea that the receptor for different CDTs might not be the same. Additional studies will be required to determine whether or not differences in intracellular trafficking pathways between Ec-CDT and Hd-CDT directly contribute to the disparity in the potencies exhibited by the two toxins towards sensitive cells. Nonetheless, we speculate that differential cell surface requirements for toxin association is critical for targeting Ec-CDT and Hd-CDT to their respective uptake and intracellular trafficking pathways.

Another important feature of toxin-receptor interaction is to understand the determinants on the toxin important for receptor engagement. Of three CDT

proteins that are required to make holotoxin, CdtA and CdtC are believed to be responsible to engage with the cell surface as the initial point of contact with the host cell, which is then followed by toxin uptake and cellular intoxication, delivering the active moiety, CdtB, inside the cell (Nesic et al., 2004). One of the unusual features highlighted by the crystal structure of Hd-CDT is a region of aromatic and heterocyclic amino acids exposed on the surface of CdtA (Nesic et al., 2004). Studying the topological information of Hd-CdtA, I mapped the surface exposed residues to investigate additional domains not covered by Nesic and co-workers (Nesic et al., 2004), which might be important for cell-surface binding. In fact, I found at least two additional tyrosines on the surface of Hd-CdtA, Y119 and Y168, mutating which produced almost complete loss of cell surface binding, and a significant attenuation in the cytotoxic properties of the Hd-CDT holotoxin. My results reflect on the importance of CdtA aromatic residues in host-pathogen interactions, and that the receptor binding regions are not limited to just four aromatic residues first described by Stebbins groups. Studying Aa-CDT, another group later reported similar results in which two-tyrosine residues, both homologous to my study of Hd-CdtA, lead to the loss in the binding properties of the holotoxin (Cao, Bandelac, Volgina, Korostoff, & DiRienzo, 2008).

I extended the studies on understanding the topological domains of CDT in cell binding, by characterizing residues on Hd-CdtC, which might play a role in toxin binding to the cell surface. I selected the aromatic and basic residues that were around the putative cell-binding groove on CdtC, hypothesizing that their mutation will result in a phenotype different from wild-type toxin. Mutating two

aromatic residues, F79 and F121, and two basic residues, R23 and K82, I investigated the effect on cell binding and cytotoxic properties of the holotoxin. Contrary to our expectations, single mutants, or all mutants put together as a tetramutant, did not demonstrate results different from the wild-type, suggesting the aromatic or basic residues around Hd-CdtC groove may not play a role in toxin binding. Further studies will be required to map domains present on CdtC and characterize their role in the cytotoxic properties of CDT.

Taken together, my findings suggest that CdtA predominantly mediates cell surface receptor binding. Further studies will be required to fully characterize all subdomains on the surface of CdtA and CdtC, and their role in cell surface binding, which will be important for developing strategies to block the activity of CDTs.

5.2.2. Trafficking through the endolysosomal system

Following docking and binding to the mammalian cell membrane, toxins are endocytosed inside the cell using one of several differentially regulated endocytic mechanisms, which sometimes may operate in parallel (Lamaze et al., 2001; Nichols & Lippincott-Schwartz, 2001; Sandvig & van Deurs, 2000, 2002). Limited studies done on CDT-endocytosis suggest that the toxin internalization is dynamin-dependent, which may or may not follow the clathrin-dependent pathway (Cortes-Bratti, Chaves-Olarte, Lagergard, & Thelestam, 2000). Induction of CDT's cytotoxic activity is completely inhibited under conditions that block the

fusion of the endosomal vesicles with downstream compartments, indicating that the toxin is further trafficked through the endosomal compartment (Cortes Bratti 2000). Depending on the toxin and host cell type, researchers have reported differing findings on the mechanism of toxin transition through the endolysosomal system. Several earlier models of CDT intoxication predicted that the CDT holotoxin, rather than a CdtA-CdtB or CdtB-CdtC dimer, or CdtB alone, is taken up by early endosomes (Boesze-Battaglia et al., 2009; Cortes-Bratti et al., 2000; Guerra et al., 2009), but a conclusive evidence on the fate of CDT subunits post-internalization is lacking.

Because of the changing conditions within endosomal lumen with the vesicle maturation, which includes drop in luminal pH and a shift in molecular components associated with endosomal vesicle, cargo might respond to the pH trigger and undergo conformational change that may allow it to escape to the cytosol, or may engage with specific components of the vesicle thus allowing itself to be transported to its subsequent target (Huotari & Helenius, 2011). If toxins cannot escape the endosomal compartments, most likely they are degraded in the lysosomes (Huotari & Helenius, 2011). In my studies, I addressed the differential fate of CDTs while being transported through endosomal compartments.

For the toxins following retrograde pathway, most cargoes exit the endolysosomal system out of the early endosomes. Our initial hypothesis was that, just like cholera toxin and shiga toxin, CDTs might the directed to the Golgi apparatus from the early endosomes, thus escaping the degradation fate in the

lysosomes (Lauvrak, Torgersen, & Sandvig, 2004; Lencer, Hirst, & Holmes, 1999). In fact my studies demonstrate that Ec-CDT does not transition through the late endosomes, as it was insensitive to the perturbations in the endosomal pH, or the molecular components involved in late endosome to Golgi trafficking (Gargi et al., 2013), suggesting that CDTs might not traffic through late endosomes at all. But the unexpected results were obtained when I evaluated the trafficking of Hd-CDT (Gargi et al., 2013), and later of Cj-CDT (unpublished data) through the endolysosomal system. I demonstrated that blocking endosomal maturation, or perturbing the molecular machinery that directs cargo from late-endosomes to the Golgi apparatus, alters the trafficking and activity of Hd-CDT and Cj-CDT, but not of Ec-CDT (Gargi et al., 2013). I did not study endosomal trafficking model for Aa-CDT, but given its structural and functional similarities with Hd-CDT, we predict that Aa-CDT might transition through the late endosomes before being trafficked to the Golgi apparatus.

5.2.3. Trafficking through the Golgi apparatus

Being the central cargo-sorting platform of eukaryotic cells, Golgi apparatus not only can modify transitioning biomolecules, but it plays a critical role both in anterograde, and retrograde trafficking of the cargo. Current model of CDT trafficking suggests that the toxin transitions through the Golgi apparatus after exiting endolysosomal system. But the understanding is speculative, and the model is based merely on the effect of small molecule inhibitors that

disintegrate the Golgi apparatus. As it is well know that small molecule inhibitors like brefeldin A have strong pleiotropic effects (Klausner, Donaldson, & Lippincott-Schwartz, 1992), it is hard to characterize precise involvement of the Golgi apparatus in toxic trafficking and activity. One report comes close to confirming that CDT is trafficked through the Golgi apparatus. By observing sulfation of CdtB, containing an engineered tag that could be sulfated, one group demonstrated the toxin transitions through the Golgi when holotoxin is applied on the cells (Guerra et al., 2005). But this study still doesn't address the absolute requirement of CDT transition through the Golgi apparatus, or identify the molecular mechanism of trafficking through the central sorting portal of the cell.

My studies address several of these questions: is trafficking through the Golgi apparatus absolutely essential for the toxin activity? What are the kinetics of toxin trafficking through the Golgi apparatus? What compartments within the Golgi apparatus play a role in toxin trafficking? What are the molecular components on the Golgi apparatus, that interact with CDT-containing cargo vesicles.

Using localization studies and specific inhibitors for Golgi sub-compartments, I demonstrated that CdtB traverse through all stacks of the Golgi apparatus, from trans- to cis-Golgi. First instance when CdtB is detected in the Golgi apparatus is at 20 minutes, positioning CDT's retrograde trafficking through the Golgi apparatus between endolysosomal system, where it is detected between 5 to 15 minutes of intoxication, and the ER, where it is observed at one hour post-intoxication. This is first such evidence, supported by toxin kinetics and

controlled disruption of cellular functions, in which the itinerary of CDT's retrograde trafficking is mapped inside a eukaryotic cell. I also identified the absolute importance of the Golgi apparatus on the activity and trafficking of the members of CDT-family. All CDT holotoxins, which were tested for their reliance on a functional Golgi apparatus, showed that disruption in the Golgi apparatus confers resistance to the intoxicated cells. This is one instance where all CDTs agree on the commonality of a single subcellular compartment involved in the toxin trafficking and activity. I further characterized the molecular components that play a role in CdtB transition through the Golgi apparatus. Evaluating the components involved in CdtB trafficking from the endolysosomes to the Golgi apparatus, I discovered that the conserved oligomeric Golgi (COG) complex plays a critical role in receiving CdtB containing cargo at the Golgi apparatus. COG complex is a resident member of the Golgi apparatus membrane. Perturbations in the trafficking factors that associate with COG complex, i.e. STX10, or altering the presence of the complex on the Golgi apparatus, led to loss in the activity of CDT, which was detected to be because of disruption in the retrograde trafficking of the toxin. Taken together, my studies not only underscore the importance of the Golgi apparatus in the transport and activity of CDT, but it also identifies the molecular machinery that plays a role in toxin trafficking through the central sorting machinery of the cell. This is first such volume of work that dissected the molecular mechanism of CDT pathogenesis at the organelle that is used by all members of CDT-family for their transport to the nucleus.

5.2.4. Trafficking through the Endoplasmic Reticulum

Endoplasmic Reticulum (ER) is the site used by several AB toxins to exit to the cytosol, making it an important portal for toxins to be able to access their intracellular target. Using fluorescence microscopy, and also by studying the glycosylation of engineered CdtB, CDT also has been shown to transition through the ER before it can reach nucleus (Eshraghi et al., 2014; Gargi et al., 2013; Guerra et al., 2005).

There are two main pathways that the toxin might take to reach the nucleus from ER: directly from ER lumen to the nucleus, or by exiting ER lumen and reaching cytosol, and then targeting the nucleus. In CDT field there are conflicting opinions on how CdtB is trafficked from ER to the nucleus. While failing to detect CdtB in the cytosol of the nucleus, one group inferred that CdtB is trafficked directly from ER to the nucleus (Guerra et al., 2009). In contrast, our research, in collaboration with Ken Bradley's, believes that CdtB must first escape to the cytosol before it can reach the nucleus (Eshraghi et al., 2014). We identified the importance of ERAD-pathway, a system that transports cargo across the ER membrane, on the trafficking and intoxication properties of Ec-CDT and Hd-CDT, which clearly supports the model that CDT must traffic from ER lumen to the cytosol before it can exert its cytotoxic effect inside the nucleus (Eshraghi et al., 2014). One exception to this model is when we tested the effect of Derlin 2 or Hrd1 mutants, both important factors in ERAD-pathway, on the activity of Cj-CDT. Contrary to the inhibition of intoxication properties of Ec-CDT and Hd-CDT, Cj-CDT was resistant to any perturbations in the ERAD-pathway,

suggesting that it might take an alternate route to reach the nucleus (data not published). Further studies will be required to evaluate the transportation mechanism of Cj-CDT from ER to the nucleus, and underlying physiological importance of this divergence in retrograde trafficking.

5.2.5. Trafficking to the nucleus

Several reports have expounded on the requirement of CdtB reaching the host cell nucleus to cause DNA-damage, and trigger a series of signaling events leading to cell cycle arrest. Studies involving transient transfection, direct microinjection of CdtB, or mutation of toxin's nuclear localization signal (NLS) underscored the importance of accessing host cell nucleus as a requisite for CDT to elaborate its cytotoxic effects (McSweeney & Dreyfus, 2004; Nishikubo et al., 2003). But none of previous studies conclusively established the presence of CdtB inside the host cell nucleus. I presented first physical evidence that the catalytically active subunit of the holotoxin could be detected in the nucleus of intoxicated mammalian cells (Gargi et al., 2013).

By testing the ability of CdtB to reach nucleus, I demonstrated that when applied externally, the catalytically active subunit of holotoxin CDT has the capability to reach nucleus within 60 minutes for Ec-CDT and Hd-CDT (Gargi et al., 2013), and by 90 minutes for Cj-CDT (unpublished data). Most cytotoxic effects of CDT, like H2AX phosphorylation and cell cycle arrest, were observed at time points much later than CdtB arrival at the nucleus. These findings support

the model that the cytotoxic effects of CDT are downstream of CdtB reaching the nucleus, and that trafficking to the nucleus might be necessary for the toxin activity. This implies that perturbations in the trafficking of CdtB to the nucleus must block the cytotoxic effect of the holotoxin. In fact, I tested and demonstrated that under conditions non-permissive for CdtB trafficking leading to the nucleus, i.e. endosomal acidification, Golgi disruption, or disruption of ERAD-pathway, depending on the path taken by different CdtBs, the transport of toxin to the nucleus was blocked, which was followed by failure of CDT to produce DNA-damage or trigger events downstream of dsDNA-break.

Of the toxins evaluated, comparing the trafficking properties of three different CDTs, Cj-CDT, Ec-CDT, and Hd-CDT, I discovered that the toxin-trafficking pathway converge and diverge at certain organelles, giving each CDT a unique transport map, which might be dependent on the site of pathogen-colonization and intoxication of the mammalian tissue. While blocking endosomal maturation affected transport of Cj-CdtB and Hd-CdtB, it had no effect on Ec-CdtB trafficking to the nucleus, suggesting that Ec-CDT might bypass the trafficking through the late endosomes. Further, transport and activity of all CDTs investigated in this study were affected by Golgi apparatus disruption, clearly suggesting that Golgi apparatus might be the bottleneck for the trafficking and activity of all CDTs. Interesting, just like trafficking through the endolysosomal system, mechanism of exiting the ER might not be similar for all CDTs. While Ec-CDT and Hd-CDT were clearly affected by the perturbations in ERAD-pathway, a major protein translocation system required for cargo transport across ER lumen

and the cytosol, biological activity of Cj-CDT was unaffected by disruptions in the ERAD-pathway. In summary, Hd-CDT trafficking and activity is affected by endosomal, Golgi, and ERAD-pathway perturbations. Cj-CDT is also affected by endosomal and Golgi apparatus perturbations, but not by ERAD-pathway disruption. While Ec-CDT is unaffected by endosomal pH perturbations, its trafficking and cytotoxic activity is sensitive to the Golgi apparatus and ERAD-pathway disruptions. One question that remains unanswered, is how does the CdtB from *C. jejuni* escape the ER, and is targeted to the nucleus. There is a possibility that Cj-CdtB utilize an alternate route to the nucleus that does not involve the ERAD-pathway. Another exciting area to explore is to find the precise role of the Golgi apparatus and ER in toxin trafficking and activity. My studies show that if CdtB is allowed to escape to the cytosol directly from endosomes, effectively bypassing transition through the Golgi apparatus and the ER, toxin is still capable of exerting DNA-damage in the intoxicated cells. But the toxin concentrations used in the studies, for detection purpose, were several-fold higher than the cytotoxic dose, which might question the overall potency and physiological relevance of method in our study. Overall, my studies not only characterize the transport path taken by CdtBs to reach nucleus, but also supports the idea that trafficking to the nucleus is indispensible for the toxin to exert its cellular activity.

5.3. Conclusion

The fact that CDT is one of few, or in some instances, only exotoxin in the arsenal of CDT-producing Gram-negative pathogens, makes it an intriguing model to understand its role in microbial pathogenesis (Gargi et al., 2012). Another outstanding feature that warrants investigating the intoxication model of CDT-family is the fact that CDTs are one of only few bacterial toxins known to produce cytotoxic effects within the nucleus of the host cell, making them an important model to study the nuclear microbiology (Nougayrede et al., 2005). One of the interesting pieces of CDT complexity is the significant structural and functional difference within the members of the family (Gargi et al., 2012; Hu, Nesic, & Stebbins, 2006). Members of CDT-family exhibit significant differences and similarities, ranging from primary sequence diversity, heterogeneity in cell attachment mechanisms, toxin-potency and sensitivities to different mammalian tissues, to variability in the way it carries out mammalian cell intoxication. Some CDTs appear to bind specifically structured glycan residues on glycoproteins or glycolipids, others were shown to engage with cholesterol rich microdomains, bind certain gangliosides, or transmembrane G-protein-coupled receptor proteins. Also, intoxication by some CDTs leads to cell cycle arrest at either the G_1 or G_2/M checkpoint or cell death via an apoptotic pathway. Exhaustive phylogenetic analyses and comparisons within each of the three subunits across the species-specific CDTs have been performed to attempt to understand this heterogeneity (Gargi et al., 2012). This approach has been yielded mixed results, which unfortunately, doesn't always translate to functional relationships. Arguably,

underlying difference in functional outcomes of CDT activity might be due to tissue tropism, or the influence of CDT-subunits of the cognate holotoxin. Further studies will be required to dissect the phenotypical differences among members of CDT family, despite carrying significant primary sequence, and structural similarities.

Current challenges are to uncover the details of the CDT intoxication process, determine whether there are truly multiple distinct receptors for each CDT, or interplay between components in highly specialized regions of the cell membrane, and identify if this specificity relates back to the tissue tropism. Moreover, the precise role of cellular compartments in the intoxication properties of specific CDTs is still unclear, and would it would be exciting to study how CDT trafficking may dictate different outcomes for CDT behavior, which may further explain the commonality and evolutionary relationship among the species-specific CDTs.

5.4. Future Work

The degree to which the large sequence diversity among CDTs reflects functional differences between individual members of the CDT family is largely unexplored. Nonetheless, as discussed in this study, there are some hints from several recent studies that CDTs may in fact be highly divergent in their potencies and host requirements for intoxication. It will be interesting to test the premise that the functional differences between CDTs may reflect the diversity of

host cells and tissues that comprise the infection microenvironments targeted by CDT-producing pathogenic bacteria.

One of the true challenges in the CDT field is to understand the *in vivo* consequences of CDT action during infection. Studies to understand, from an evolutionary perspective, the benefit of CDT-mediated genotoxicity for promoting host-pathogen interactions, remain a particular challenge, because any benefits may in fact be highly idiosyncratic to the specific pathogen and the host niche occupied by that pathogen.

5.5. Figures

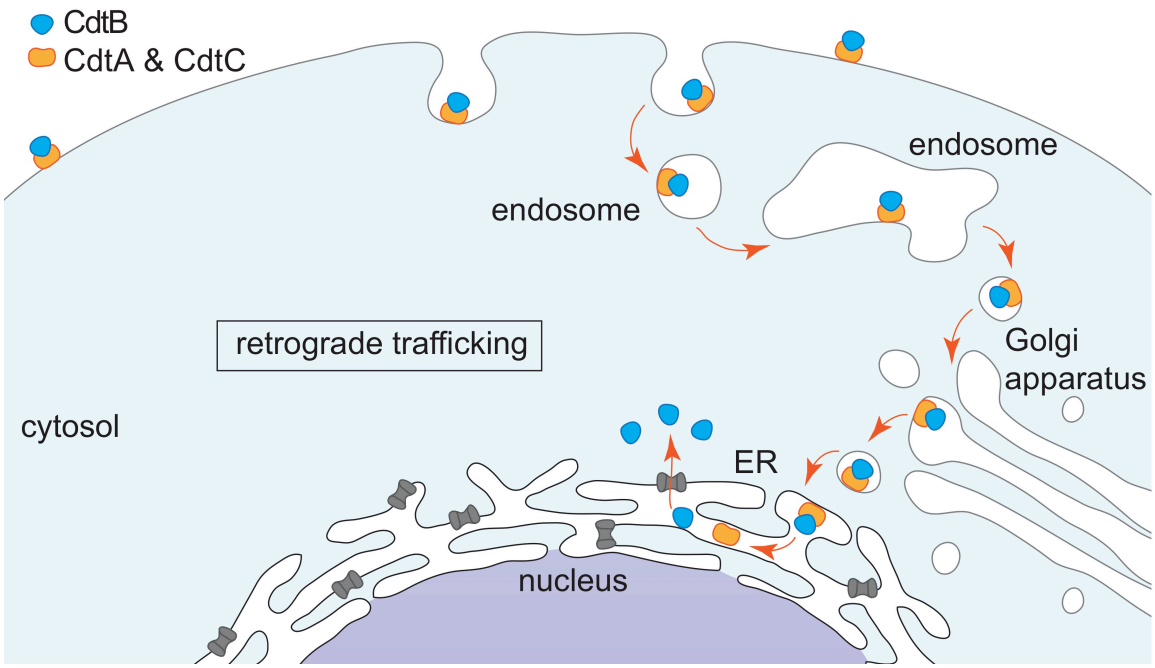

Figure 5.1. CDT is trafficked retrogradely to the host cell nucleus. CDT is an AB toxin that has a two component architecture, with A moiety, composed of CdtB, carrying the toxic activity, and B moiety, composed of CdtA and CdtC, responsible for cell binding and facilitating CdtB delivery to its target. Following cellular uptake, CDT is trafficked through the endolysosomal system to the Golgi apparatus, from where it is further targeted to the endoplasmic reticulum. Using the ERAD-pathway, CdtB escapes to the cytosol, from where it is subsequently transported to the nucleus to exert genotoxic activity.

5.6. References

1. Blanke, S. R. (2006). Portals and Pathways: Principles of Bacterial Toxin Entry into Host Cells. *Microbe, 1*, 26 - 32.

2. Boesze-Battaglia, K., Brown, A., Walker, L., Besack, D., Zekavat, A., Wrenn, S., Krummenacher, C., & Shenker, B. J. (2009). Cytolethal distending toxin-induced cell cycle arrest of lymphocytes is dependent upon recognition and binding to cholesterol. *Journal of Biological Chemistry, 284*(16), 10650-10658.

3. Cao, L., Bandelac, G., Volgina, A., Korostoff, J., & DiRienzo, J. M. (2008). Role of aromatic amino acids in receptor binding activity and subunit assembly of the cytolethal distending toxin of *Aggregatibacter actinomycetemcomitans*. *Infect Immun, 76*(7), 2812-2821.

4. Carette, J. E., Guimaraes, C. P., Varadarajan, M., Park, A. S., Wuethrich, I., Godarova, A., Kotecki, M., Cochran, B.H., Spooner, E., Ploegh, H.L., & Brummelkamp, T. R. (2009). Haploid genetic screens in human cells identify host factors used by pathogens. *Science, 326*(5957), 1231-1235.

5. Cortes-Bratti, X., Chaves-Olarte, E., Lagergard, T., & Thelestam, M. (2000). Cellular internalization of cytolethal distending toxin from *Haemophilus ducreyi*. *Infect Immun, 68*(12), 6903-6911.

6. Eshraghi, A., Dixon, S. D., Tamilselvam, B., Kim, E. J., Gargi, A., Kulik, J. C., Damoiseaux, R., Blanke, S.R., &Bradley, K. A. (2014). Cytolethal distending toxins require components of the ER-associated degradation pathway for host cell entry. *PLoS Pathog, 10*(7), e1004295.

7. Eshraghi, A., Maldonado-Arocho, F. J., Gargi, A., Cardwell, M. M., Prouty, M. G., Blanke, S. R., & Bradley, K. A. (2010). Cytolethal distending toxin family members are differentially affected by alterations in host glycans and membrane cholesterol. *Journal of Biological Chemistry, 285*(24), 18199-18207.

8. Gargi, A., Reno, M., & Blanke, S. R. (2012). Bacterial toxin modulation of the eukaryotic cell cycle: are all cytolethal distending toxins created equally? *Front Cell Infect Microbiol, 2*, 124.

9. Gargi, A., Tamilselvam, B., Powers, B., Prouty, M. G., Lincecum, T., Eshraghi, A., Maldonado-Arocho, F.J., Wilson, B.A., Bradley, K.A., & Blanke, S. R. (2013). Cellular interactions of the cytolethal distending toxins from *Escherichia coli* and *Haemophilus ducreyi*. *Journal of Biological Chemistry, 288*(11), 7492-7505.

10. Guerra, L., Nemec, K. N., Massey, S., Tatulian, S. A., Thelestam, M., Frisan, T., & Teter, K. (2009). A novel mode of translocation for cytolethal distending toxin. *Biochim Biophys Acta, 1793*(3), 489-495.

11. Guerra, L., Teter, K., Lilley, B. N., Stenerlow, B., Holmes, R. K., Ploegh, H. L., Sandvig, K., Thelestam, M., & Frisan, T. (2005). Cellular internalization of cytolethal distending toxin: a new end to a known pathway. *Cellular Microbiology, 7*(7), 921-934.

12. Hu, X., Nesic, D., & Stebbins, C. E. (2006). Comparative structure-function analysis of cytolethal distending toxins. *Proteins, 62*(2), 421-434.

13. Huotari, J., & Helenius, A. (2011). Endosome maturation. *EMBO Journal, 30*(17), 3481-3500.

14. Johnson, W. M., & Lior, H. (1988a). A new heat-labile cytolethal distending toxin (CLDT) produced by *Campylobacter spp*. *Microbial Pathogenesis, 4*(2), 115-126.

15. Johnson, W. M., & Lior, H. (1988b). A new heat-labile cytolethal distending toxin (CLDT) produced by *Escherichia coli* isolates from clinical material. *Microbial Pathogenesis, 4*(2), 103-113.

16. Klausner, R. D., Donaldson, J. G., & Lippincott-Schwartz, J. (1992). Brefeldin A: insights into the control of membrane traffic and organelle structure. *Journal of Cell Biology, 116*(5), 1071-1080.

17. Lamaze, C., Dujeancourt, A., Baba, T., Lo, C. G., Benmerah, A., & Dautry-Varsat, A. (2001). Interleukin 2 receptors and detergent-resistant membrane domains define a clathrin-independent endocytic pathway. *Mol Cell, 7*(3), 661-671.

18. Lauvrak, S. U., Torgersen, M. L., & Sandvig, K. (2004). Efficient endosome-to-Golgi transport of Shiga toxin is dependent on dynamin and clathrin. *Journal of Cell Science, 117*(Pt 11), 2321-2331.

19. Lencer, W. I., Hirst, T. R., & Holmes, R. K. (1999). Membrane traffic and the cellular uptake of cholera toxin. *Biochim Biophys Acta, 1450*(3), 177-190.

20. Lin, C. D., Lai, C. K., Lin, Y. H., Hsieh, J. T., Sing, Y. T., Chang, Y. C., Chen, K., Wang, W., Su, H., & Lai, C. H. (2011). Cholesterol depletion reduces entry of *Campylobacter jejuni* cytolethal distending toxin and attenuates intoxication of host cells. *Infect Immun, 79*(9), 3563-3575.

21. McSweeney, L. A., & Dreyfus, L. A. (2004). Nuclear localization of the *Escherichia coli* cytolethal distending toxin CdtB subunit. *Cellular Microbiology, 6*(5), 447-458.

22. Nesic, D., Hsu, Y., & Stebbins, C. E. (2004). Assembly and function of a bacterial genotoxin. *Nature, 429*(6990), 429-433.

23. Nichols, B. J., & Lippincott-Schwartz, J. (2001). Endocytosis without clathrin coats. *Trends Cell Biol, 11*(10), 406-412.

24. Nishikubo, S., Ohara, M., Ueno, Y., Ikura, M., Kurihara, H., Komatsuzawa, H., Oswald, E., & Sugai, M. (2003). An N-terminal segment of the active component of the bacterial genotoxin cytolethal distending toxin B (CDTB) directs CDTB into the nucleus. *Journal of Biological Chemistry, 278*(50), 50671-50681.

25. Nougayrede, J. P., Taieb, F., De Rycke, J., & Oswald, E. (2005). Cyclomodulins: bacterial effectors that modulate the eukaryotic cell cycle. *Trends Microbiol, 13*(3), 103-110.

26. Sandvig, K., & van Deurs, B. (2000). Entry of ricin and Shiga toxin into cells: molecular mechanisms and medical perspectives. *EMBO Journal, 19*(22), 5943-5950.

27. Sandvig, K., & van Deurs, B. (2002). Membrane traffic exploited by protein toxins. *Annual Review of Cell & Developmental Biology, 18*, 1-24.

28. Smith, J. L., & Bayles, D. O. (2006). The contribution of cytolethal distending toxin to bacterial pathogenesis. *Crit Rev Microbiol, 32*(4), 227-248.

29. Yamada, T., Komoto, J., Saiki, K., Konishi, K., & Takusagawa, F. (2006). Variation of loop sequence alters stability of cytolethal distending toxin (CDT): crystal structure of CDT from Actinobacillus actinomycetemcomitans. *Protein Sci, 15*(2), 362-372.

30. Young, K. T., Davis, L. M., & Dirita, V. J. (2007). *Campylobacter jejuni*: molecular biology and pathogenesis. *Nat Rev Microbiol, 5*(9), 665-679.

31. Zhou, M., Zhang, Q., Zhao, J., & Jin, M. (2012). *Haemophilus parasuis* encodes two functional cytolethal distending toxins: CdtC contains an atypical cholesterol recognition/interaction region. *PLoS ONE [Electronic Resource], 7*(3), e32580.